MODELING OF NON-LINEAR EFFECT IN REMOTE CONTROLLED STABILIZED GUN SYSTEMS

UZAKTAN KOMUTALI STABİLİZE SİLAH SİSTEMLERİNDE LİNEER OLMAYAN ETKİLERİN MODELLENMESİ

AHMET TATAR

PROF.DR. BORA YILDIRIM
Supervisor

Submitted to Graduate School of Science and Engineering of Hacettepe University as a Partial Fulfillment to the Requirements for the award of the Degree of Master in Mechanical Engineering

2018

This work named **"Modeling of Non-Linear Effect in Remote Controlled Stabilized Gun Systems"** by **AHMET TATAR** has been approved as a thesis for the Degree of **MASTER OF SCIENCE IN MECHANICAL ENGINEERING** by the below mentioned Examining Committee Members.

Assistant Prof. Dr. Osman Selim TÜRKBAŞ
Head ....

Prof. Dr. Bora YILDIRIM
Supervisor ....

Associate Prof. Dr. Barış SABUNCUOĞLU
Member ....

Assistant Prof. Dr. Can Ulaş DOĞRUER
Member ....

Assistant Prof. Dr. Okan GÖRTAN
Member ....

This thesis has been approved as a thesis for the Degree of **MASTER OF SCIENCE IN MECHANICAL ENGINEERING** by Board of Directors of the Institute for Graduate School of Science and Engineering.

Prof. Dr. Menemşe GÜMÜŞDERELİOĞLU
Director of the Institute of
Graduate School of Science and Engineering

YAYINLAMA VE FİKRİ MÜLKİYET HAKLARI BEYANI

Enstitü tarafından onaylanan lisansüstü tezimin/raporumun tamamını veya herhangi bir kısmını, basılı (kağıt) ve elektronik formatta arşivleme ve aşağıda verilen koşullarla kullanıma açma iznini Hacettepe üniversitesine verdiğimi bildiririm. Bu izinle Üniversiteye verilen kullanım hakları dışındaki tüm fikri mülkiyet haklarım bende kalacak, tezimin tamamının ya da bir bölümünün gelecekteki çalışmalarda (makale, kitap, lisans ve patent vb.) kullanım hakları bana ait olacaktır.

Tezin kendi orijinal çalışmam olduğunu, başkalarının haklarını ihlal etmediğimi ve tezimin tek yetkili sahibi olduğumu beyan ve taahhüt ederim. Tezimde yer alan telif hakkı bulunan ve sahiplerinden yazılı izin alınarak kullanması zorunlu metinlerin yazılı izin alarak kullandığımı ve istenildiğinde suretlerini Üniversiteye teslim etmeyi taahhüt ederim.

☑ **Tezimin/Raporumun tamamı dünya çapında erişime açılabilir ve bir kısmı veya tamamının fotokopisi alınabilir.**
(Bu seçenekle teziniz arama motorlarında indekslenebilecek, daha sonra tezinizin erişim statüsünün değiştirilmesini talep etseniz ve kütüphane bu talebinizi yerine getirse bile, tezinin arama motorlarının önbelleklerinde kalmaya devam edebilecektir.)

☐ **Tezimin/Raporumun .... tarihine kadar erişime açılmasını ve fotokopi alınmasını (İç Kapak, Özet, İçindekiler ve Kaynakça hariç) istemiyorum.**
(Bu sürenin sonunda uzatma için başvuruda bulunmadığım taktirde, tezimin/raporumun tamamı her yerden erişime açılabilir, kaynak gösterilmek şartıyla bir kısmı ve ya tamamının fotokopisi alınabilir)

☐ **Tezimin/Raporumun .... tarihine kadar erişime açılmasını istemiyorum, ancak kaynak gösterilmek şartıyla bir kısmı veya tamamının fotokopisinin alınmasını onaylıyorum.**

☐ **Serbest Seçenek/Yazarın Seçimi**

15 / 05 / 2018

A. Tatar

(İmza)

Ahmet TATAR

To my family and all friends…

ETHICS

In this thesis study, prepared in accordance with the spelling rules of Institute of Graduate Studies in Science of Hacettepe University

I declare that

- All the information and documents have been obtained in the base of the academic rules
- All audio-visual and written information and results have been presented according to the rules of science ethics
- In case of using other Works, related studies have been cited in accordance with the scientific standards
- All cited studies have been fully referenced
- I did not do any distribution in the data set
- And any part of this thesis has not been presented as another thesis study at this or any other university

15/05/2018

AHMET TATAR

ABSTRACT

MODELING OF NON-LINEAR EFFECT IN REMOTE CONTROLLED STABILIZED GUN SYSTEMS

Ahmet TATAR
Master of Science Degree, Department of Mechanical Engineering
Supervisor: Prof. Dr. Bora YILDIRIM

May 2018, 136 pages

The defense industry is the fastest growing sector with technological developments all over the world. Autonomous and remote controlled weapons are regarded the most advanced weapons in today's battlefields. In this study, the effects of the flexible behavior of the steering gears in the remote controlled weapons on the aiming precision was investigated. System was modeled in ANSYS software for observing material flexibilities at maximum motion ranges. Analysis run for flexible and rigid material conditions and solutions were compared. The vertical dynamics of the seven degrees of freedom four wheels and nine degrees of freedom six wheels vehicles simulate in MATLAB software for creating a realize environment. Turret system was integrated on the vehicles, and when vehicles pass on an obstacle, turret stabilization is provided with PID controller. In final step of the study, ANSYS turret model, and MATLAB vehicle model were connected. Turret system behavior was observed on the realized vehicles with this ANSYS integrated MATLAB algorithm. Disturbance on the turret caused by vehicle vibration was controlled with MATLAB Artificial Neural Network Tool.

Keywords: analysis, PID, remote controlled gun system, simulation, vehicle vibration, turret,

ÖZET

UZAKTAN KOMUTALI STABİLİZE SİLAH SİSTEMLERİNDE LİNEER OLMAYAN ETKİLERİN MODELLENMESİ

Ahmet TATAR

Yüksek Lisans, Makine Mühendisliği Bölümü

Tez danışmanı: Prof. Dr. Bora YILDIRIM

Mayıs 2018, 136 sayfa

Savunma sanayii teknolojik gelişimleriyle tüm dünyada en hızlı ilerleyen sektör konumundadır. Bugünün savaş alanlarında, otonom ve uzaktan yönlendirilebilen silahlar en gelişmiş silahlar olarak kabul görmektedir. Bu çalışmada, uzaktan komuta edilen bir silah sisteminde kullanılan yönlendirme dişlilerinin esnek davranışlarının nişan alma kararlılığı üzerindeki etkileri incelenecektir. Malzeme esnekliğini inceleyebilmek için taret sistemi ANSYS yazılımında modellenerek maksimum hareket açıklıklarındaki rijit ve esnek durum için kıyas yapılacaktır. Ardından sistemin gerçek koşullar altındaki davranışlarını inceleyebilmek için yedi serbestlik dereceli dört lastik tekerlekli ve dokuz serbestlik dereceli altı lastik tekerlekli aracın düşey dinamik etkileri MATLAB yazılımında benzetim edilecektir. Taret sistemi araçlar üzerine entegre edilerek, araçlar belirlenen engeller üzerinden geçerken PID kontrolcü ile stabilizasyon sağlanacaktır. Çalışmanın son adımında ANSYS yazılımında modellenen taret ile MATLAB yazılımında modellenen araçlar, MATLAB programı üzerinden haberleştirilerek benzetim yapılacaktır. Kurulan bu ANSYS bütünleşik MATLAB algoritması ile sistemin gerçek bir araç üzerindeki davranışları incelenecektir. Taret üzerinde oluşan araç titreşiminden kaynaklı pozisyon bozulmaları MATLAB'in yapay sinir ağları (Artificial Neural Network) ile kontrol edilerek, algoritmaya yapay zeka eklenecektir.

Anahtar Kelimeler : analiz, araç titreşimleri, PID, simülasyon, taret, Uzaktan Komutalı Silah Sistemleri

ACKNOWLEDGMENTS

Firstly, I express my sincere appreciation to my supervisor Prof. Dr. Bora YILDIRIM for his valuable commands and helpfulness.

I would like to thank to Lecturer Dr. Can Ulaş DOĞRUER for his valuable comments and helpfulness.

I would like to thank to Ceren ÖZCAN for her great support for this study and my life.

Finally, many thanks to my chief engineer Özgür DOĞAN for valuable support and positive approach.

TABLE OF CONTENT

Pages

LIST OF TABLES

LIST OF FIGURES

NOMENCLATURE

α	: elevation angle of the weapon
Θ	: azimuth angle of the weapon
ω	: roll angle
λ	: pitch angle
δz	: displacement of turret on z-axis
T	: kinetical energy
x_i	: particle coordinate
$\dot{x}_i$	: velocity on x direction
$\ddot{x}_i$	: acceleration on x direction
V	: potential energy
F_i	: acting force on the particle
p_i	: momentum
L	: Lagrangian
Q	: damping energy
A,B,C,D, E,F	: body-suspension system contact points
$c, c_1, c_2, c_3, c_4, c_5, c_6, c_7, c_8, c_9, c_{10}, c_{11}, c_{12}$	: damping coefficients
J_Θ , J_α	: moment of inertias
$k, k_1, k_2, k_3, k_4, k_5, k_6, k_7, k_8, k_9, k_{10}, k_{11}, k_{12}$	: stiffness coefficients
$K, K', L_W, L, L_1, L_2, L_3, L_4, L_5, L_6, L_7$	: distances
$m, m_1, m_2, m_3, m_4, m_5, m_6, m_7$	: masses
$x_1, x_2, x_3, x_4, x_5, x_6, x_7, \Theta, \alpha$	: vibration amplitudes
$x_A, x_B, x_C, x_D, x_E, x_F$	: position points
$x_{y1}, x_{y2}, x_{y3}, x_{y4}, x_{y5}, x_{y6}$	: track amplitudes
A', B, C, C', D, D'	: last positions of the muzzle end
XA, XA',XB, XC, XC'	: last position of muzzle end at x-axis

YA, YA’, YB, YC, YC’, YD, YD’	: last position of muzzle end at y-axis
ZA, ZA’ ZB, ZC, ZC’, ZD, ZD’	: last position of muzzle end at z-axis

SYMBOLS AND ABBREVIATIONS

DOF	: Degree of freedom
PID	: Proportional-Integral-Derivative
WWI	: World War-I
WWII	: World War-II
APDL	: ANSYS Parametric Design Language
ANN	: Artificial Neural Network
APG	: Abeerden Proving Ground

1 INTRODUCTION

1.1 Background

Modern threats have contributed defense industry. Today’s warfare technic based on fighting with asymmetric elements. Countries lose their soldier especially city-wars against the enemies. Isolating the human element from the battlefield as much as possible is the main mission of the defense industry.

Nowadays, remotely controllable systems are widely using at battlefield areas. One of these systems is the Remote Controlled Gun System. This system is best advantage controlled at the protective area, inside the hull of the vehicles, ships, buildings. In this way, operator life is taken safely.

Quality of this weapons measure with the precision of the target hit. Weapon directs with a mechanism which name is a turret. Used material rigidities of the turret are very critical for target hit precision. High flexibility of the materials causes to increasing bias between weapon and target.

1.2 Motivation

Although these weapons usage increase every day, some analysis has been made on the real prototype model. Stabilization is necessary for mobile platforms as a ground vehicle, ships, and air vehicles. Some stabilization development processes of these systems carried out with real prototypes like material flexibility, the backlash of the gear and bearings. Creating a virtual model with analysis tool is benefit for cost and time of these applications. In the literature, some analysis made for similar mechanism but not fully covered these systems.

1.3 Thesis Objectives and Scope of Research

The objective of this study is creating a virtual environment for stabilization processes. Remote Controlled Gun Systems are widely used for the ground vehicle. Disturbances of the ground vehicle are affected to aiming of the turret and turret try to stabilize itself against to disturbances.

Another effect on the aiming, comes from the flexibility of the used materials. Steering of the mechanism is providing with gear systems in a turret system. In this study flexibility effects of the gears and vehicle vertical dynamics motions were investigated on target hit precision.

4 different simulation was design for simulating to the system. Firstly, 4 wheel 7 DOF and 6 wheels 9 DOF vehicles were modeled for simulating vertical dynamics effects of the

vehicle in MATLAB SIMULINK. There are two obstacle on the track, one of right and the other is left side. Vehicles are passed over these obstacles and motion characteristics was observed.

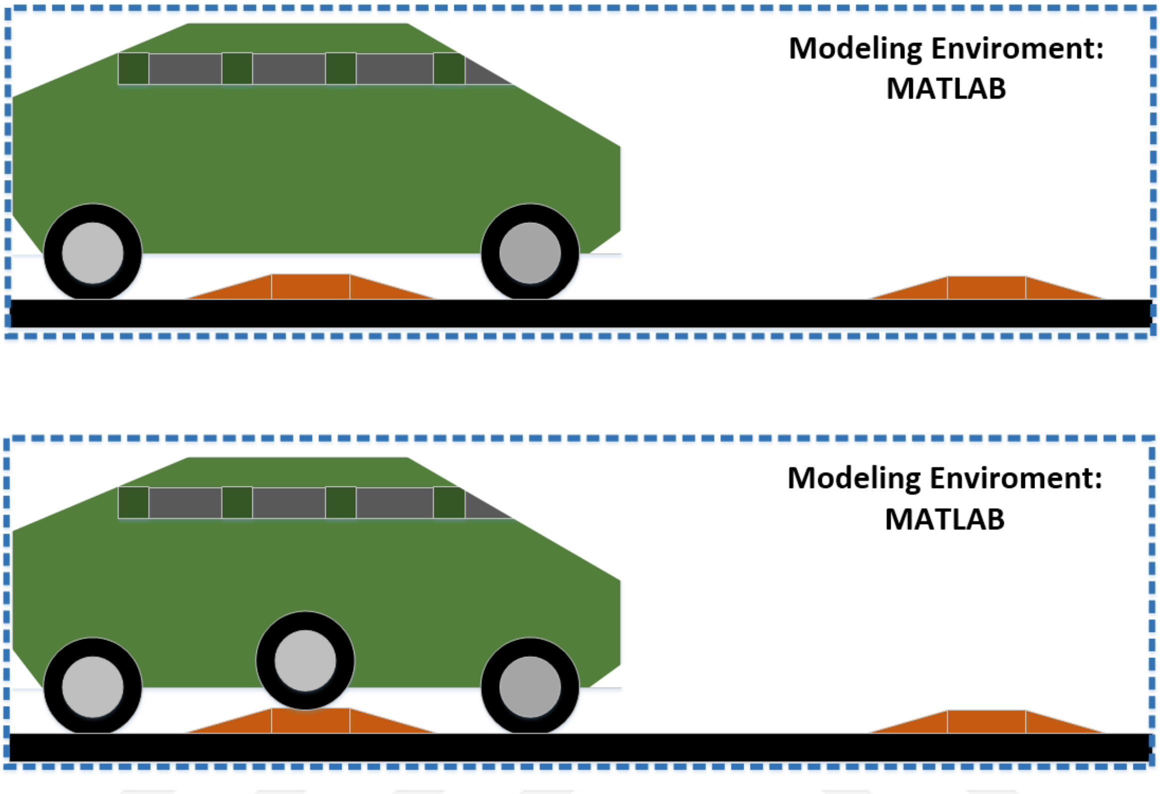

Figure 2-1 7 DOF and 9 DOF vehicles MATLAB simulations

After simulation of the vehicles, Remote Controlled Gun System (Turret system) was modeled at MATLAB SIMULINK with using SIMULINK physical blocks. Turret was installed on the 7 DOF and 9 DOF vehicles. Vehicles were passed over obstacles, and vibration profiles generated. The turret was affected by these vibration profiles and tried to stabilize itself with PID controller.

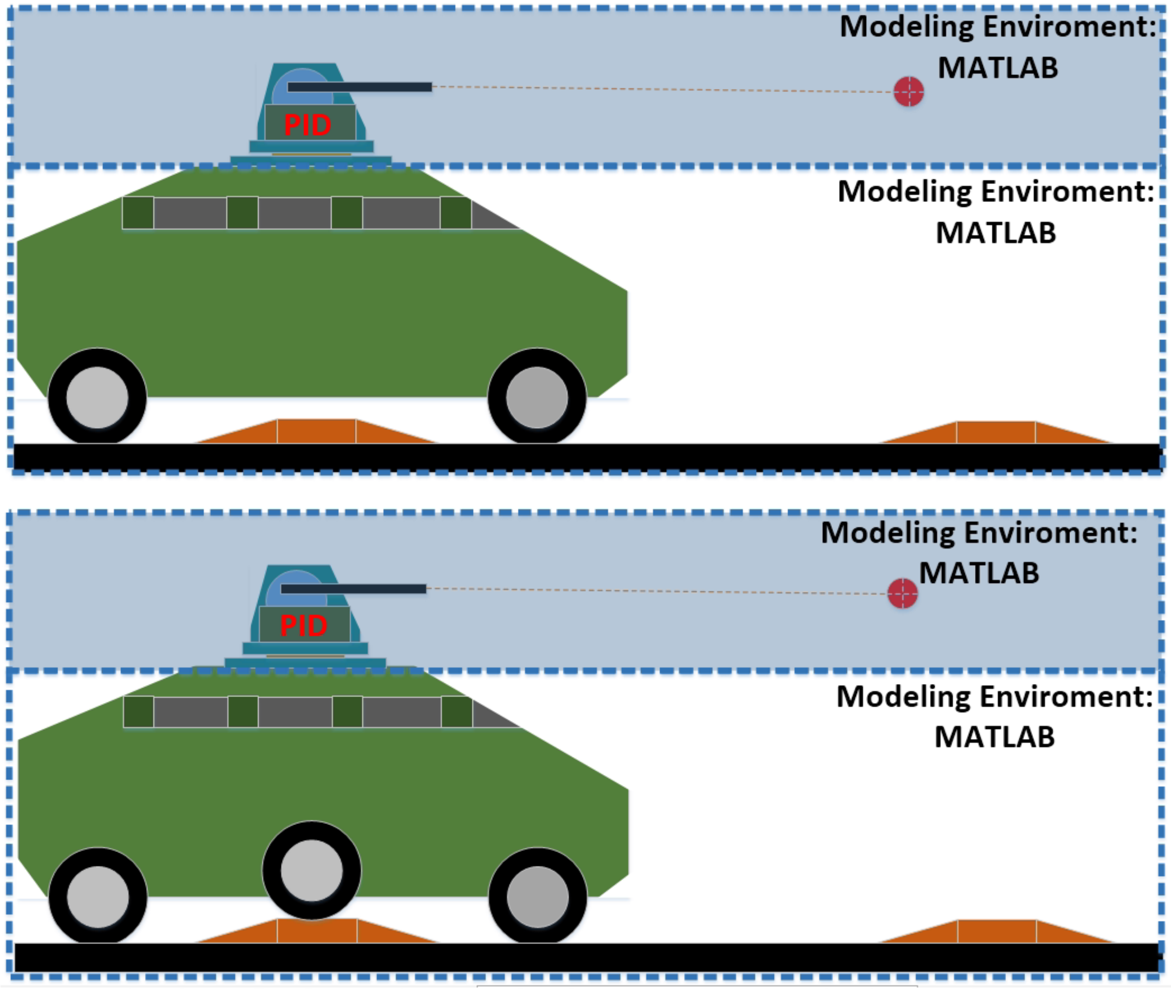

Figure 2-2 7 DOF and 9 DOF Vehicle Remote Controlled Gun System installed MATLAB simulations

System has to be moved specific acceleration and velocities. Steering of the gears are provided with gear systems. Flexibility of the gears is affected aiming precisions. For seeing flexibility effects of the system, virtual physical model of the Remote Gun System was built in ANSYS. System was analyzed under maximum motion conditions and results were compared for flexible and rigid gear conditions. Gears fatigue life was analyzed according to these conditions.

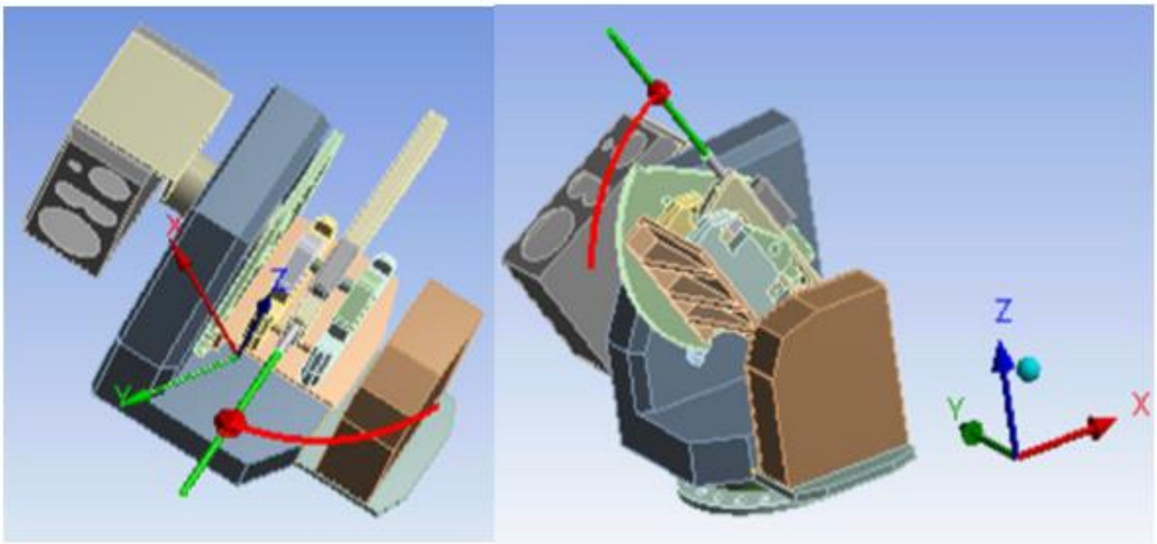

Figure 2-3 ANSYS model of the Remote Controlled Gun System Turret

At the final step, turret ANSYS model was connected with MATLAB vehicle vertical vibration model. In this step, ANSYS and MATLAB were worked integrated. According to the algorithm, MATLAB is run the vehicle models and generate the vibration profiles and run the ANSYS with generated profiles and stabilization parameters. Stabilization parameters were generated by Artificial Neural Network tool of MATLAB for this simulation.

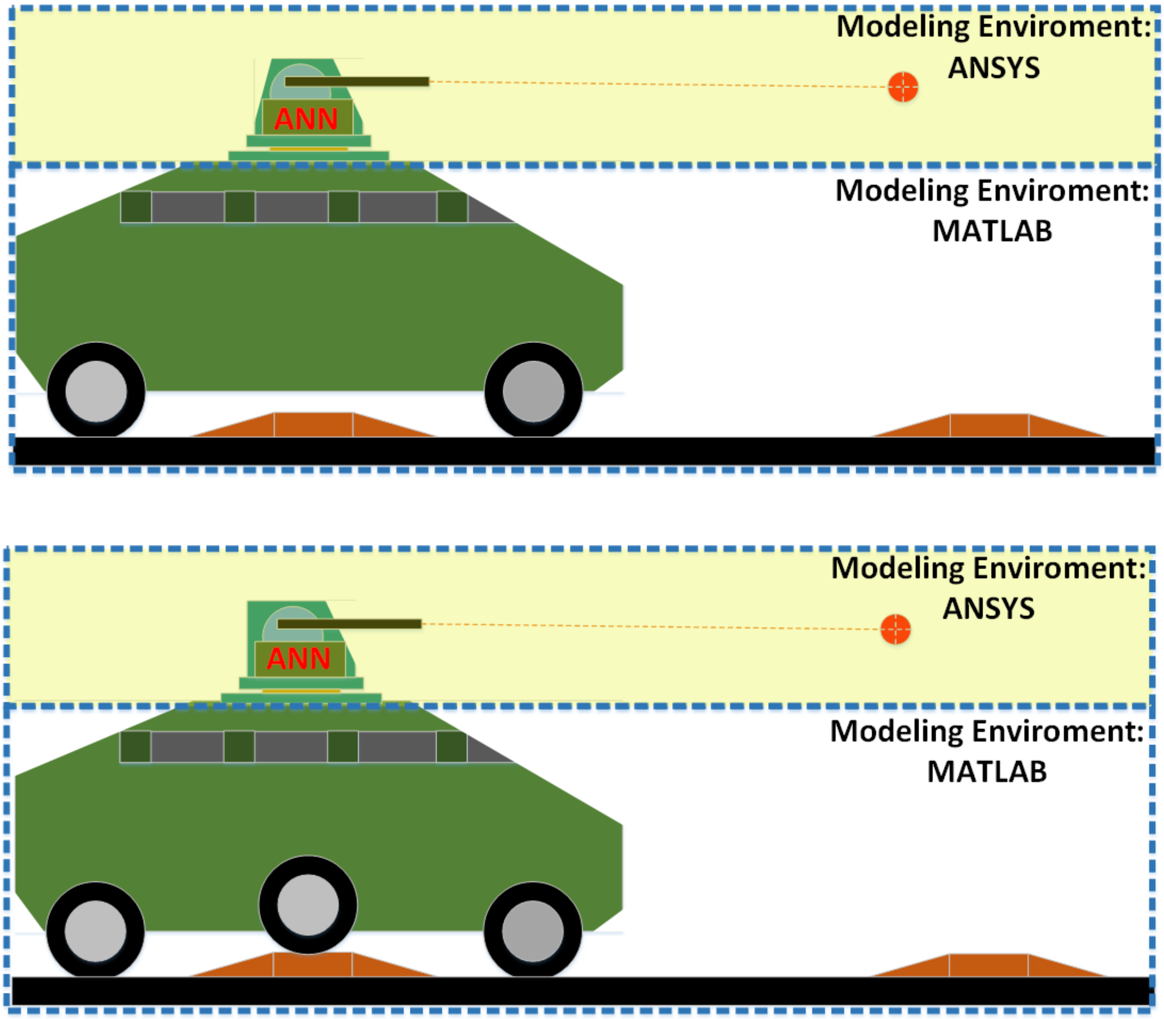

Figure 2-4 MATLAB ANSYS integrated analysis

1.4 Organization and Content Thesis

Non-linear analysis of the remote controlled gun system in this study is explained in six chapters. In the first chapter aim, scope and general information was given. Similar studies in the literature were given at the second chapter. An analytical model of the turret system, information about the vehicle dynamics, vibration equations of the vehicles, information about Artificial Neural Network were given at the third chapter. Information about creating simulation models of the vehicles and turret were given at the fourth chapter. Simulation results were given at the fifth chapter. Finally, general information about outputs and future works were given at the sixth chapter.

2 LITERATURE REVIEW

2.1 Remote Controlled Stabilized Gun System

Remote controlled gun systems are the modern element of the battlefield area. This weapon development increase with the protection of soldier life and target hit precision necessity. These systems can be integrated air, naval and ground platforms.

Figure 2-1 Application area of the remote controlled gun systems

These systems usually use on ground platforms. Attacking from ground targets include more risk than naval and air because of the ground is the living area of the humanity. Main advantageous of the system control area of the gunner is more protective than the system. Gunner decision-making ability increases with this system; because gunner is not affected from meteorological conditions, shielded position with armor in fire line, vision capabilities are developed with electro-optic systems and target hit precision is more sensitive than human capabilities. System can be mount fixed platforms, like army or police stations, or mobile platforms.

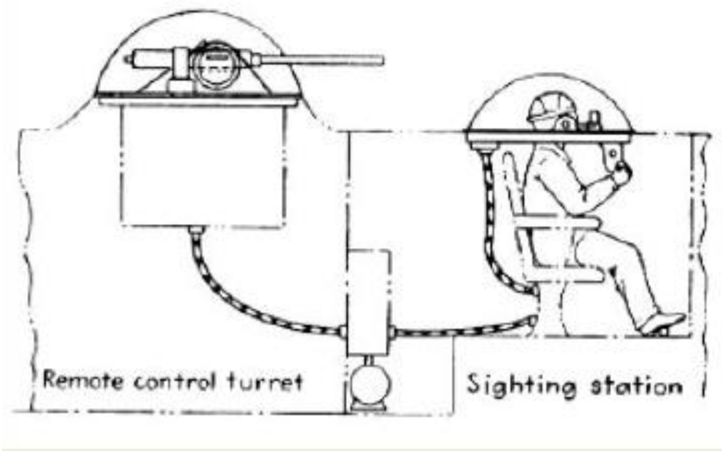

Figure 2-2 Remote controlled turret

ASELSAN INC. is one of the most successful company in this area. ASELSAN INC. has various type products which named SARP, SARP-L, SARP-DUAL, STAMP, STOP, MUHAFIZ, NEFER for wide application areas and requirements. [1]

Figure 2-3 ASELSAN remote controlled weapon systems [1]

2.2 Stabilization of Guns

A gun stabilizer is a device intended to facilitate aiming a gun by compensating for the motion of the platform on which the gun is mounted. First stabilization necessity came up for battle tanks. Development of the battle tanks based on at WWI. Primary tanks designs are rude, noisy and difficult to operate. At this stage, battle tanks fired while standing and this cause open target for the enemies. Designers worked for shorter firing time while standing. [2]

After the WWII, battle tanks were equipped with gun stabilization capability using gyroscopes for stabilization. This was a huge development for fighting machines because vehicles had fire-on-move capabilities for this innovative idea. At first generation gun stabilization, the gun is kept horizontal concerning earth and deviation from the target was only translational independently of the target distance in the azimuth axis. These caused angular and translational errors. [3]

Figure 2-4 Battle Tank [2]

The main purpose of the Weapon Control System on a Main Battle Tank is providing high hitting precision for mobile and fixed targets. This process has to realize in the shortest time and lowest iteration. At the designing stage of the tanks, designers are tried to place center of gravity at the muzzle. Conflicting center of gravity of the tank and muzzle is provided more precision stabilization. If the tank is not designed according to this, stabilization of the muzzle will be markedly reduced. [4] Complete equilibrium can only provide for a fixed muzzle on a horizontal surface. If the gun is effected externally on the muzzle elevation axis, additional mass forces on the center of gravity of the muzzle elevation motion parts cause to disturbances. These effects are valid for naval, ground and air gun systems and equilibrators are not used for these systems. For this reason, guns are mounted center of gravity of the muzzle. [5]

Equilibrators use only static system for balancing to unbalanced parts. In the dynamic case, acceleration forces of move on the center of the gravity of the elevation mass. Conventional equilibrator cannot balance the system and this cause to variable stabilization states. For preventing to this effects, conventional equilibrators are not used dynamic stabilized applications. [6]

First applications of the gun stabilization changed the rules of games in terms of the main battle tanks on the battlefields. However stabilization performance of the tanks was not enough for the single hit precisions. Tanks still have to fire a few iteration for hitting the targets. [7] Before the stabilization of the muzzle, the battle tanks fired while standing although they were mobile platforms. With muzzle stabilization, tanks become a main power of the battlefields. The first generation stabilization system was used gyroscope for each elevation and azimuth axis. The gyroscopes were detected the disturbances on the same axis. Disturbances values were used for holding that axis fixed while tanks moving. Early applications of the stabilization systems was using rate errors between the gyro feedback and command signals. For this reason, stabilization system is need to an error for its operation. [3]

Stabilization processes use for various kind of sectors. Such as movie or photography sectors are using for camera systems too for taking quality images. In the automotive sector, stabilization applies for security systems like ESC (electronic stability control) ABS (Anti-lock Braking System).

2.3 Vehicle Vibrations

1990s are the unexpected times for automotive industry and market structure. There has been large scale requests from the global scales like safer automobiles, saving environment and intelligent driving and media systems. After this time, producers were used for their product rising computer technology, simulation and artificial intelligent technologies. Automotive industry were grown with working on vehicle dynamics. Primary research on the vehicle dynamics are included operation and service conditions under external effects. [8]

Suspension system and its parameters of the vehicles depends on the producers and wide range of models. Suspension system plays an important role on vehicle dynamics. Primary duty of the suspension system is providing safer driving capability. Disturbances of the track geometry cause oscillation motion on the tire of the vehicle and this motion conduct to axle. Suspension system connect the axle to the chassis of the vehicle and regulate to the vibrations and shocks during to the motions. Suspension system has to provide good driving capability and comfortable riding at the uneven track geometry. A quality suspension system has to prevent large scale oscillations under uneven track surface. If the large scale oscillation indicate, the system has to be removed, as short as possible. The vehicle suspension has to design based on a purpose like good driving capability, comfortable or safety riding. [9]

For investigating a vehicle vertically, the number of degree of freedom can be two, nine or more. For example a vehicle can be modeled 2 DOF on the lateral and yaw axis, 3 DOF on the longitudinal, lateral and yaw axis, and 4 DOF longitudinal, lateral, yaw, roll axis. 2 DOF (quarter) vehicle model mostly use for while lateral acceleration is less than 0.3g. [8]

2 DOF (quarter) vehicle model uses for independent axle suspension systems. Rear or front axle of the vehicle can be modeled with this model because each axle vibrate independently. The quarter vehicle model is the simplest one dimensional model. This model is used for designing active and semi-active suspension system. A vehicle can be analyze on three dimensional axis with using lumped mass model. Model can be 7, 8 or more degree of freedom. Heave, pitch and roll motions can be observed with lumped mass model. Cebon built a three dimensional vehicle model with 14 DOF. This model include longitudinal and lateral tire forces and non-linear suspension system. [10]

3 THEORY

In this chapter; turret analytic models were explained with equations for fixed and mobile platforms. This work scope on the observing motion characteristics of the turret while installed a vertically modeled ground vehicle. Therefore; basic ground vehicle vibration model were investigated. Turret was stabilized with using Artificial Neural Network at ANSYS integrated MATLAB analysis. Theory and development of the Artificial Neural Network were explained.

3.1 ANALYTICAL MODEL OF THE TURRET SYSTEM

Turret system has 2 Degree of Freedom. One of elevation axis for controlling the weapon high (rotation around X'-axis), the other one is azimuth axis for controlling the direction of the weapon (rotation on Z-axis). The weapon can be rotated along the elevation axis in the limits of upper and lower stroke. However there is no limit on azimuth axis, the weapon can be turned endless.

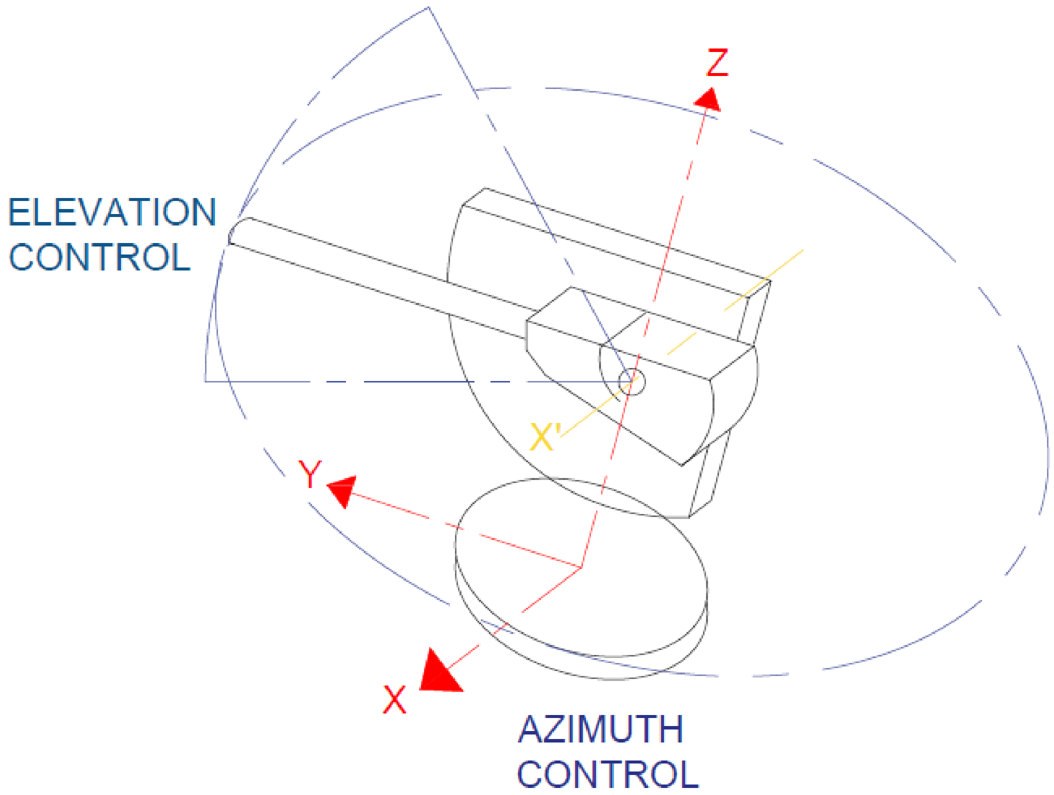

Figure 3-1 Motion characteristics of the turret system

Turret system works for directing to weapon muzzle and electro-optic vision systems in the right position.

Whole calculations were made for muzzle endpoint of the weapon. If we scan the weapon muzzle endpoint (represented with A) motion in the space, we can observe trajectories which is given in Figure 3-2.

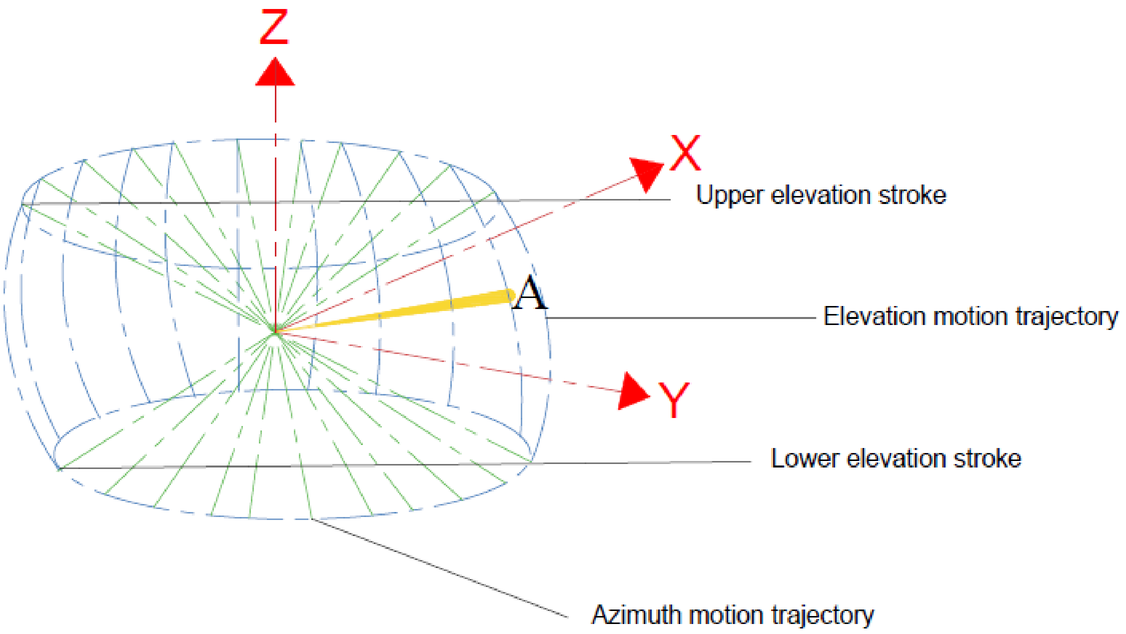

Figure 3-2 Trajectories of the motion of weapon

Turret systems can be installed mobile and fixed platforms. The main difference between fixed and mobile platforms is the stabilization necessity. There is no stabilization requirement for the fixed platforms.

3.1.1 Fixed Platform Model

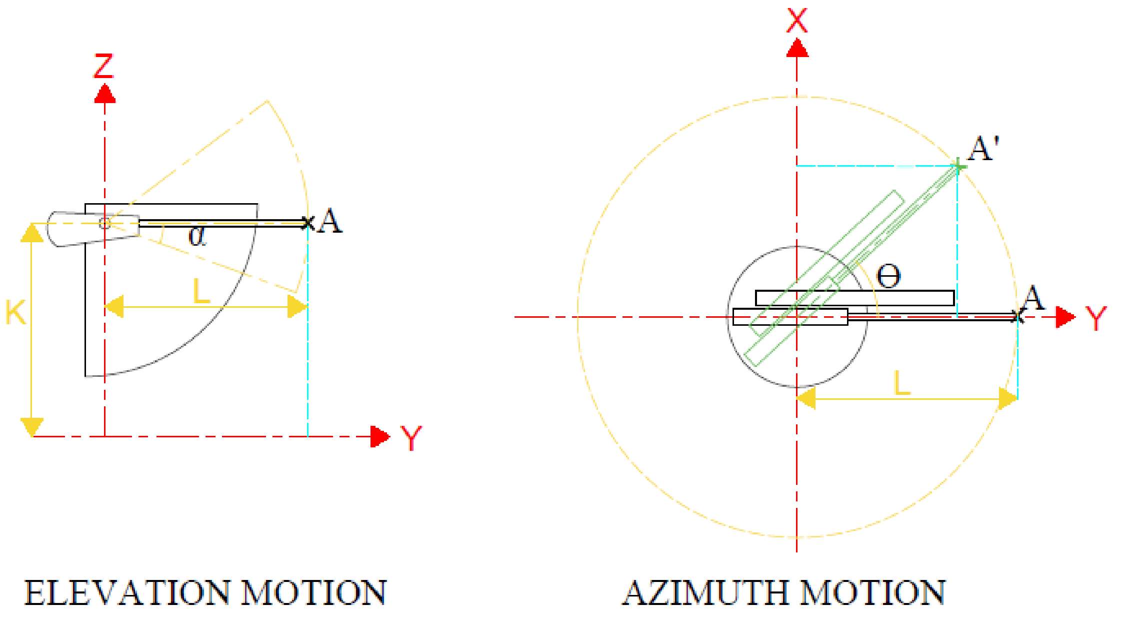

Figure 3-3 Motion of endpoint for fixed platforms

In the fixed platform conditions, equations can be written for the muzzle end as follows,

A : first position of the muzzle end

A’ : last position of the muzzle end

XA’ : last position of muzzle end at x-axis

YA’ : last position of muzzle end at y-axis

ZA’ : last position of muzzle end at z-axis

α : elevation angle of the weapon

ϴ : azimuth angle of the weapon

L_w : length of the muzzle from muzzle-end to rotation point of the elevation axis

K : high of the rotation point of the elevation axis at z-axis

We can define the position of A’ according to Cartesian coordinate system,

$$XA' = L_w cos(\alpha)\sin(\Theta) \quad (3.1)$$

$$YA' = L_w cos(\alpha)\cos(\Theta) \quad (3.2)$$

$$ZA' = K + L_w sin(\Theta) \quad (3.3)$$

3.1.2 Mobile Platform Model

The turret is affected by the motions of mobile platforms. The system can be installed ground, navy and air platforms. Dynamics of each platform are different. Navy and air platforms are out of scope for this study.

Ground platform dynamics investigate under three main title; lateral, longitudinal and vertical dynamic. In this scope, the system analyzes for only vertical dynamic conditions.

A ground vehicle makes three different movements in the vertical dynamics, roll, pitch and heaves on the z-axis. Turret affects these three motions and stabilizes itself according to the target position.

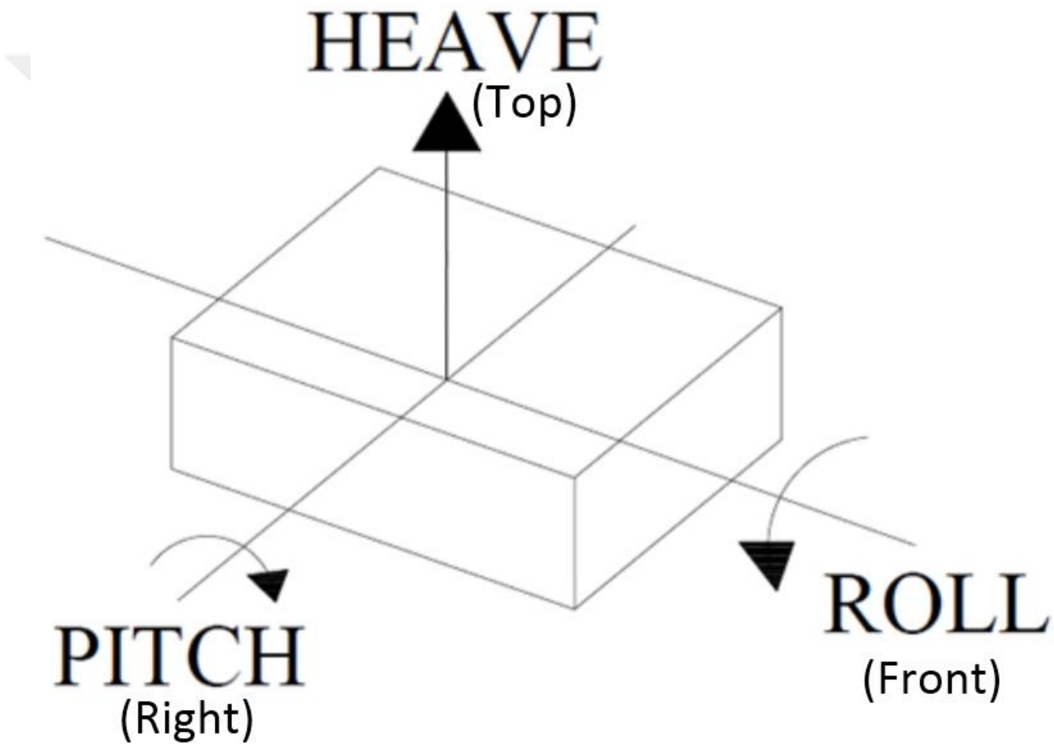

Figure 3-4 Motion of the vehicle in the vertical dynamic

3.1.2.1 Roll Motion Model

Vehicle rotates to around the y-axis at the roll motion. This part was investigated under two states, stabilization is passive, and stabilization is active.

While stabilization is passive;

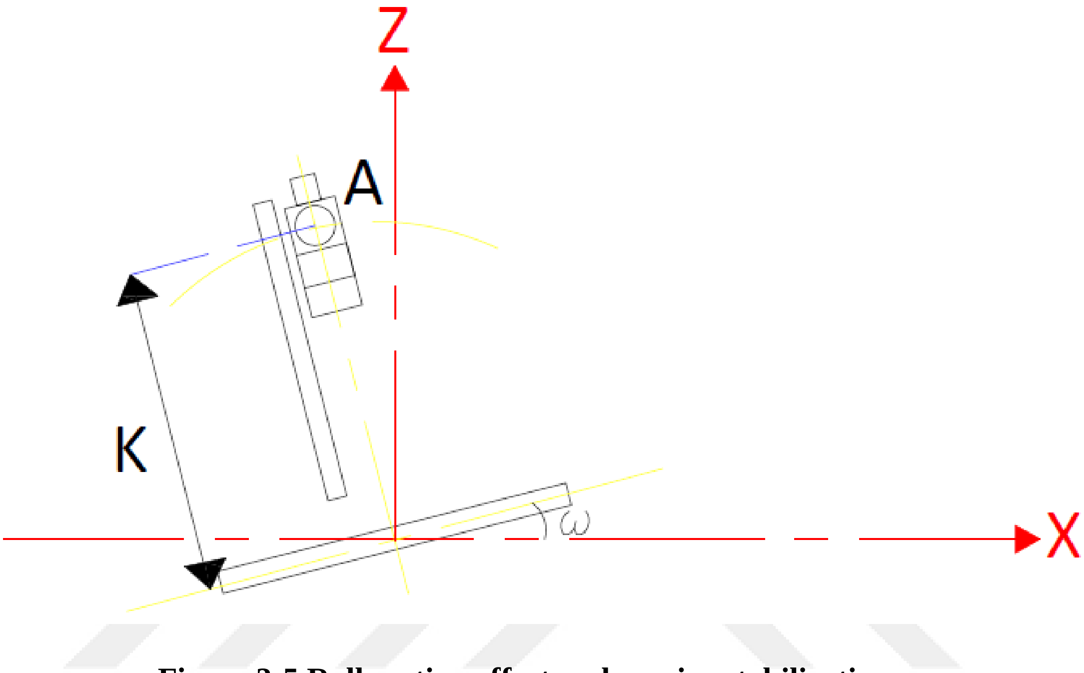

Figure 3-5 Roll motion effect and passive stabilization

A : muzzle end of the weapon

XA : position of muzzle end at x-axis

YA : position of muzzle end at y-axis

ZA : position of muzzle end at z-axis

ω : roll angle

L : distance of the target

L_w : length of the muzzle from muzzle-end to rotation point of the elevation axis

K : high of the rotation point of the elevation axis at z-axis

K' : muzzle end of the weapon after stabilization

Θ : azimuth angle of the weapon

α : elevation angle of the weapon

We can define the position of A according to Cartesian coordinate system,

$$XA = K'sin(\omega)\sin(\Theta) \qquad (3.4)$$

$$YA = \mathrm{L}_w\cos(\alpha)$$

$$ZA = K'cos(\omega)\cos(\Theta) \qquad (3.5)$$

$$K' = K + \mathrm{L}_w\sin(\alpha) \qquad (3.6)$$

While stabilization is active, system compensates for rolling effect with α and ϴ control angle;

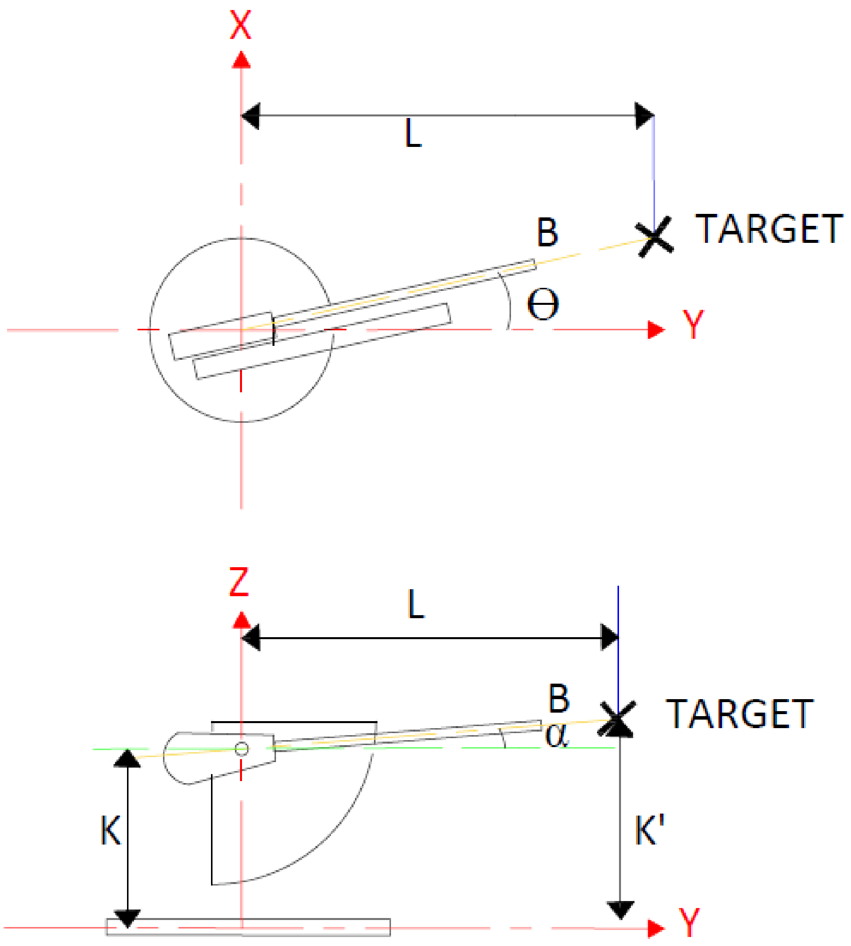

Figure 3-6 Roll angle correction

B : muzzle end of the weapon for roll angle

XB : position of muzzle end at x-axis

YB : position of muzzle end at y-axis

ZB : position of muzzle end at z-axis

K : high of the rotation point of the elevation axis at z-axis

K' : muzzle end of the weapon after stabilization

L : distance of the target

L_w : length of the muzzle from muzzle-end to rotation point of the elevation axis

α : elevation angle of the weapon

Ɵ : azimuth angle of the weapon

We can define the position of B according to Cartesian coordinate system,

$$\Theta = \arctan\left[\frac{K'\tan(\omega)]}{\mathrm{L}}\right] \tag{3.7}$$

$$\alpha = \arctan\left[\frac{K'(1 - cos(\omega))}{\mathrm{L}}\right] \tag{3.8}$$

$$XB = L_w \sin\left[\arctan\left[\frac{K'\tan(\omega)}{\mathrm{L}}\right]\right] \cos\left[\arctan\left[\frac{K'(1 - cos(\omega))}{\mathrm{L}}\right]\right] \tag{3.9}$$

$$YB = L_w \cos\left[\arctan\left[\frac{K'\tan(\omega)}{\mathrm{L}}\right]\right] \cos\left[\arctan\left[\frac{K'(1 - cos(\omega))}{\mathrm{L}}\right]\right] \tag{3.10}$$

$$ZB = \left[K + L_w \sin\left[\arctan\left[\frac{K'(1 - cos(\omega))}{\mathrm{L}}\right]\right]\right] cos(\omega) \tag{3.11}$$

$$K' = K + \mathrm{L}_w \sin\left[\arctan\left[\frac{K'(1 - cos(\omega))}{\mathrm{L}}\right]\right] \tag{3.12}$$

3.1.2.2 Pitch Motion Model

Vehicle rotates to turret around the x-axis at the pitch angle motion.

While stabilization is passive;

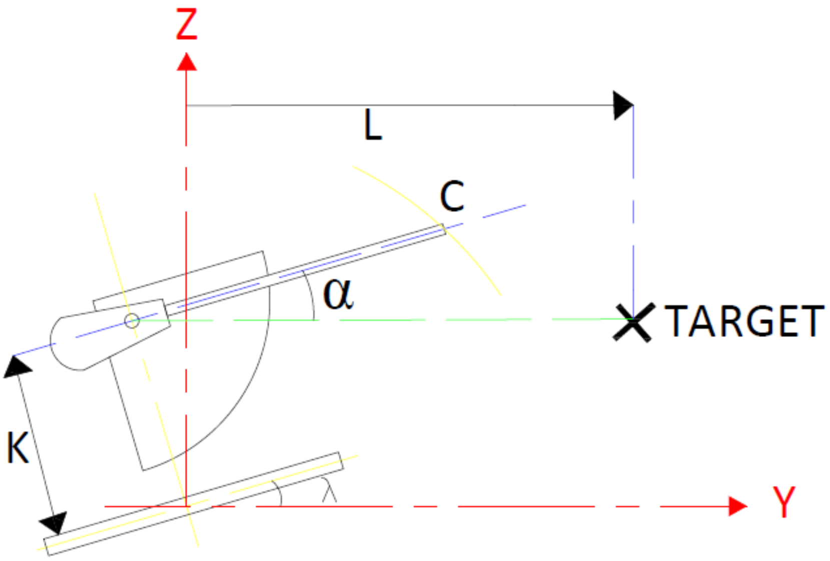

Figure 3-7 Pitch angle motion effect and passive stabilization

C : muzzle end of the weapon for pitch angle

XC : position of muzzle end at x-axis

YC : position of muzzle end at y-axis

ZC : position of muzzle end at z-axis

K : high of the rotation point of the elevation axis at z-axis

L : distance of the target

L_w : length of the muzzle from muzzle-end to rotation point of the elevation axis

α : elevation angle of the weapon

Ө : azimuth angle of the weapon

λ : Pitch angle

We can define the position of C according to Cartesian coordinate system,

$$YC = (L_w - Kcos(\lambda))cos(\lambda) \quad (3.13)$$

$$ZC = Kcos(\lambda) + Ksin(\lambda)tan(\lambda) + (L_w - Kcos(\lambda)sin(\lambda) \quad (3.14)$$

While stabilization is active, system tries to compensate pitch effect only with α control angle;

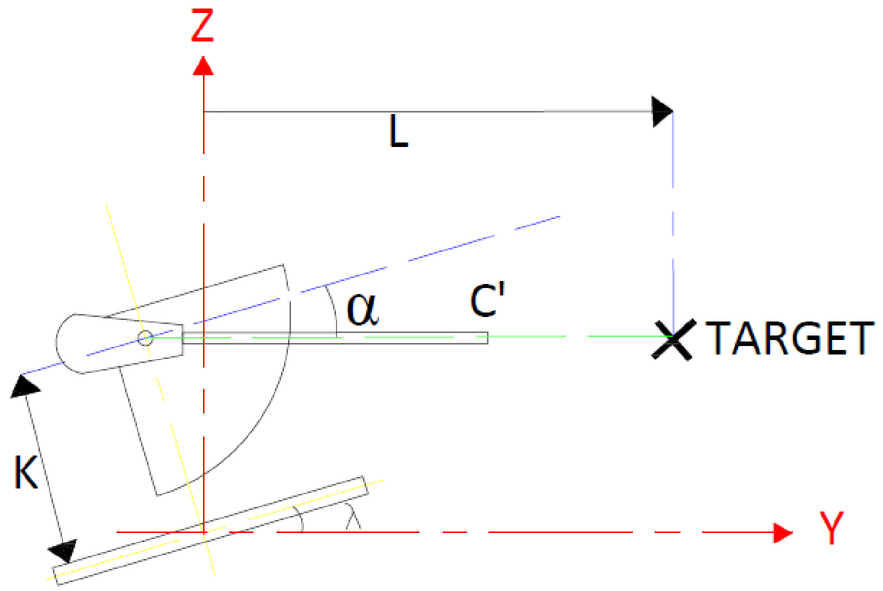

Figure 3-8 Pitch angle motion effect after stabilization

C’ : muzzle end of the weapon for pitch angle after stabilization

XC’ : position of muzzle end at x-axis

YC’ : position of muzzle end at y-axis

ZC’ : position of muzzle end at z-axis

L_w : length of the muzzle from muzzle-end to rotation point of the elevation axis

λ : Pitch angle

We can define the position of C’ according to Cartesian coordinate system,

$$YC' = L_w - Ksin(\lambda) \tag{3.15}$$

$$ZC' = Kcos(\lambda) \tag{3.16}$$

$$\alpha = -\lambda \tag{3.17}$$

3.1.2.3 Heave Motion Model

Heave motion of the vehicle moves at the z-axis.

While stabilization is passive;

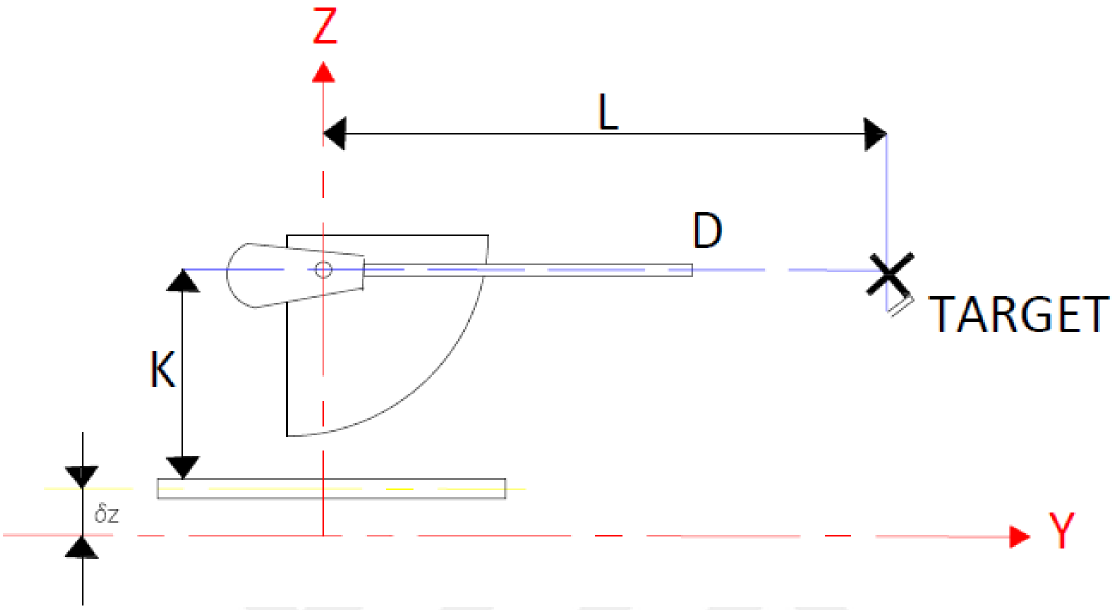

Figure 3-9 Heave motion effect and passive stabilization

D : muzzle end of the weapon for heave motion

YD : position of muzzle end at y-axis

ZD : position of muzzle end at z-axis

K : high of the rotation point of the elevation axis at z-axis

L : distance of the target

L_w : length of the muzzle from muzzle-end to rotation point of the elevation axis

α : elevation angle of the weapon

δz : displacement of turret on z-axis

We can define the position of D according to Cartesian coordinate system,

$$\alpha = \arctan\left[\frac{K'(1 - cos(\omega))}{\mathrm{L}}\right] \quad (3.18)$$

$$ZD = K + \delta z - Lsin(\alpha) \quad (3.19)$$

$$\alpha = \arctan\left[\frac{\delta z}{L}\right] \tag{3.20}$$

While stabilization is active, system tries to compensate heave effect only α control angle;

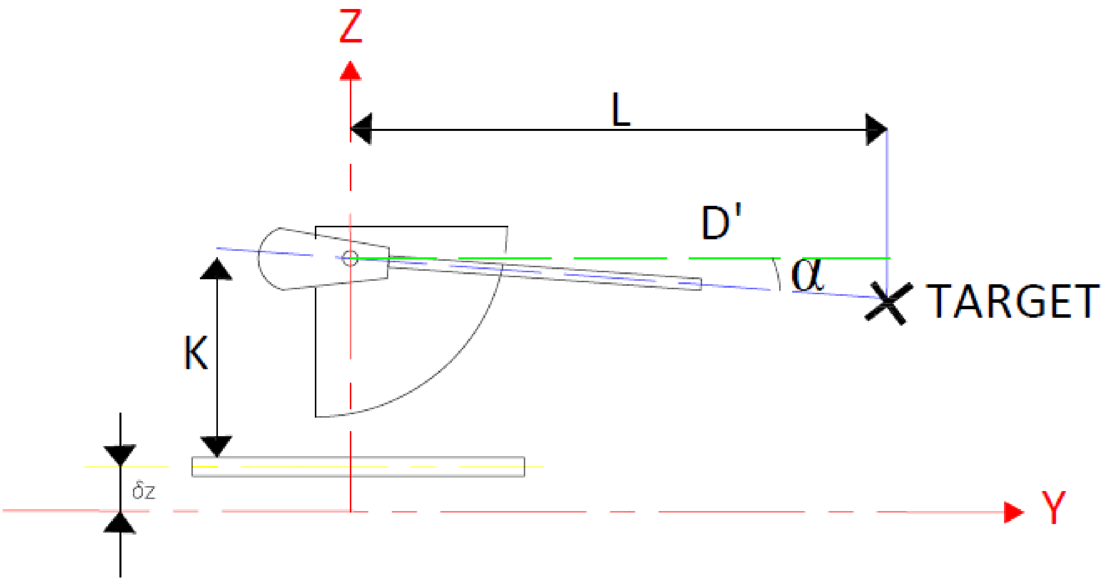

Figure 3-10 Heave motion effect after stabilization

heave deflection on the turret corrects with elevation axis.

D' : muzzle end of the weapon for heave motion after stabilization

ZD' : position of muzzle end at z-axis

L_w : length of the muzzle from muzzle-end to rotation point of the elevation axis

α : elevation angle of the weapon

K : high of the rotation point of the elevation axis at z-axis

δz : displacement of the turret on the z-axis

We can define the position of D' according to Cartesian coordinate system,

$$YD' = L_w cos(\alpha) \tag{3.21}$$

$$ZD' = K + \delta z - L_w sin(\alpha) \tag{3.22}$$

3.1.2.4 Total Motion Control Equations

All vertical motions effect can be described on elevation and azimuth axis as following equations;

$$\alpha = \arctan\left[\frac{K'(1 - cos(\omega))}{\mathrm{L}}\right] + \arctan\left[\frac{\delta z}{L}\right] - \lambda \qquad (3.23)$$

$$\Theta = \arctan\left[\frac{K'\tan(\omega)}{\mathrm{L}}\right] \qquad (3.24)$$

$$K' = K + L_w \sin(\alpha) \qquad (3.25)$$

3.2 Modeling the Vehicles

3.2.1 Basic Vehicle Dynamics

The vehicle can affect various kind of effect during to movement both environmental and internally. The vehicle is exposed to many kinds of forces during the motion and can be investigated at the vertical, lateral and longitudinal axis.

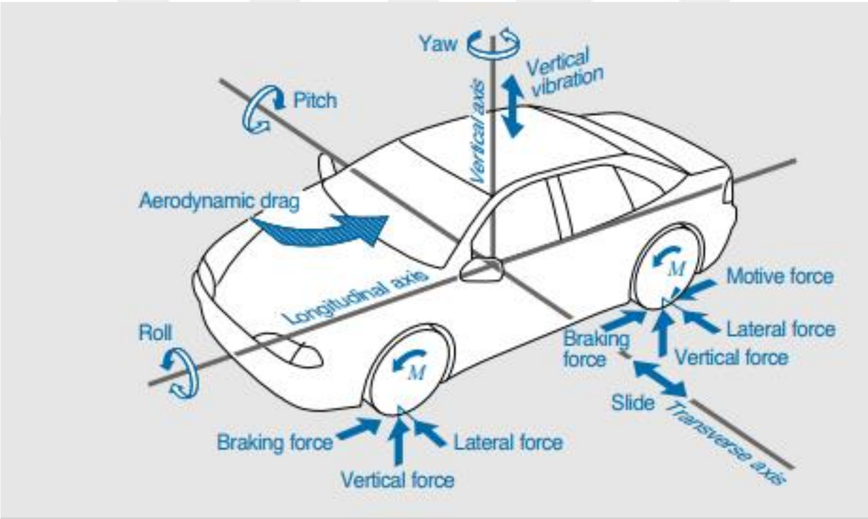

Figure 3-11 Acting forces of a vehicle [11]

3.2.1.1 Longitudinal dynamics of the vehicle

The system can be investigated under three main effects in longitudinal dynamics, inertia, the slope of the road and aerodynamic.

Newton's first law of motion states that "an object at rest stays at rest and an object in motion stays in motion with same speed and the same direction unless acted upon by an unbalanced force." Simply, objects tend to keep on doing what they are doing. This resistance to changes calls inertia. Like every physical object, there is inertia of the vehicles also. Acceleration, cornering, braking and other motions are affected by inertia.

The slope of the road is another lateral force effect. If vehicle move on a positive slope road conditions, sinus function of the road slope and mass of the vehicle act the backward direction of the vehicle and keeping the moving vehicle has to defeat this force.

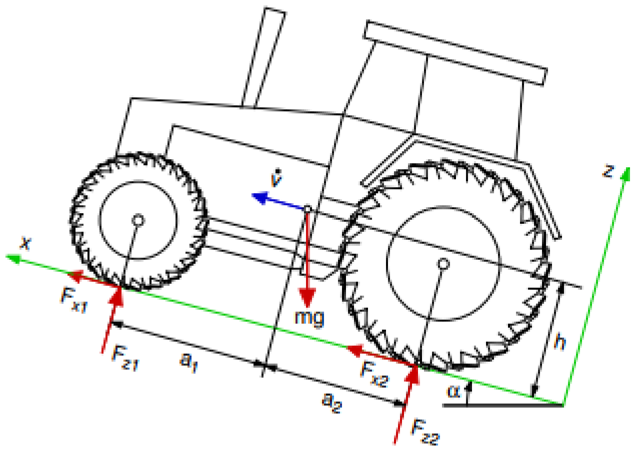

Figure 3-12 Slope resistance [12]

Another longitudinal effect is aerodynamic. The shape of the vehicle is significant for aerodynamic forces. Fluid on the car produces resistance force and torques. This winding effect can be used for positively like “down-forces” act on the rear and front axle and increase the dynamic driving conditions.

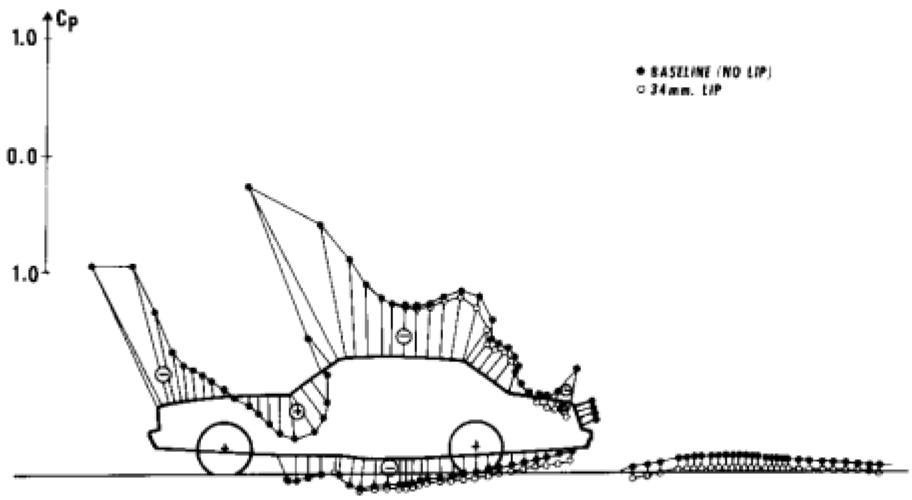

Figure 3-13 Pressure distribution on a vehicle [13]

3.2.1.2 Lateral dynamics of the vehicle

Lateral forces acting on a vehicle, while vehicle turning, centrifugal forces act depends on velocity, mass, of vehicle friction and radius of the road. Centrifugal forces changes to rolling and pitch angle because of the stiffness of the suspension systems and tires this cause to change pitch and yaw angles. Turning process is a complex state and controlled electronic systems today's vehicles. Design of the suspension, steering, and powertrain systems are very critical for lateral dynamic stabilizations.

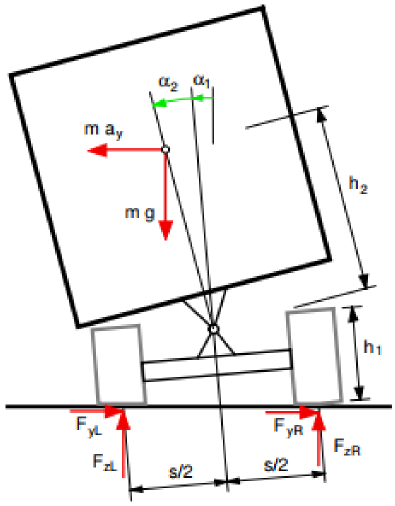

Figure 3-14 Lateral forces on a vehicle [12]

Tire and road relation is also critical for lateral forces. The shape of tires can be changed while vehicle cornering. Distortions of the tires change friction surface and stiffness of the tire. Various non-linear effects can be observed during this motion.

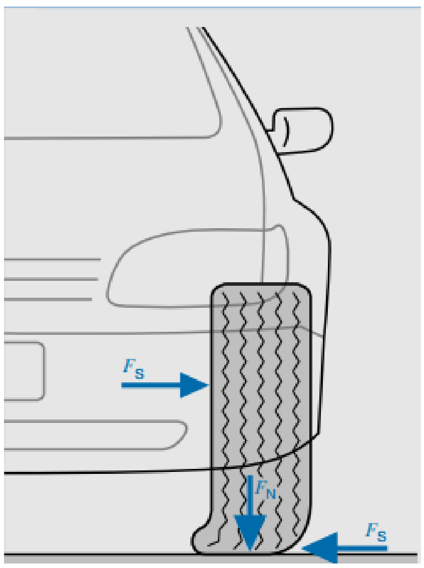

Figure 3-15 Lateral forces on tire [11]

3.2.1.3 Vertical dynamics of the vehicle

In this scope, turret motions were investigated under vertical dynamic conditions so that this subject was discussed in full details.

Vertical dynamics of the vehicles focus on the comfortable and safe riding capability. The aim of the researches arranging to the spring and damping constants and reducing the stresses which act on the vehicle body. Comfortable driving is determined by driver. There are many kind of searches of the human sense under the vehicle vibration effects. Body accelerations on the car are sensed by driver. For comfortable driving vibration amplitudes has to between specific values. Designers measure the vehicle vibrations and amplitudes and judged their design objective criteria in practice. [12]. The main component of the vertical dynamics is tire and suspension systems. Each components were investigated separate heading.

3.2.1.3.1 Tires

Motion begins with tires on the vehicle. Tires provide contact between vehicle and road. For safety journey tires and road, relationships are significant. Tires conduct the motion, breaking, acceleration and other lateral forces on the road. Also be effected vertical forces because of the road topography, roughness lateral and longitudinal forces. Tires have to be stable running ability, compatible with weather and different road conditions, good steering capacity and ride comfort. There are many kinds of tire types nowadays, and radial tires are the most comprehensive used.

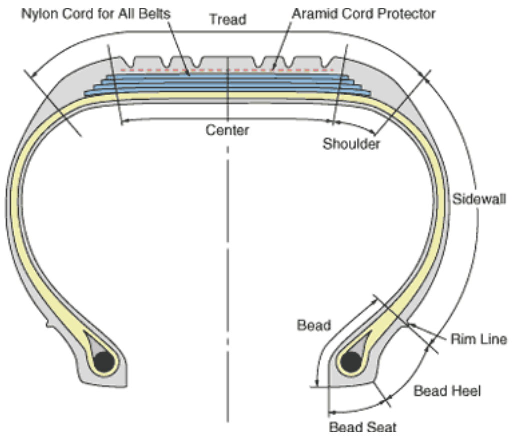

Figure 3-16 Structure of the radial tire [11]

There is some kind of non-uniformities because of imbalanced mass, dimensional variations, and stiffness variations. These non-uniformities effect on vertical dynamics of the vehicle.

Imbalances forces affect driving comfort and strength of the structural parts of the vehicle. The imbalance force is given by the equation;

$$Fi = mr\omega_t^2 \tag{3.26}$$

F_i : imbalance force

m : imbalance mass

r : radius

ω_t : wheel rotational velocity

A non-uniform and asymmetric mass distribution along the axis of rotation causes dynamic imbalance. Dynamic imbalance creates a rotating torque on the wheel, appearing as variations in overhunting moment and aligning torque at the wheel rotational frequency. The dynamic imbalance is most important on steered wheels which may experience steering vibrations as a result of the excitation. Static imbalance can exist in the absence of dynamic imbalance. The tires, wheels, hubs and brake drums may all contribute to imbalance effects, [13].

The tire can be modeled like a radial spring because of its elastic structure. This physical approach provides us a mathematical model of tire. Tire changes its shape under load, and this called loaded radial run out. Unloaded states call free radial run out. If vehicle gravitational force divided by difference between loaded and free radial run out, stiffness coefficient of the tire can be found.

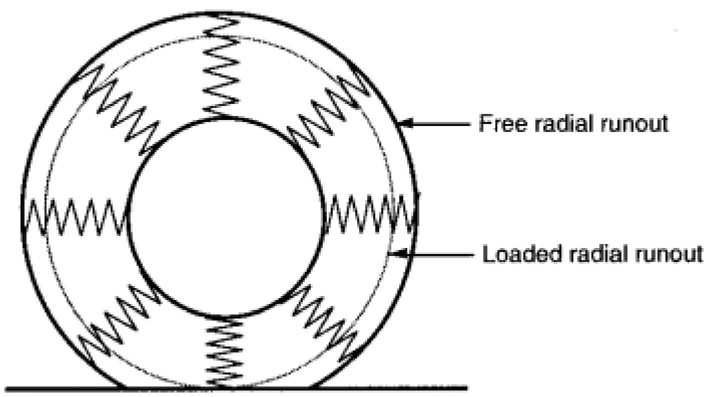

Figure 3-17 Tire radial spring model [13]

The stiffness of tire depends on used materials in the tire and fluid inflation pressure. When the inflation pressure increase, the tire will be getting stiffer.

Pressure 1.3bar		
Load kg	Def. mm	Stiffness N/mm
300	17.8	165.33
400	24.6	159.51
500	31.7	154.73
600	38.5	152.88
700	44.4	154.66
800	49	160.16

Pressure 1.7 bar		
Load kg	Def. mm	Stiffness N/mm
300	15.7	187.45
400	21.9	179.17
500	28.44	172.46
600	34.4	171.10
700	39.7	172.97
800	42.3	185.53

Pressure 2 bar		
Load kg	Def. mm	Stiffness N/mm
300	14.8	198.85
400	20.1	195.22
500	27.6	177.71
600	31.09	189.32
700	36.04	190.53
800	40.05	195.95

Pressure 2.4bar		
Load kg	Def. mm	Stiffness N/mm
300	14	210.21
400	20	196.2
500	26	188.65
600	30.5	192.98
700	34.9	196.76
800	38.3	204.90

Pressure 2.7bar		
Load kg	Def. mm	Stiffness N/mm
300	12.72	231.36
400	18.34	213.95
500	24.02	204.20
600	28.84	204.09
700	33.7	203.76
800	37.1	211.53

Figure 3-18 Inflation pressure-deflection changes [14]

Under real conditions, tire stiffness changes each angle of the tire during to motion. The road surface is not perfectly flat; it has macro and micro-roughness. These roughness cause accelerations on the tire, so acting force in the stiffness equation always changes. The same scene can be observed breaking phase of the vehicle. However, these conditions are ignored because of simplifying the calculation.

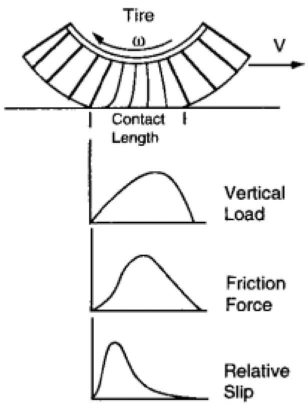

Figure 3-19 Breaking deformation of the contact surface [13]

Damping coefficient of the tires depends on same conditions of the stiffness. Inflation pressure, load value and material of the tire effects damping.

Modeling the contact between road and tire is also another important problem. Road and tire contact assumes as the point. This model mostly used for dynamic analysis of the vehicles.

For evaluating this model Kyongsu used road surface which is being a six sinusoidal waves and found to tire force. Finally calculated tire force was found close to the real case [12]. Other studies in the literature show that point contact is the realistic approach and there is no significant difference between other approaches. Besides, the point contact model between road and tire is used for only the vertical dynamic analysis.

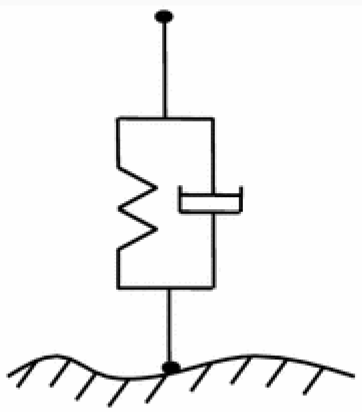

Figure 3-20 Single-point contact between tire and road [8]

3.2.1.3.2 Suspension System

The first known suspension system was used at the cart of Tutankhamon the Pharaoh at 1350 BC. Thick leathers were cut in strips and integrated between wheel and chassis. In this way travel on the cart was being gotten more comfortable.

The usage of metal springs has begun end of the 16th century. However, these springs were used widely at the beginning of 18th century. The structure of this primitive spring system is that metal sheets were cut constant width but different length. Each sheet was bent with a specific radius and located shortest one is upper longest one is lower of the system. The longest sheets were connected to the chassis of the vehicle. Thus, the vibration was being reduced highly.

Constructing spring was being first usage area of the rubber. H.C. Lacy took a patent for producing rubber spring for a vehicle at the Manchester City, England in 1826. Rubber springs were being begun to seeing since 1845.

Helical springs were seen firstly in the middle of the 18th century. These springs are being used various kinds of area. In 1950, French car producer Citroen developed hydraulic suspension system. The system includes nitrogen gas being a vibration absorber.

The primary properties of a suspension are in the kinematic motion behavior and its response to forces and moments. Suspension system transmits these effects from tires to chassis. Suspension system can be seen in a two main group, solid axle, and independent angle.

Wheels are mounted on a rigid beam in the solid axle. Any effect on a tire will be transmitted the opposite. Solid axle is seen the rear of many cars any also commonly used for the front of the heavy vehicles.

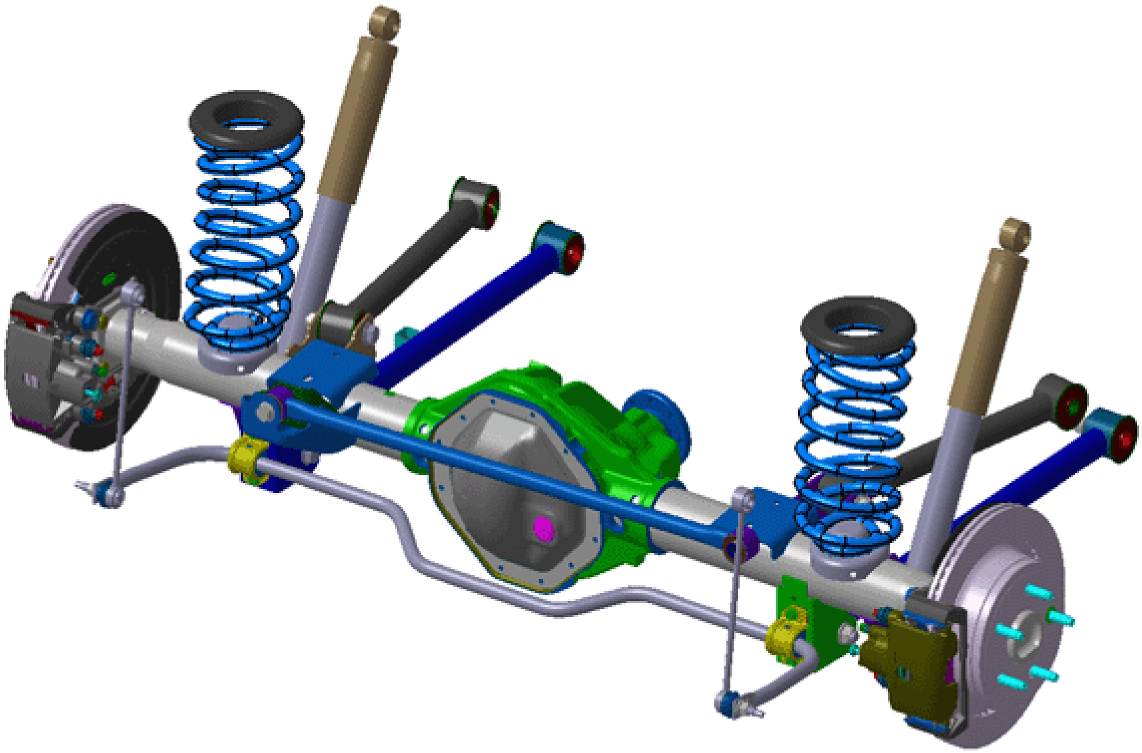

Figure 3-21 Solid axle [15]

Independent suspension allows for each vertical wheel movement independently. Wheels are not affected by opposites. Today’s most of the cars and light vehicles use independent suspensions because of the low volume requirement. Further advantages of the independent suspension are higher roll stiffness according to vertical spring rate.

Figure 3-22 Independent Suspension [15]

Main parts of suspension systems are spring and dampers. There are many types of damper and springs. Different mechanisms were developed with time and technological development according to necessities.

Vehicle stand on the springs and springs carry vehicle weight. Springs absorb the impact forces cause of the road non-linearitys. They are the connections between tires and chassis. Any instant vertical impact absorbs with a spring mechanism, thence conducting to shocks are blocked. The various types of springs are air, leaf, coil springs, and torsion bars. Vehicle types, system requirements, weights, performances are the parameters for spring selections. Leaf and coil springs widely used today’s applications.

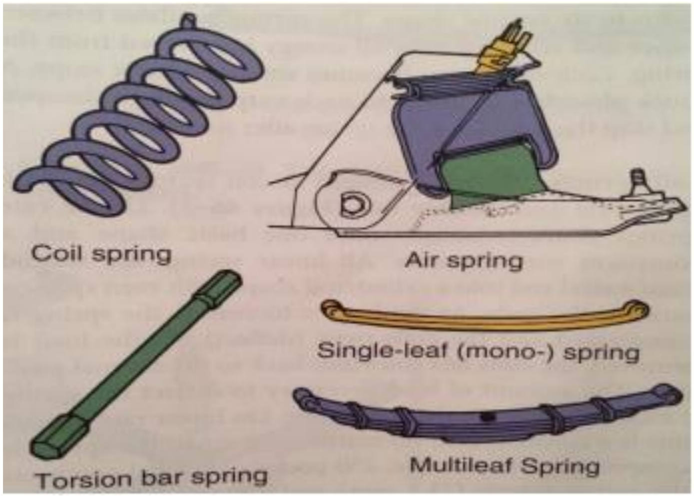

Figure 3-23 Types of springs

The leaf spring was designed by Obediah Elliot in 1804 and was used by horse and buggies. Over time, a design developed and installed the automobiles. Leaf springs are still using at heavyweight vehicles. Leaf quantities are increased for heavier loads. Single-leaf spring is stable and low lateral movements.

Coil springs can be called helical compression springs. These springs are producing for today's vehicles and other mechanical mechanisms. The coil springs can store more than twice the energy per unit volume than leaf springs. Vertical separation between chassis and axle is higher than leaf spring in the helical spring applications.

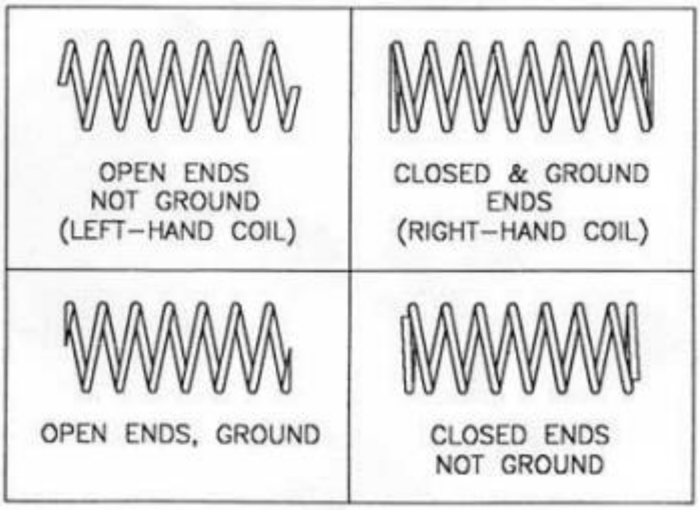

Figure 3-24 Helical spring types

Dampers (absorbers) use for to damp of the spring motions. Springs and dampers work together in a vehicle. Dampers absorb the shocks and reduce vibration, amplitude, and oscillations of the spring motion. This provides come back to the desired position in the spring. Springs continue to oscillation motion, after the stimulant effect until its natural damping are stopped itself. Natural damping coefficient depends on the material of spring. Damper provides for decreasing this oscillation and spring come to the desired position as soon as possible. Thus, spring is prepared for next stimulants. There are various types of absorbers which are hydraulic, gas and air pressure type.

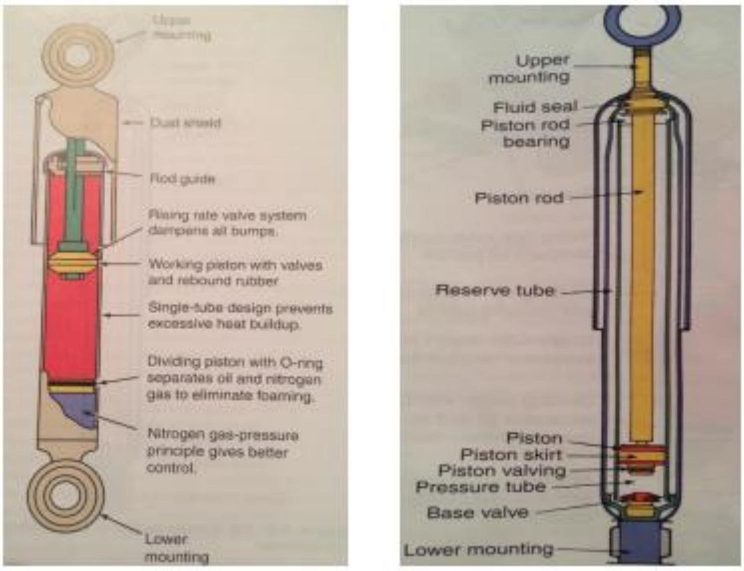

Figure 3-25 Hydraulic and gas pressure absorbers

3.2.2 Vibration Model of the Vehicles

The subject of vertical dynamics of the vehicle is concerned with the movement on the road surface. The primary goal of the vertical dynamics is tuning the suspension and damping constant for absorbing the shocks, safety, and comfortable riding characteristic. The most used modeling method is lumped parameter modeling. According to this model, the vehicle is comprised of mass, spring and damper elements. The lumped model can be a quarter car, half car, and a full car. In this scope four-wheel (7DOF) and six-wheels (9DOF), full cars are modeled.

Vibration model of the vehicles can be built with The Newton-Euler and Lagrange Methods. In this scope, Lagrange Motion Equations were used. Main advantageous of the Lagrange Equations in the mechanical vibrations is having a symmetric coefficient matrix.

The equation of motion of n DOF linear mechanical vibration system can be arranged second-order differential equation.

$$[m]\ddot{x} + [c]\dot{x} + [k]x = F \tag{3.27}$$

In which x is a column array of describing a coordinate system, and F is an array of describing applied force. The square matrices [m], [c], [k] is mass, damping and stiffness matrices of the system.

Creating the mathematical vibration model, following assumptions were considered,

- Spring and damping characteristics are linear,
- All wheels contact with track and Hook Law is valid,
- The effect points of the forces from track to wheels are mid-point of the contact surface and vertical to contact surface.

3.2.2.1 Derivation of the Lagrange Motion Equation

According to conservation equations for a large number (n) of particles in a conservative force field using Cartesian coordinates of positions x_i. For this system total kinetic energy as,

$$T = \sum_{n=1}^{M} \frac{1}{2} m_i {\dot{x}_i}^2 \tag{3.28}$$

where M is the degree of the freedom of the system.

The momentum of a particle in a given direction can be obtained by differentiating this expression concerning x_i coordinate. This gives the momentum p_i,

$$\frac{\partial T}{\partial x_i} = p_i \tag{3.29}$$

where T is kinetical energy

Time derivative of the momentum,

$$\frac{d}{dt}\left(\frac{\partial T}{\partial x_i}\right) = m_i \ddot{x}_i \tag{3.30}$$

The force on the particle is given by the derivative of the potential at the particle position in the given direction,

$$F_i = \frac{\partial V}{\partial x_i} \tag{3.31}$$

where V is potential energy.

According to Newton Law,

$$F_i = \frac{dp_i}{dt} \tag{3.32}$$

Kinetic and potential energy of a conservative force field,

$$\frac{d}{dt}\left(\frac{\partial T}{\partial x_i}\right) = -\frac{\partial V}{\partial x_i} \tag{3.33}$$

$$\frac{\partial T}{\partial x_i} = 0 \tag{3.34}$$

$$\frac{\partial V}{\partial \dot{x}_i} = 0 \tag{3.35}$$

According to this results rewriting the equation (3.33)

$$\frac{d}{dt}\left(\frac{\partial (T - V)}{\partial x_i}\right) - \frac{\partial (T - V)}{\partial x_i} = 0 \tag{3.36}$$

We can define,

$$L = T - V \tag{3.37}$$

where L is the Lagrangian

Equation (3.36) arrange for final form

$$\frac{d}{dt}\left(\frac{\partial (L}{\partial x_i}\right) - \frac{\partial (L)}{\partial x_i} = 0 \tag{3.38}$$

Damping coefficient can be added as,

$$\frac{d}{dt}\left(\frac{\partial (L}{\partial x_i}\right) - \frac{\partial (L)}{\partial x_i} + \frac{\partial (Q)}{\partial x_i} = 0 \tag{3.39}$$

where Q is damping energy.

3.2.3 7 DOF Vehicle Mathematical Vibration Equations

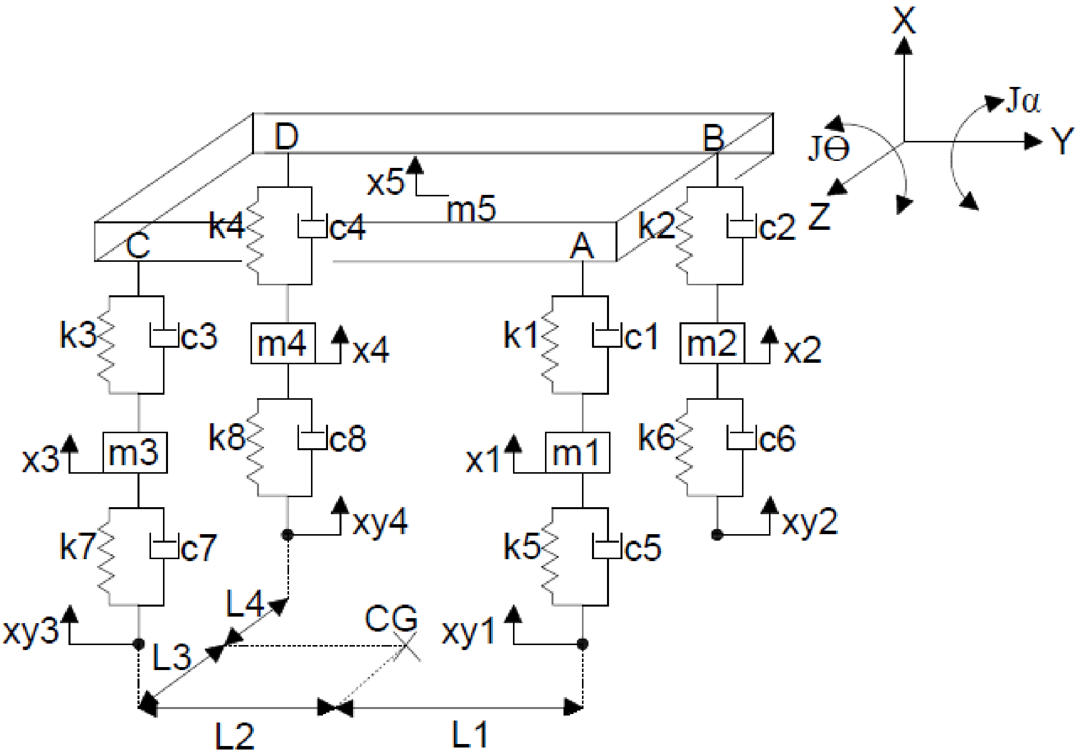

Figure 3-26 9 DOF vehicle vibration model

where,

A,B,C,D body-suspension system contact points,

c_1, c_2, c_3, c_4 damping coefficients of the suspension systems,

c_5, c_6, c_7, c_8 damping coefficients of the wheels,

J_Θ moment of inertia of the pitch axis,

J_α moment of inertia of the roll axis,

k_1, k_2, k_3, k_4 stiffness of the suspension systems,

k_5, k_6, k_7, k_8 stiffness of the wheels,

L_1 distance on y-axis of the rear suspensions with respect to in center of the gravity of the vehicle,

L_2 distance on y-axis of the front suspensions with respect to in center of the gravity of the vehicle,

L_3 distance on z-axis of the right suspensions with respect to in center of the gravity of the vehicle,

L_4 distance on z-axis of the left suspensions with respect to in center of the gravity of the vehicle,

m_5 mass of the body of the vehicle,

m_1,m_2, m_3, m_4 mass of the axle and wheel,

x_5 vibration amplitude of the body,

x_1,x_2, x_3, x_4, vibration amplitude of the wheels,

ϴ vibration amplitude of the pitch angle,

α vibration amplitude of the roll angle,

x_A, x_B, x_C, x_D vertical movement of the body-suspension points,

x_{y1}, x_{y2}, x_{y3}, x_{y4} track amplitudes

Assumptions for variables;

$x_1 < x_A$, $x_2 < x_B$, $x_3 < x_C$, $x_4 < x_D$,

$x_{y1} < x_1$, $x_{y2} < x_2$, $x_{y3} < x_3$, $x_{y4} < x_4$,

Lagrange equation has applied the system. Kinetic energy of the system;

Vibration model of the vehicle for each wheel and suspension system can be shown follows,

$$T = \sum_{n=1}^{M} \frac{1}{2} m_i \dot{x}_i{}^2 = \frac{1}{2} m_1 \dot{x}_1{}^2 + \frac{1}{2} m_2 \dot{x}_2{}^2 + \frac{1}{2} m_3 \dot{x}_3{}^2 + \frac{1}{2} m_4 \dot{x}_4{}^2 + \frac{1}{2} m_5 \dot{x}_5{}^2 + \frac{1}{2} J_\Theta \dot{\Theta}^2 + \frac{1}{2} J_\alpha \dot{\alpha}^2 \tag{3.40}$$

Potential energy of the system;

$$V = \sum_{n=1}^{M} \frac{1}{2} k_i x_i{}^2 = \frac{1}{2} k_1 (x_1 - x_A)^2 + \frac{1}{2} k_2 (x_2 - x_B)^2 + \frac{1}{2} k_3 (x_3 - x_C)^2 + \frac{1}{2} k_4 (x_4 - x_D)^2 + \frac{1}{2} k_5 (x_1 - x_{y1})^2 + \frac{1}{2} k_6 (x_2 - x_{y2})^2 + \frac{1}{2} k_7 (x_3 - x_{y3})^2 + \frac{1}{2} k_8 (x_4 - x_{y4})^2 \tag{3.41}$$

Damping energy of the system;

$$Q = \sum_{n=1}^{M} \frac{1}{2} c_i {\dot{x}_i}^2 = \frac{1}{2} c_1 (\dot{x}_1 - \dot{x}_A)^2 + \frac{1}{2} c_2 (\dot{x}_2 - \dot{x}_B)^2 + \frac{1}{2} c_3 (\dot{x}_3 - \dot{x}_C)^2$$
$$+ \frac{1}{2} c_4 (\dot{x}_4 - \dot{x}_D)^2 + \frac{1}{2} c_5 (\dot{x}_1 - \dot{x}_{y1})^2 + \frac{1}{2} c_6 (\dot{x}_2 - \dot{x}_{y2})^2 \tag{3.42}$$
$$+ \frac{1}{2} c_7 (\dot{x}_3 - \dot{x}_{y3})^2 + \frac{1}{2} c_8 (\dot{x}_4 - \dot{x}_{y4})^2$$

Displacement equations,

$$x_A = x_5 - \Theta L_1 - \alpha L_3 \tag{3.43}$$

$$x_B = x_5 - \Theta L_1 - \alpha L_4 \tag{3.44}$$

$$x_C = x_5 + \Theta L_2 - \alpha L_3 \tag{3.45}$$

$$x_B = x_5 + \Theta L_2 + \alpha L_4 \tag{3.46}$$

Energy equations are substituted into the Lagrange Equation and arranged,

$$m_1 \ddot{x}_1 - c_1 \left(\dot{x}_5 - \dot{\Theta} L_1 - \dot{\alpha} L_3 - \dot{x}_1 \right) + c_5 (\dot{x}_1 - \dot{x}_{y1}) - k_1 (x_5 - \Theta L_1 - \alpha L_3$$
$$- x_1) + k_5 (x_1 - x_{y1}) = 0 \tag{3.47}$$

$$m_2 \ddot{x}_2 - c_2 \left(\dot{x}_5 - \dot{\Theta} L_1 + \dot{\alpha} L_4 - \dot{x}_2 \right) + c_6 (\dot{x}_2 - \dot{x}_{y2}) - k_2 (x_5 - \Theta L_1$$
$$+ \alpha L_4 - x_2) + k_6 (x_2 - x_{y2}) = 0 \tag{3.48}$$

$$m_3 \ddot{x}_3 - c_3 \left(\dot{x}_5 + \dot{\Theta} L_2 - \dot{\alpha} L_3 - \dot{x}_3 \right) + c_7 (\dot{x}_3 - \dot{x}_{y3}) - k_3 (x_5 + \Theta L_2$$
$$- \alpha L_3 - x_3) + k_7 (x_3 - x_{y3}) = 0 \tag{3.49}$$

$$m_4 \ddot{x}_4 - c_4 \left(\dot{x}_5 + \dot{\Theta} L_2 + \dot{\alpha} L_4 - \dot{x}_4 \right) + c_8 (\dot{x}_4 - \dot{x}_{y4}) - k_4 (x_5 + \Theta L_2$$
$$+ \alpha L_4 - x_4) + k_8 (x_4 - x_{y4}) = 0 \tag{3.50}$$

$$m_5 \ddot{x}_5 + c_1 \left(\dot{x}_5 - \dot{\Theta} L_1 - \dot{\alpha} L_3 - \dot{x}_1 \right) + c_2 \left(\dot{x}_5 - \dot{\Theta} L_1 + \dot{\alpha} L_4 - \dot{x}_2 \right)$$
$$+ c_3 \left(\dot{x}_5 + \dot{\Theta} L_2 - \dot{\alpha} L_3 - \dot{x}_3 \right) + c_4 \left(\dot{x}_5 + \dot{\Theta} L_2 + \dot{\alpha} L_4 - \dot{x}_4 \right) \tag{3.51}$$

$$+k_1(x_5-\Theta L_1-\alpha L_3-x_1)+k_2(x_5-\Theta L_1+\alpha L_4-x_2)$$

$$+k_3(x_5+\Theta L_2-\alpha L_3-x_3)+k_4(x_5+\Theta L_2+\alpha L_4-x_4=0$$

$$J_\Theta\ddot{\Theta}-c_1L_1(\dot{x_5}-\dot{\Theta}L_1-\dot{\alpha}L_3-\dot{x}_1)+c_2L_1(\dot{x_5}-\dot{\Theta}L_1+\dot{\alpha}L_4-\dot{x}_2)$$

$$+c_3L_2(\dot{x_5}+\dot{\Theta}L_2-\dot{\alpha}L_3-\dot{x}_3)+c_4L_2(\dot{x_5}+\dot{\Theta}L_2+\dot{\alpha}L_4-\dot{x}_4) \quad (3.52)$$

$$-k_1L_1(x_5-\Theta L_1-\alpha L_3-x_1)-k_2L_1(x_5-\Theta L_1+\alpha L_4-x_2)$$

$$+k_3L_2(x_5+\Theta L_2-\alpha L_3-x_3)+k_4L_2(x_5+\Theta L_2+\alpha L_4-x_4=0$$

$$J_\Theta\ddot{\alpha}-c_1L_3(\dot{x_5}-\dot{\Theta}L_1-\dot{\alpha}L_3-\dot{x}_1)+c_2L_4(\dot{x_5}-\dot{\Theta}L_1+\dot{\alpha}L_4-\dot{x}_2)$$

$$-c_3L_3(\dot{x_5}+\dot{\Theta}L_2-\dot{\alpha}L_3-\dot{x}_3)+c_4L_4(\dot{x_5}+\dot{\Theta}L_2+\dot{\alpha}L_4-\dot{x}_4) \quad (3.53)$$

$$-k_1L_3(x_5-\Theta L_1-\alpha L_3-x_1)+k_2L_4(x_5-\Theta L_1+\alpha L_4-x_2)$$

$$-k_3L_3(x_5+\Theta L_2-\alpha L_3-x_3)+k_4L_5(x_5+\Theta L_2+\alpha L_4-x_4=0$$

3.2.4 9 DOF Vehicle Mathematical Vibration Equations [16]

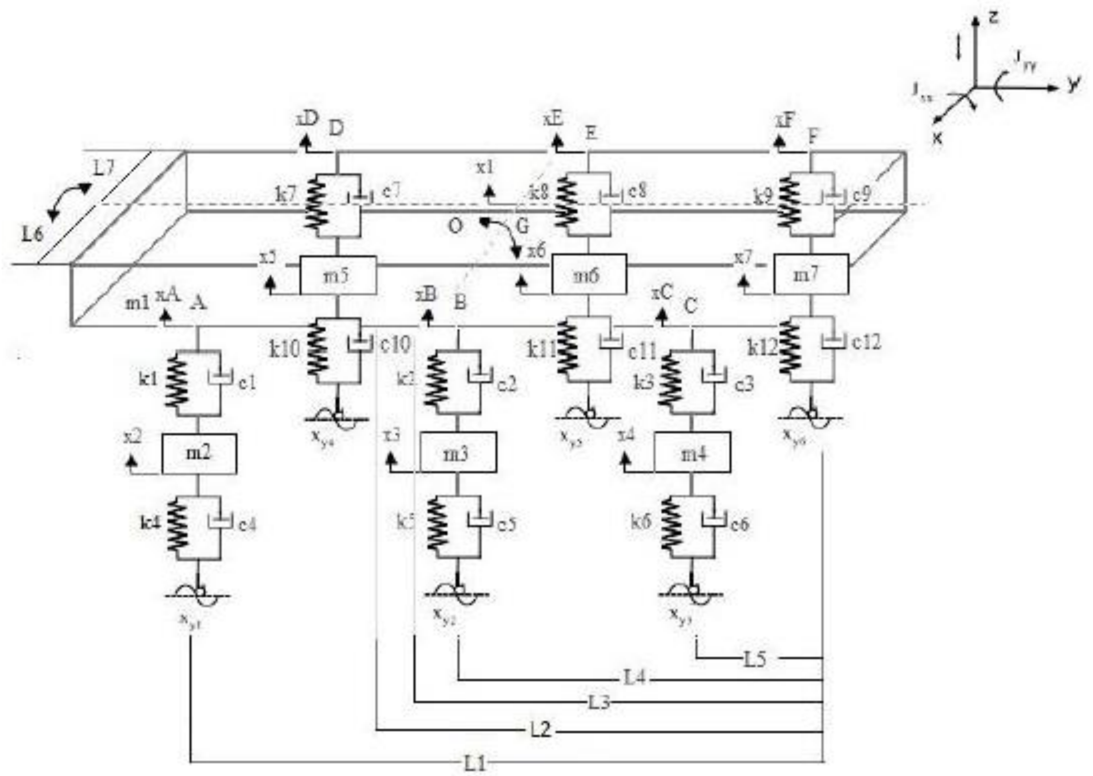

Figure 3-27 9 DOF vehicle vibration model

where,

A,B,C,D,E,F body-suspension system contact points,

$c_1, c_2, c_3, c_7, c_8, c_9$ damping coefficients of the suspension systems,

$c_4, c_5, c_6, c_{10}, c_{11}, c_{12}$ damping coefficients of the wheels,

J_Θ moment of inertia of the pitch axis,

J_α moment of inertia of the roll axis,

$k_1, k_2, k_3, k_7, k_8, k_9$ stiffness of the suspension systems,

$k_4, k_5, k_6, k_{10}, k_{11}, k_{12}$ stiffness of the wheels,

L_1 distance on y-axis of the rear suspensions with respect to in front of the vehicle,

L_2 distance on y-axis of the middle of the body with respect to in front of the vehicle,

L_3 distance on y-axis of the center of mass with respect to in front of the vehicle,

L_4 distance on y-axis of the center suspensions with respect to in front of the vehicle,

L_5 distance on y-axis of the front suspensions with respect to in front of the vehicle,

L_6 distance on x-axis of center of mass with respect to left suspensions,

L_7 distance on x-axis of center of mass with respect to right suspensions,

m_1 mass of the body of the vehicle,

$m_2, m_3, m_4, m_5, m_6, m_7$ mass of the axle and wheel,

x_1 vibration amplitude of the body,

$x_2, x_3, x_4, x_5, x_6, x_7$ vibration amplitude of the wheels,

Θ vibration amplitude of the pitch angle,

α vibration amplitude of the roll angle,

$x_A, x_B, x_C, x_D, x_E, x_F$ vertical movement of the body-suspension points,

$x_{y1}, x_{y2}, x_{y3}, x_{y4}, x_{y5}, x_{y6}$ track amplitudes

Assumptions for variables;

$x_2 < x_A, x_3 < x_B, x_4 < x_C, x_5 < x_D, x_6 < x_E, x_7 < x_F,$

$x_F < x_C, x_E < x_B, x_D < x_A,$

$x_{y1} < x_2, x_{y2} < x_3, x_{y3} < x_4, x_{y4} < x_5, x_{y5} < x_6, x_{y6} < x_7,$

Lagrange equation has applied the system. Kinetic energy of the system;

$$T=\sum_{n=1}^{M}\frac{1}{2}m_i\dot{x}_i{}^2=\frac{1}{2}m_1\dot{x}_1{}^2+\frac{1}{2}m_2\dot{x}_2{}^2+\frac{1}{2}m_3\dot{x}_3{}^2+\frac{1}{2}m_4\dot{x}_4{}^2+ \frac{1}{2}m_5\dot{x}_5{}^2+\frac{1}{2}m_6\dot{x}_6{}^2+\frac{1}{2}m_7\dot{x}_7{}^2+\frac{1}{2}J_\Theta\dot{\Theta}^2+\frac{1}{2}J_\alpha\dot{\alpha}^2 \tag{3.54}$$

Potential energy of the system;

$$V=\sum_{n=1}^{M}\frac{1}{2}k_ix_i{}^2=\frac{1}{2}k_1(x_2-x_A)^2+\frac{1}{2}k_2(x_3-x_B)^2 +\frac{1}{2}k_3(x_4-x_C)^2+\frac{1}{2}k_7(x_5-x_D)^2+\frac{1}{2}k_8(x_6-x_E)^2+\frac{1}{2}k_9(x_7-x_F)^2 +\frac{1}{2}k_4(x_2-x_{y1})^2+\frac{1}{2}k_5(x_3-x_{y2})^2+\frac{1}{2}k_6(x_4-x_{y3})^2 +\frac{1}{2}k_{10}(x_5-x_{y4})^2+\frac{1}{2}k_5(x_6-x_{y5})^2+\frac{1}{2}k_6(x_7-x_{y6})^2 \tag{3.55}$$

Damping energy of the system;

$$Q=\sum_{n=1}^{M}\frac{1}{2}c_i\dot{x}_i{}^2=\frac{1}{2}c_1(\dot{x}_2-\dot{x}_A)^2+\frac{1}{2}c_2(\dot{x}_3-\dot{x}_B)^2+\frac{1}{2}c_3(\dot{x}_4-\dot{x}_C)^2 +\frac{1}{2}c_7(\dot{x}_5-\dot{x}_D)^2+\frac{1}{2}c_8(\dot{x}_6-\dot{x}_E)^2+\frac{1}{2}c_9(\dot{x}_7-\dot{x}_F)^2+\frac{1}{2}c_4(\dot{x}_2-\dot{x}_{y1})^2 +\frac{1}{2}c_5(\dot{x}_3-\dot{x}_{y2})^2+\frac{1}{2}c_6(\dot{x}_4-\dot{x}_{y3})^2+\frac{1}{2}c_{10}(\dot{x}_5-\dot{x}_{y4})^2 +\frac{1}{2}c_{11}(\dot{x}_6-\dot{x}_{y5})^2+\frac{1}{2}c_{12}(\dot{x}_7-\dot{x}_{y6})^2 \tag{3.56}$$

Displacement equations;

$$x_A=x_1+\Theta(L_1-L_3)+\alpha L_6 \tag{3.57}$$

$$x_B=x_1-\Theta(L_3-L_4)+\alpha L_6 \tag{3.58}$$

$$x_C=x_1-\Theta(L_3-L_5)+\alpha L_6 \tag{3.59}$$

$$x_D=x_1+\Theta(L_1-L_3)-\alpha L_7 \tag{3.60}$$

$$x_E = x_1 - \Theta(L_3 - L_4) - \alpha L_7 \tag{3.61}$$

$$x_F = x_1 - \Theta(L_3 - L_5) - \alpha L_7 \tag{3.62}$$

Energy equations are substituted into the Lagrange Equation,

$$\begin{gathered} m_1\ddot{x}_1 + \dot{x}_1(c_1 + c_2 + c_3 + c_7 + c_8 + c_9) - \dot{x}_2c_1 - \dot{x}_3c_2 - \dot{x}_4c_3 - \dot{x}_5c_7 \\ -\dot{x}_6c_8 - \dot{x}_7c_9 + \dot{\Theta}(c_1(L_1 - L_3) - c_2(L_3 - L_4) - c_3(L_3 - L_5) \\ +c_7(L_1 - L_3) - c_8(L_3 - L_4) - c_9(L_3 - L_5)) + \dot{\alpha}(c_1L_6 + c_2L_6 + c_3L_6 \\ -c_7L_7 - c_8L_7 - c_9L_7) + x_1(k_1 + k_2 + k_3 + k_7 + k_8 + k_9) \\ -x_2k_1 - x_3k_2 - x_4k_3 - x_5k_7 - x_6k_8 - x_7k_9 + \Theta(k_1(L_1 - L_3) \\ -k_2(L_3 - L_4) - k_3(L_3 - L_5) + k_7(L_1 - L_3) - k_8(L_3 - L_4) \\ -k_9(L_3 - L_5)) + \alpha(k_1L_6 + k_2L_6 + k_3L_6 - k_7L_7 \\ -k_8L_7 - k_9L_7) = 0 \end{gathered} \tag{3.63}$$

$$\begin{gathered} m_2\ddot{x}_2 - \dot{x}_1c_1 + \dot{x}_2(c_1 + c_4) - \dot{\Theta}c_1(L_1 - L_3) - \dot{\alpha}c_1L_6 - x_1k_1 \\ +x_2(k_1 + k_4) + \Theta k_1(L_1 - L_3) - \alpha k_1L_6 - \dot{x}_{y1}c_4 - x_{y1}k_4 = 0 \end{gathered} \tag{3.64}$$

$$\begin{gathered} m_3\ddot{x}_3 - \dot{x}_1c_2 + \dot{x}_3(c_2 + c_5) + \dot{\Theta}c_2(L_3 - L_4) - \dot{\alpha}c_2L_6 - x_1k_2 \\ +x_3(k_2 + k_5) + \Theta k_2(L_3 - L_4) - \alpha k_2L_6 - \dot{x}_{y2}c_5 - x_{y2}k_5 = 0 \end{gathered} \tag{3.65}$$

$$\begin{gathered} m_4\ddot{x}_4 - \dot{x}_1c_3 + \dot{x}_4(c_3 + c_6) + \dot{\Theta}c_3(L_3 - L_5) - \dot{\alpha}c_3L_6 - x_1k_2 \\ +x_4(k_3 + k_6) + \Theta k_3(L_3 - L_5) - \alpha k_3L_6 - \dot{x}_{y3}c_6 - x_{y3}k_6 = 0 \end{gathered} \tag{3.66}$$

$$\begin{gathered} m_5\ddot{x}_5 - \dot{x}_1c_7 + \dot{x}_5(c_7 + c_{10}) - \dot{\Theta}c_7(L_1 - L_3) + \dot{\alpha}c_7L_7 - x_1k_7 \\ +x_5(k_7 + k_{10}) - \Theta k_7(L_1 - L_3) + \alpha k_7L_7 - \dot{x}_{y4}c_{10} - x_{y4}k_{10} = 0 \end{gathered} \tag{3.67}$$

$$\begin{gathered} m_6\ddot{x}_6 - \dot{x}_1c_8 + \dot{x}_6(c_8 + c_{11}) + \dot{\Theta}c_8(L_3 - L_4) + \dot{\alpha}c_8L_7 - x_1k_8 \\ +x_6(k_8 + k_{11}) + \Theta k_8(L_3 - L_4) + \alpha k_8L_7 - \dot{x}_{y5}c_{11} - x_{y5}k_{11} = 0 \end{gathered} \tag{3.68}$$

$$m_7\ddot{x}_7 - \dot{x}_1c_9 + \dot{x}_7(c_9 + c_{12}) + \dot{\Theta}c_9(L_3 - L_5) + \dot{\alpha}c_9L_7 - x_1k_9 \tag{3.69}$$

$$+x_7(k_9+k_{12})+\Theta k_9(L_3-L_5)+\alpha k_9L_7-\dot{x}_{y6}c_{12}-x_{y6}k_{12}=0$$

$$\begin{gathered}J\ddot{\Theta}+\dot{x}_1(c_1(L_1-L_3)-c_2(L_3-L_4)-c_3(L_3-L_5)+c_7(L_1-L_3)\\ -c_8(L_3-L_4)-c_9(L_3-L_5))-\dot{x}_2c_1(L_1-L_3)+\dot{x}_3c_2(L_3-L_4)\\ +\dot{x}_4c_3(L_3-L_5)-\dot{x}_5c_7(L_1-L_3)+\dot{x}_6c_8(L_3-L_4)+\dot{x}_7c_9(L_3-L_5)\\ +\dot{\Theta}(c_1(L_1-L_3)^2+c_2(L_3-L_4)^2+c_3(L_3-L_5)^2+c_7(L_1-L_3)^2\\ c_8(L_3-L_4)^2+c_9(L_3-L_5)^2)+\dot{\alpha}(c_1L_6(L_1-L_3)-c_2L_6(L_3-L_4)\\ -c_3L_6(L_3-L_5)-c_7L_7(L_1-L_3)+c_8L_7(L_3-L_4)+c_9L_7(L_3-L_5))\\ x_1(k_1(L_1-L_3)-k_2(L_3-L_4)-k_3(L_3-L_5)+k_7(L_1-L_3)\\ -k_8(L_3-L_4)-k_9(L_3-L_5))-x_2k_1(L_1-L_3)+x_3k_2(L_3-L_4)\\ +x_4k_3(L_3-L_5)-x_5k_7(L_1-L_3)+x_6k_8(L_3-L_4)+x_7k_9(L_3-L_5)\\ +\Theta(k_1(L_1-L_3)^2+k_2(L_3-L_4)^2+k_3(L_3-L_5)^2+k_7(L_1-L_3)^2\\ +k_8(L_3-L_4)^2+k_9(L_3-L_5)^2)+\alpha(k_1L_6(L_1-L_3)-k_2L_6(L_3-L_4)\\ -k_3L_6(L_3-L_5)-k_7L_7(L_1-L_3)+k_8L_7(L_3-L_4)k_9L_7(L_3-L_5))=0\end{gathered} \tag{3.70}$$

$$\begin{gathered}J\ddot{\alpha}+\dot{x}_1(c_1L_6+c_2L_6+c_3L_6-c_7L_7-c_8L_7-c_9L_7)-\dot{x}_2c_1L_6\\ -\dot{x}_3c_2L_6-\dot{x}_4c_3L_6+\dot{x}_5c_7L_7+\dot{x}_6c_8L_7+\dot{x}_7c_9L_7+\dot{\Theta}(c_1L_6(L_1-L_3)\\ -c_2L_6(L_3-L_4)-c_3L_6(L_3-L_5)-c_7L_7(L_1-L_3)+c_8L_7(L_3-L_4)\\ +c_9L_7(L_3-L_4))+\dot{\alpha}(c_1{L_6}^2+c_2{L_6}^2+c_3{L_6}^2+c_7{L_7}^2+c_8{L_7}^2+c_9{L_7}^2)\\ +x_1(k_1L_6+k_2L_6+k_3L_6-k_7L_7-k_8L_7-k_9L_7)-x_2k_1L_6-x_3k_2L_6\\ -x_4k_3L_6+x_5k_7L_7+x_6k_8L_7+x_7k_9L_7+\Theta(k_1L_6(L_1-L_3)\\ -k_2L_6(L_3-L_3)-k_3L_6(L_3-L_5)-k_7L_7(L_1-L_3)+k_8L_7(L_3-L_4)\\ k_9L_7(L_3-L_5))+\alpha\left(k_1{L_6}^2+k_2{L_6}^2+k_3{L_6}^2+k_7{L_7}^2+k_8{L_7}^2+k_9{L_7}^2\right)\\ =0\end{gathered} \tag{3.71}$$

3.3 Neural Networks

Neural networks are algorithms modeled similar to the brain and be identified to machine learning. Communication units of the human brains are neuron. Each neuron occurs nucleus, dendrite, cell body, axon, and synapses. Dendrite receives the signals from other neurons. Cell body gets the incoming signals and generates output signals. Axon distributes the generated signal to the other neurons and synapses are the connection points with other axons. Cell body decides to generate a signal by reaching the threshold value.

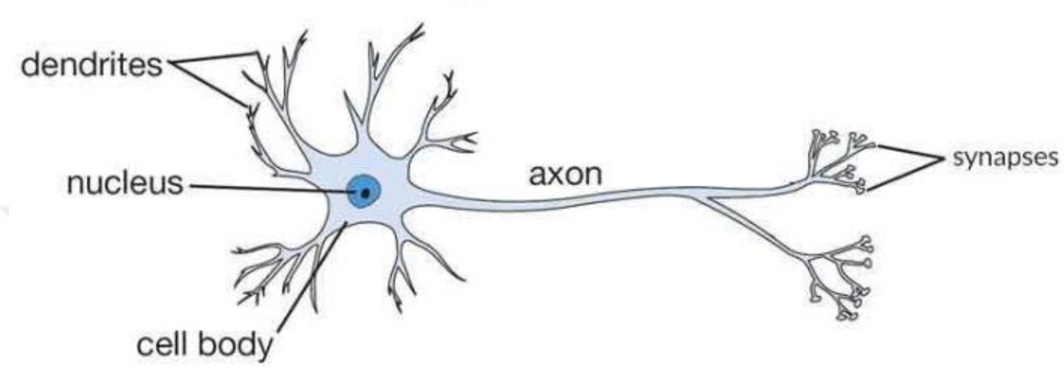

Figure 3-28 Structure of the neuron [17]

Neural networks look like human brains. Their structures, connection lines are similar to neurons. In neural networks, dendrites are the weight inputs based on their interconnection in the artificial neural network. Cell body comprises of summation and threshold, so it decides to send output. Axon carries outputs to the other networks.

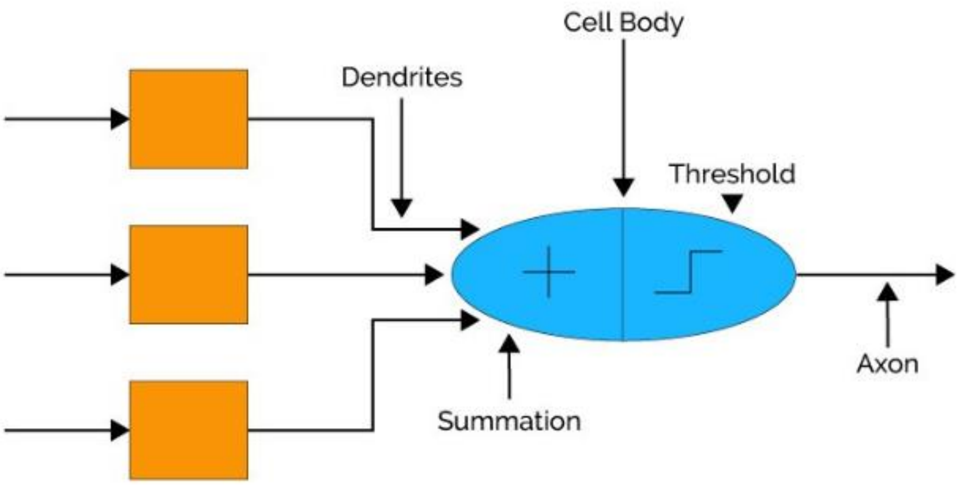

Figure 3-29 Artificial Neural Network-Neuron Similarities [17]

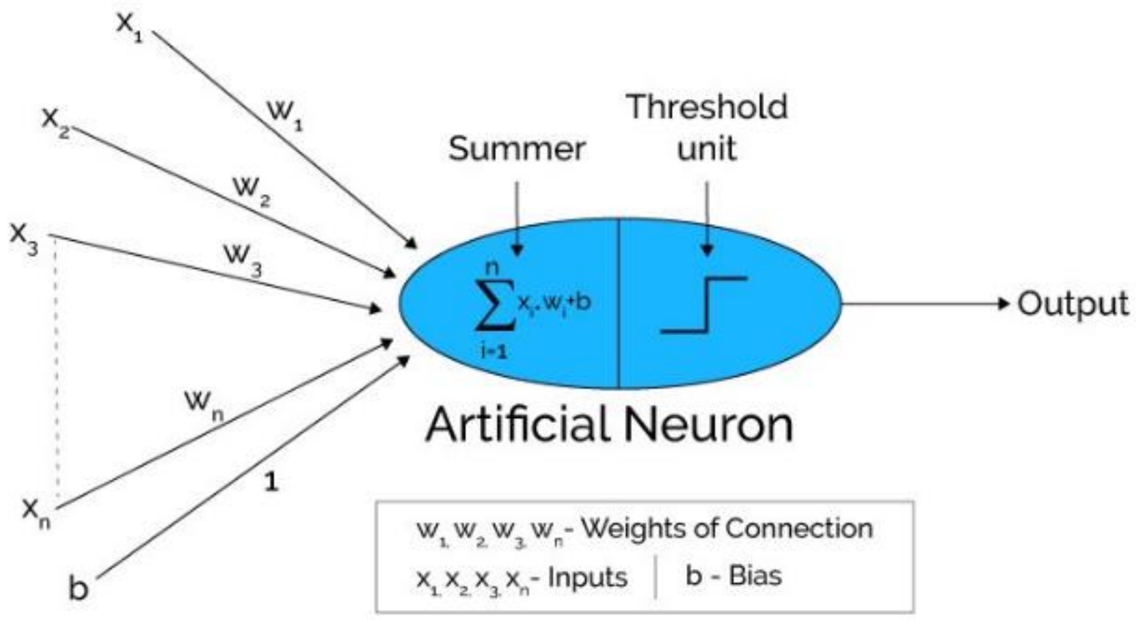

Figure 3-30 Structure of the Artificial Neural Network [17]

Neural network data mostly moves only one-direction (feedforward). An individual node can be connected several nodes in the layer. Some nodes receive data, and some nodes take data. Node assigns a known number, which can be called weight, for each input connections. If the connection path active, nodes can take data. Each input multiplies with the weight of the connection than reach the neuron. If multiplied data is over the threshold, neuron sends to outputs.

Values of the weight and threshold assign randomly at the training stage. Training data use for input layer and pass into other layers, at this stage data multiplied and added. This iteration continue until data transform at the output layer.

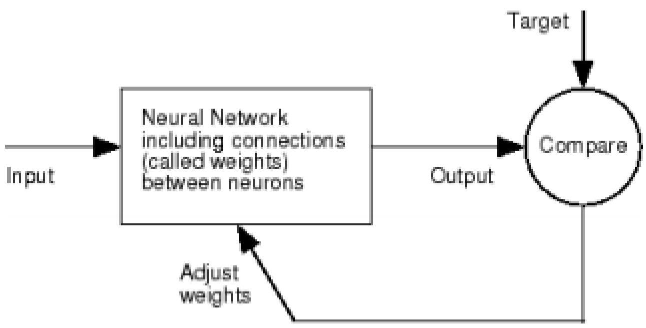

Figure 3-31 Algorithm of the Neural Network [18]

There are several of type transfer functions in the Neural Network. However linear and Log-Sigmoid transfer functions are mostly used.

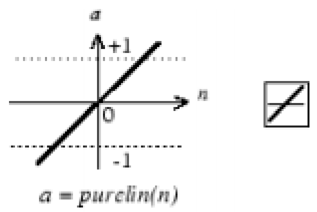

Figure 3-32 Linear transfer function [18]

Sigmoid transfer function inputs can be plus and minus infinity. Outputs will be zero to one range.

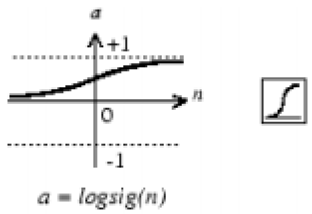

Figure 3-33 Log-Sigmoid transfer function [18]

Transfer functions used in the hidden layers of the multilayer network because of they are differentiable.

Neuron input can be vectors. All input element will be multiplied by weights and weighted values fed to summing function.

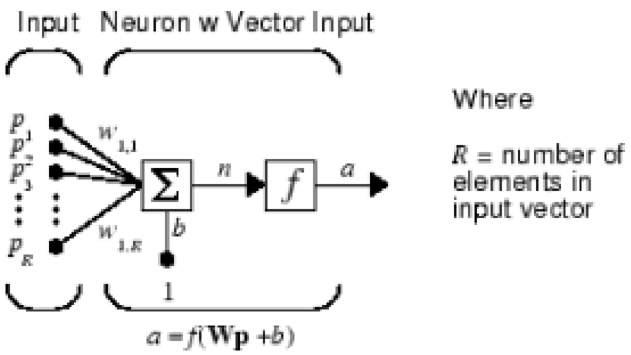

Figure 3-34 Vector input in Neural Network [18]

Networks can be one and multiple layers. In one layer network, each input connected to the whole neurons.

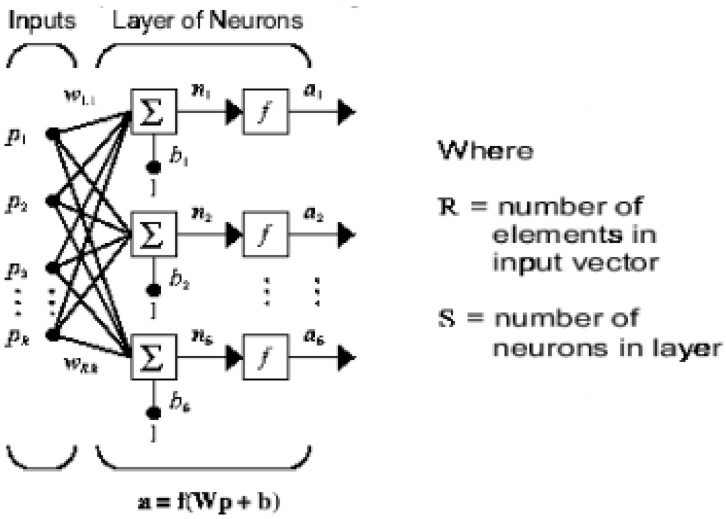

Figure 3-35 One layer neurons [18]

The network can be several layers. Each input connected with first layer neurons. Each layer has their weight, bias and output value. Multiple layer networks are quite robust.

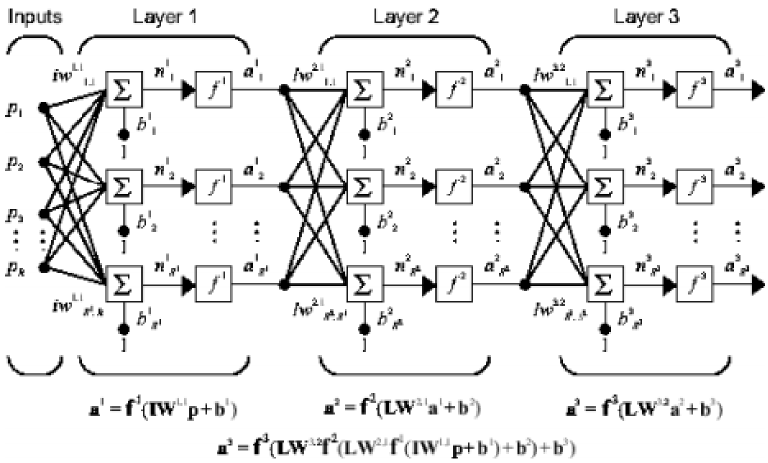

Figure 3-36 Multiple layer neurons [18]

Today, artificial intelligent uses many type application from industrial, defense and financial sector to the game sector. It can be seen following figure, a sectoral table prepared by MATLAB developer.

Industry	Business Applications
Defense	Weapon steering, target tracking, object discrimination, facial recognition, new kinds of sensors, sonar, radar and image signal processing including data compression, feature extraction and noise suppression, and signal/image identification
Electronics	Code sequence prediction, integrated circuit chip layout, process control, chip failure analysis, machine vision, voice synthesis, and nonlinear modeling
Entertainment	Animation, special effects, and market forecasting
Financial	Real estate appraisal, loan advising, mortgage screening, corporate bond rating, credit-line use analysis, credit card activity tracking, portfolio trading program, corporate financial analysis, and currency price prediction
Industrial	Prediction of industrial processes, such as the output gases of furnaces, replacing complex and costly equipment used for this purpose in the past
Insurance	Policy application evaluation and product optimization
Manufacturing	Manufacturing process control, product design and analysis, process and machine diagnosis, real-time particle identification, visual quality inspection systems, beer testing, welding quality analysis, paper quality prediction, computer-chip quality analysis, analysis of grinding operations, chemical product design analysis, machine maintenance analysis, project bidding, planning and management, and dynamic modeling of chemical process system
Medical	Breast cancer cell analysis, EEG and ECG analysis, prosthesis design, optimization of transplant times, hospital expense reduction, hospital quality improvement, and emergency-room test advisement
Oil and gas	Exploration
Robotics	Trajectory control, forklift robot, manipulator controllers, and vision systems
Securities	Market analysis, automatic bond rating, and stock trading advisory systems
Speech	Speech recognition, speech compression, vowel classification, and text-to-speech synthesis
Telecommunications	Image and data compression, automated information services, real-time translation of spoken language, and customer payment processing systems
Transportation	Truck brake diagnosis systems, vehicle scheduling, and routing systems

Figure 3-37 Application area of the Artificial Neural Network [18]

4 METHODOLOGY

4.1 Analysis and Simulation Types

4.1.1 ANSYS Analysis of Turret

Turret system has to perform its ability under hard conditions. External and internal acceleration were forced to system limitations.

Turret was included many sub-systems. Flexibility of the sub-systems are affected the accuracy of aiming. System was steered with gear systems on the elevation and azimuth axes. Flexibility of the gear systems is especially important because of conducting motions. For example, the 1º error of the aiming on the gears causing ~1.75m bias from a hundred meters away from the target point.

For seeing flexibility effects of the elevation and azimuth gears, system was analyzed in ANSYS for flexible and rigid gear conditions and results were compered.

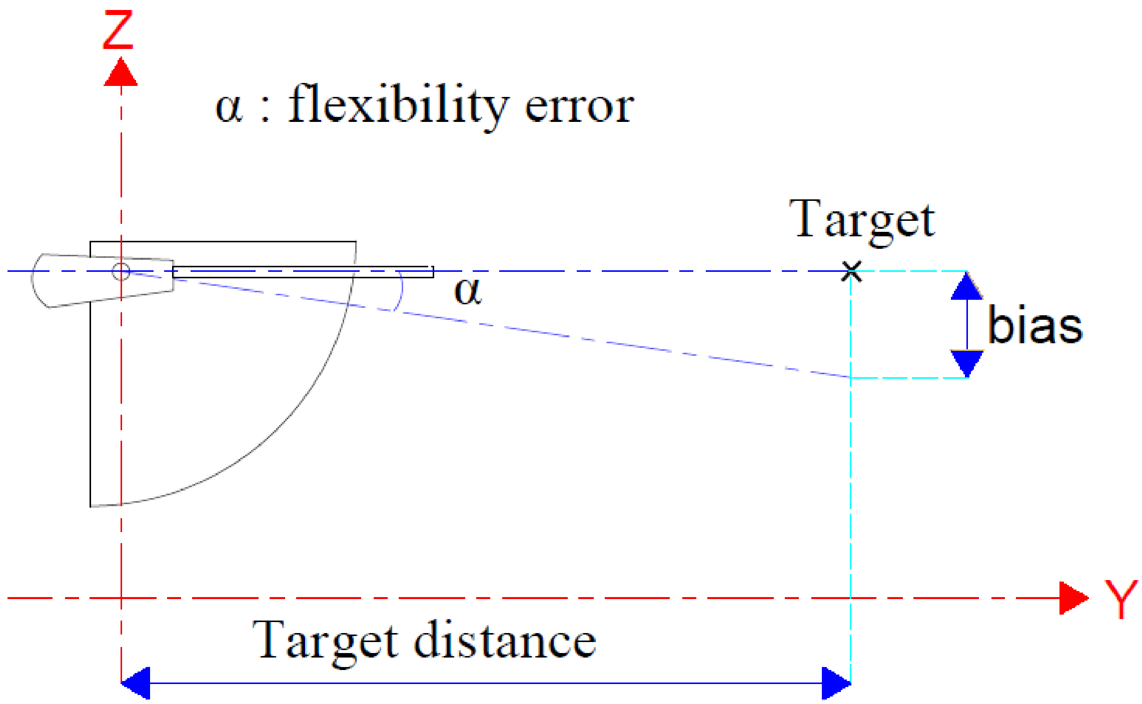

Figure 4-1 Flexibility error of elevation axis

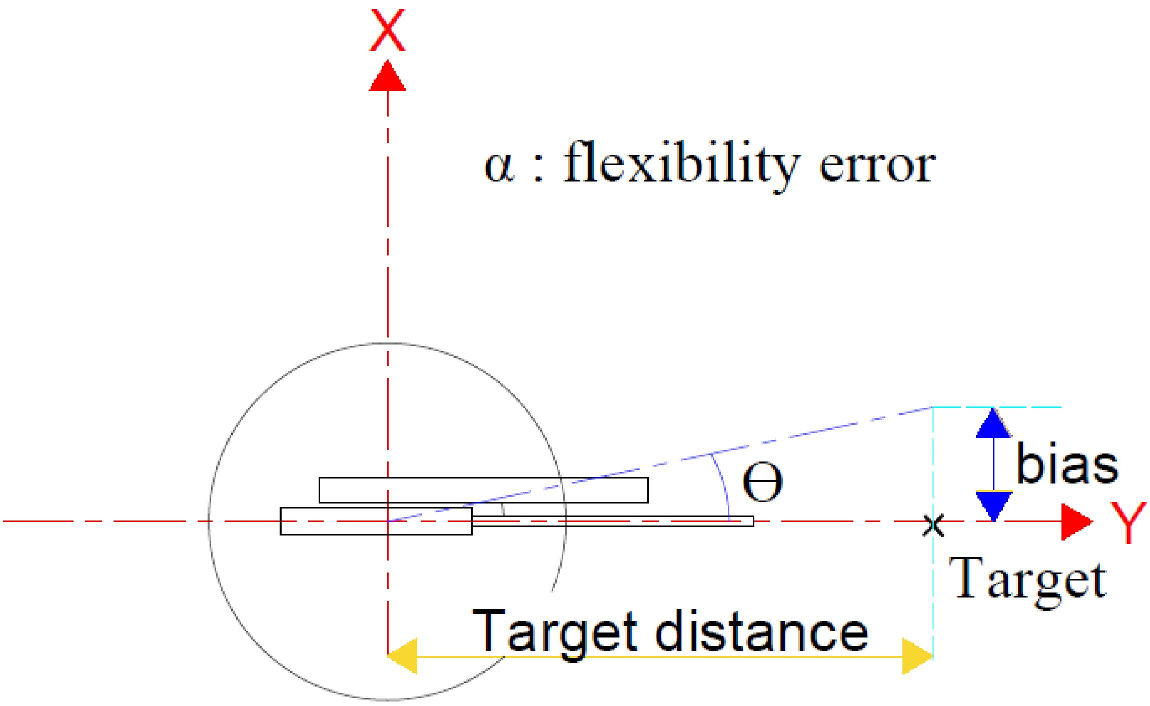

Figure 4-2 Flexibility error of azimuth axis

Dynamic parameters of the system were given in Table 4-1. Analysis were run for while turret reach to maximum velocities with maximum acceleration. Muzzle positions were obtained for flexible and rigid cases and compared each other.

Table 4-1 Dynamic Parameters of the Turret

	Azimuth Axis	Elevation Axis
Movement Limitations	-30º / +60º	nx360º
Maximum velocity	>60º/s	>60º/s
Maximum accelerations	>90º/s^2	>90º/s^2

Analysis scenarios were built according to dynamic conditions and identified as follows;

- Maximum elevation velocity while elevation gear is flexible,
- Maximum elevation velocity while elevation gear is rigid,
- Maximum azimuth velocity while azimuth gear is flexible,
- Maximum azimuth velocity azimuth gear is rigid,
- Elevation and azimuth gears fatigue life analysis,

4.1.2 MATLAB Analysis of Vehicle and Turret

The scope of this analysis is creating a vehicle vibration model, turret model in SIMULINK and observing the turret motions. The second step of this analysis, the turret was controlled against to disturbances with PID controller.

First, vehicles were stimulated for non-uniform track and results are observed. At the second step, the turret was modeled with muzzle, azimuth and elevation gears according to real positions and muzzle motions were observed. At the final step, PID controller is developed for the turret and performed under the effect of vehicle vibrations.

In this scope, following simulations were run,

- 7 DOF Vehicle vibration simulation under 15km/h, 30km/h and 50km/h velocities
- 9 DOF Vehicle vibration simulation under 15km/h, 30km/h and 50km/h velocities
- Turret integrated 7 DOF vehicle PID controlled simulation under 15km/h, 30km/h and 50km/h velocities
- Turret integrated 9 DOF vehicle PID controlled simulation under 15km/h, 30km/h and 50km/h velocities

4.1.3 MATLAB ANSYS Integrated Analysis

This simulation was run for to observe turret motions under real conditions at virtual world. Physical model of the turret can be created, close to the real, in ANSYS and physical model of the vehicle vertical dynamics can be created, close to the real, in MATLAB. The scenario of this simulation is that turret mounted a ground vehicle, ground vehicle impact with non-uniform track conditions and turret try to stabilize itself. Real simulation conditions can be created running and connecting these two programs together.

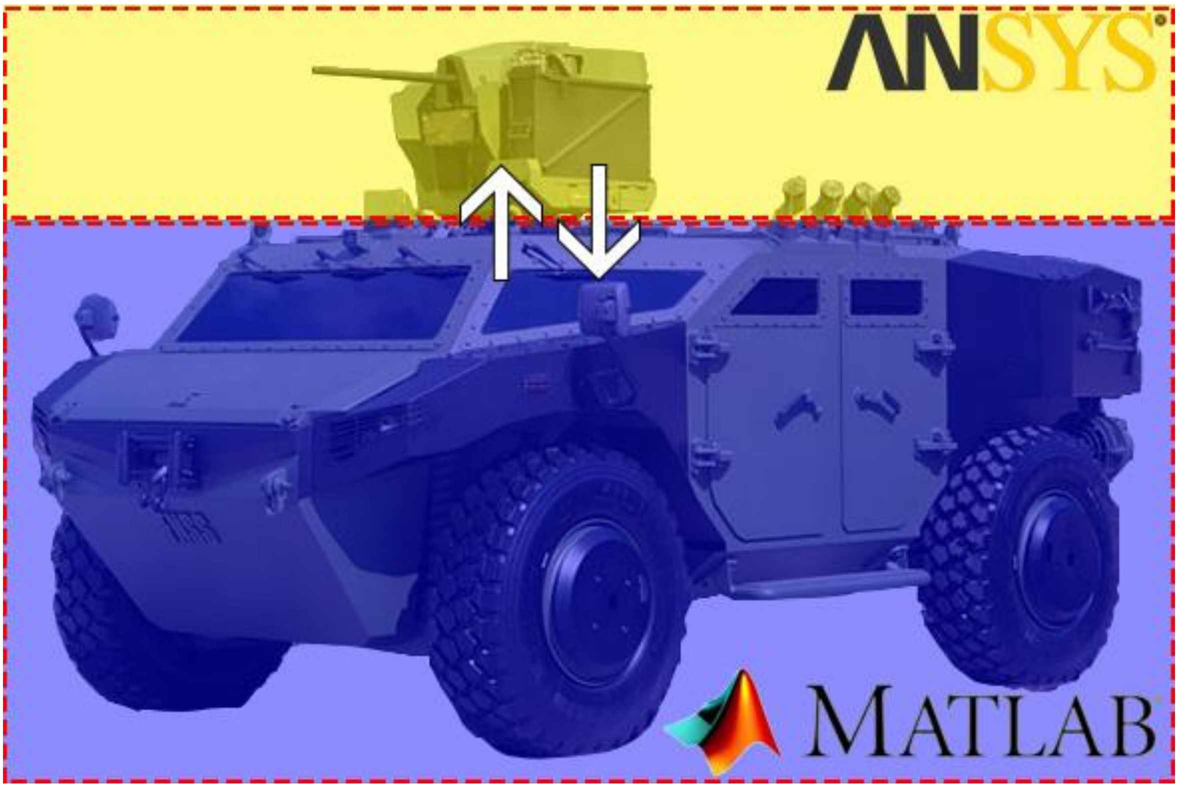

Figure 4-3 Modelling environment of systems

MATLAB is the quite powerful modelling program. It can be programmed to running other programs at batch mode and also ANSYS APDL. Simulation algorithm is that, firstly vehicle stimulate with non-uniform track conditions and heave, roll and pitch motions were taken. Peaks of the heave, roll and pitch graphs were detected. Turret responses against the vehicle vibrations were tough to program with Artificial Neural Network for 10m beyond target. Therefore, MATLAB artificial neural networks create stabilization parameter against to detecting disturbances. MATLAB open the APDL input file for writing heave, roll and pitch disturbance and stabilization parameters with time. ANSYS is run according to inputs by MATLAB.

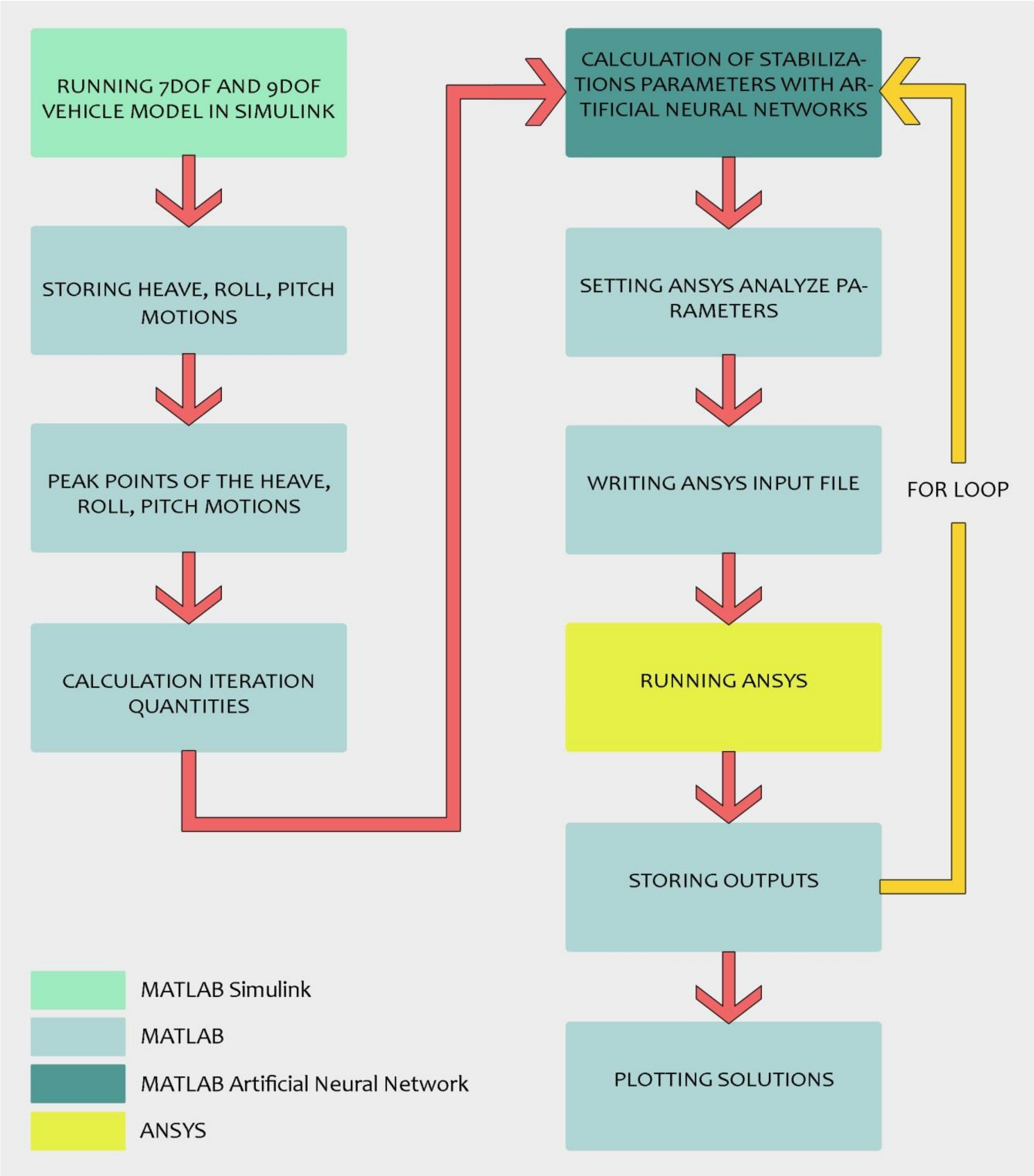

Figure 4-4 Simulation Algorithm

MATLAB are prepared the ANSYS input file which includes whole information for analysis like mechanical parts, geometrical information, material properties, loads, analysis settings. File format of the input file is text file and included FORTRAN programming language commands. This file can easily be manipulated via MATLAB.

```
/batch
/config,noeldb,1     ! force off writing results to database
*get,_wallstrt,active,,time,wall
! ANSYS input file written by Workbench version 14.0  Release
! File used for geometry attach: C:\Users\AHMET TATAR\AppData\Local\Temp\WB_AHMETTATAR_184_2\unsaved_project_files\dp0\SYS-1\DM\SYS-1.agdb
/title,unsaved_project--Transient (B5)
*DIM,_wb_ProjectScratch_dir,string,248
_wb_ProjectScratch_dir(1) = 'C:\Users\AHMET TATAR\AppData\Local\Temp\WB_AHMETTATAR_184_2\unsaved_project_files\dp0\SYS-1\MECH\'
*DIM,_wb_SolverFiles_dir,string,248
_wb_SolverFiles_dir(1) = 'C:\Users\AHMET TATAR\AppData\Local\Temp\WB_AHMETTATAR_184_2\unsaved_project_files\dp0\SYS-1\MECH\'
*DIM,_wb_userfiles_dir,string,248
_wb_userfiles_dir(1) = 'C:\Users\AHMET TATAR\AppData\Local\Temp\WB_AHMETTATAR_184_2\unsaved_project_files\user_files\'
/com,--- Data in consistent NMM units.
/units,MPA
/nopr
/wb,file,start              !  signify a WB generated input file
/prep7
! Turn off shape checking because checks already performed inside WB mesher.
! See help system for more information.
SHPP,OFF,,NOWARN
/nolist
etcon,set             ! allow ANSYS to choose best KEYOP's for 180x elements
/com,*********** Nodes for the whole assembly ***********
nblock,3
(1i8,3e20.9e3)
       1   -2.024281770E-002    1.475285303E+000    1.500000000E+001
       2    0.000000000E+000   -4.249154173E-015    1.500000000E+001
       3    0.000000000E+000   -4.249154173E-015    1.500000000E+001
       4   -2.024252087E-002    1.475285413E+000    3.000000000E+001
-1
/wb,elem,start            !  set before creation of elements
/com,*********** Elements for Body 1 "Solid" ***********
/com,*********** Send Body as a Rigid Body ***********
et,1,MASS21
keyo,1,2,1              ! Moments of inertia in nodal coordinates
keyo,1,3,0          ! 3D Mass With Rotary Intertia
r,1,7.68817779724411e-004,7.68817779724411e-004,7.68817779724411e-004,0.364853292089838,0.323564099705316,0.573587625682416
local,11,0,-2.02428177044433e-002,1.4752853033287,14.9999999999985,0.788836508504098,-5.32516476765898e-010,5.09171729504085e-010
nrot,1
csys,0
mat,1
real,1
type,1
en,1,1
/wb,elem,end               !  done creating elements
/com,*********** Send User Defined Coordinate System(s) ***********
local,12,0,0.,-4.24915417323598e-015,15.,-0.,0.,0.
csys,0
toffst,273.15,  ! Temperature offset from absolute zero
/com,*********** Set Reference Temperature ***********
```

Figure 4-5 ANSYS APDL command file

Disturbance values were generated with MATLAB SIMULINK vehicle model and stabilization parameters were produced by Artificial Neural Network. Disturbances and stabilization parameters have to put in the input file for each iteration. The relevant part of the variables are found by MATLAB and changed for each loop. Figure 4-6 shows motion and time inputs for ANSYS analysis.

```
real,2
type,2
en,8,1,4
/com,*********** Construct Remote Displacement Using RBE3/CERIG Contact ***********
*DIM,_loadvari47uy,TABLE,1,1,1,TIME,
! Time values
_loadvari47uy(1,0,1) = 1.
! Load values
_loadvari47uy(1,1,1) = 0.

*DIM,_loadvari47uz,TABLE,1,1,1,TIME,
! Time values
_loadvari47uz(1,0,1) = 1.
! Load values
_loadvari47uz(1,1,1) = 0.

*DIM,_loadvari47rotx,TABLE,1,1,1,TIME,
! Time values
_loadvari47rotx(1,0,1) = 1.
! Load values
_loadvari47rotx(1,1,1) = 0.

*DIM,_loadvari47roty,TABLE,1,1,1,TIME,
! Time values
_loadvari47roty(1,0,1) = 1.
! Load values
_loadvari47roty(1,1,1) = 0.

*DIM,_loadvari47rotz,TABLE,3,1,1,TIME,
! Time values
_loadvari47rotz(1,0,1) = 0.
_loadvari47rotz(2,0,1) = 1.
_loadvari47rotz(3,0,1) = 2.
! Load values
_loadvari47rotz(1,1,1) = 0.
_loadvari47rotz(2,1,1) = 0.174532925199433
_loadvari47rotz(3,1,1) = 0.349065850398866

/COM,*** Created for Use in Spectrum Analysis ***
CMBLOCK,REMOTEDISPALL,NODE,        1
```

Figure 4-6 Motion inputs for ANSYS input file

It is also possible to put commands in the input file which information will be output for the results. Figure 4-7 are shown to command for producing to the output file.

```
/POST1
*GET,MAXNODE,NODE,0,NUM,MAX
*GET,MINNE,NODE,0,NUM,MIN
*DO,i,MINNE,MAXNODE
/OUT,ANSYS_SOLUTIONS_V51,txt,,APPEND
*VWRITE,i,NX(i),NY(i),NZ(i),UX(i),UY(i),UZ(i),ROTX(i),ROTY(i),ROTZ(i)
(1X,F20.10,' ',F20.10,' ',F20.10,' ',F20.10,' ',F20.10,' ',F20.10,' ',F20.10,' ',F20.10,' ',F20.10,' ',F20.10)
/OUT
*ENDDO
```

Figure 4-7 Result command in the input file

Output file format was identified as text file and this file is included node numbers, coordinate of the points, displacements on x,y,z directions and rotational displacements on x,y,z directions. Figure 4-8 shows output values according to node numbers of the solutions.

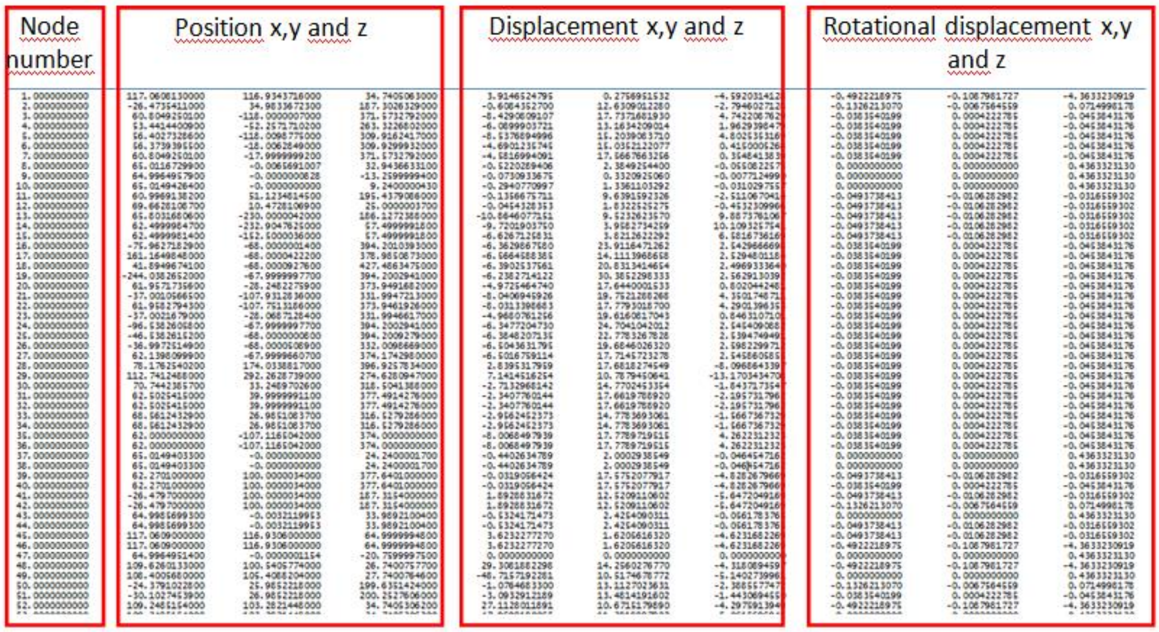

Figure 4-8 Output values according to nodes

Disturbances come from directional-z, rotational-x and rotational-y axes. Turret is opposed to disturbances with Articial Neural Network tool and tough the answers with its neural networks. Stabilization parameters were calculated with equations which were given in chapter 3.1.2. Problem was evolved to plot fitting until these point because disturbances and answers of the system are known. Therefore, in this scope Neural Fitting application was used for calculating stabilization parameters.

Inputs and targets data are put in the tool. Each data set are included approximately 2000 samples and 70% of the data was used for training 15% was used validation and %15 was used for testing. Training data is presented to the network during training and the networks is adjusted according to its error. Validation data is used to measure network generalization and to halt training when generalization stops improving. Testing data has no effect on training and so provide and independent measure of network performance during and after training. After selecting to percentages of the data, hidden neuron quantities are specified.

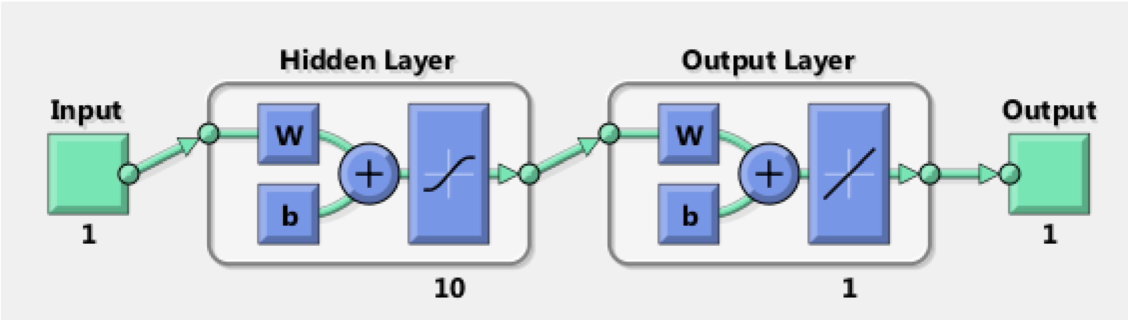

Figure 4-9 Block scheme of the neural network

There are 3 different training algorithm in the Neural Network tool and each algorithm has different behavior. Levenberg-Marquardt algorithm is used for this simulation. Finally, training is started and results are taken. Figure 4-10 shows to elevation axis corrections against to heave motions. Similar calculations were made for pitch and roll axis to calculating both elevation and azimuth axis stabilization values.

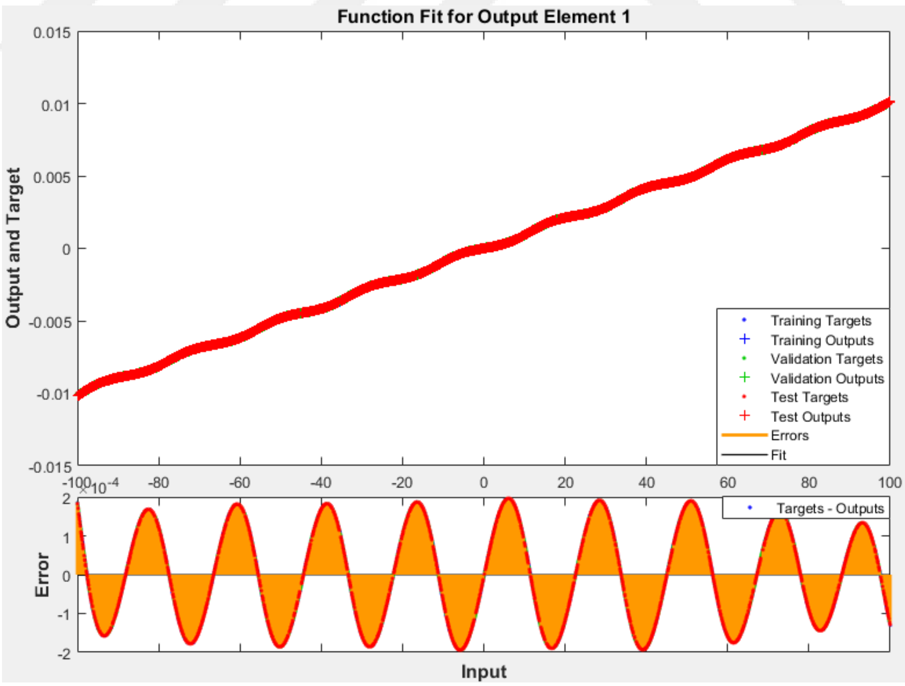

Figure 4-10 Fitting solutions of the elevation axis stabilization values against to heave disturbances

Mean squared error and regression values find as Figure 4-11. Mean squared error is the average squared difference between inputs and targets. As seen the Figure 4-11 errors are close to zero. Regression values measure the correlation between outputs and targets. Close to 1 values gives best relation.

	Samples	MSE	R
Training:	14001	1.58304e-8	9.99761e-1
Validation:	3000	1.57799e-8	9.99768e-1
Testing:	3000	1.62758e-8	9.99754e-1

Figure 4-11 Mean square error and regression values for elevation stabilization

Similar steps were proceed for other elevation and azimuth stabilization values against to pitch, roll disturbances.

4.2 Modelling Systems

4.2.1 Building Vibration model of Vehicle on MATLAB

There are several methods for building vibration model on MATLAB. The model can be built with state-space equations of the vehicle on script file or command window on the MATLAB. Furthermore, the model can be designed at Simulink tool with a few methods. Simulink is the powerful tool of MATLAB for simulating Mechanic, Electronic, Electric, Economic, etc. problems. In this study, Simulink function block method was used.

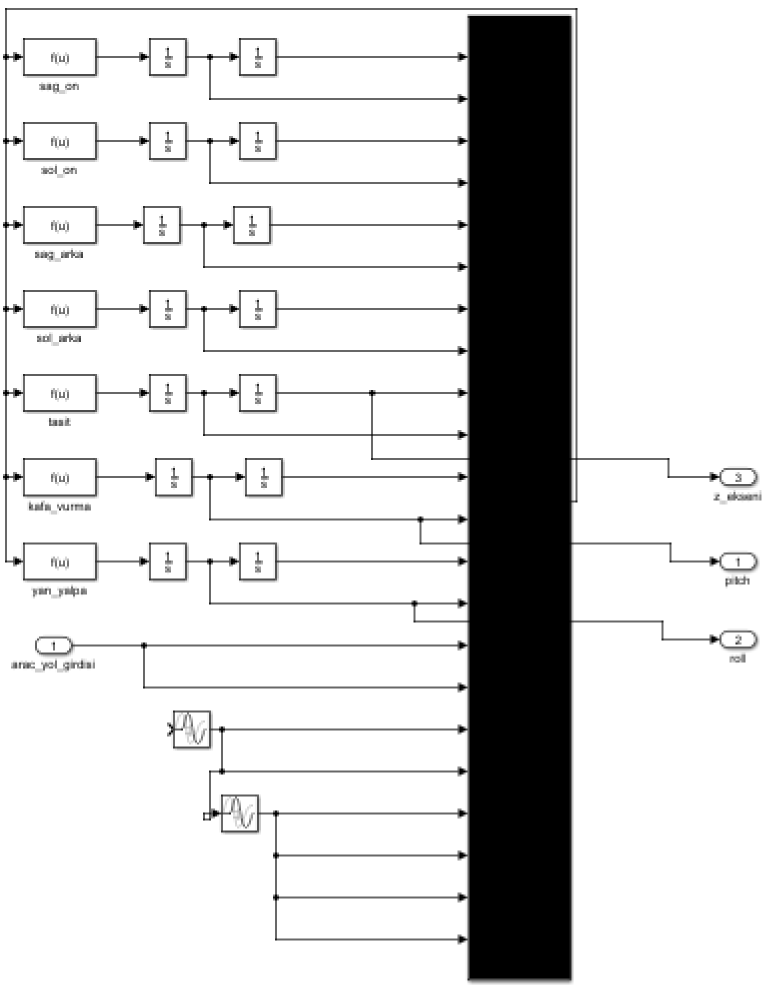

Figure 4-12 Simulink Block diagram of 7 DOF model

According to this method, each motion equations are written in the function blocks. Blocks first and second order integrals are connected with other blocks.

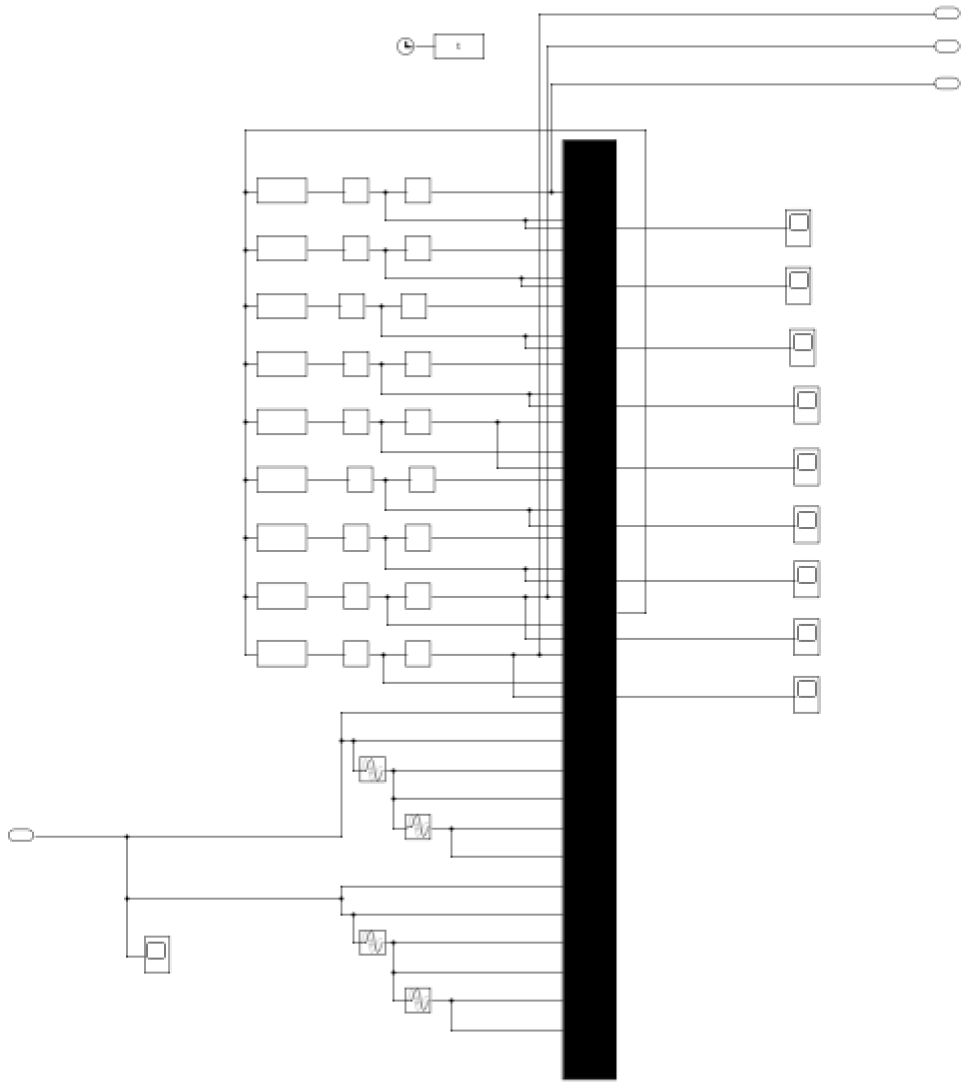

Figure 4-13 Simulink Block diagram of 9 DOF model

Vehicle wheels are stimulated with the APG (Aberdeen Proving Ground) course track while 15km/h, 30 km/h, and 50 km/h.

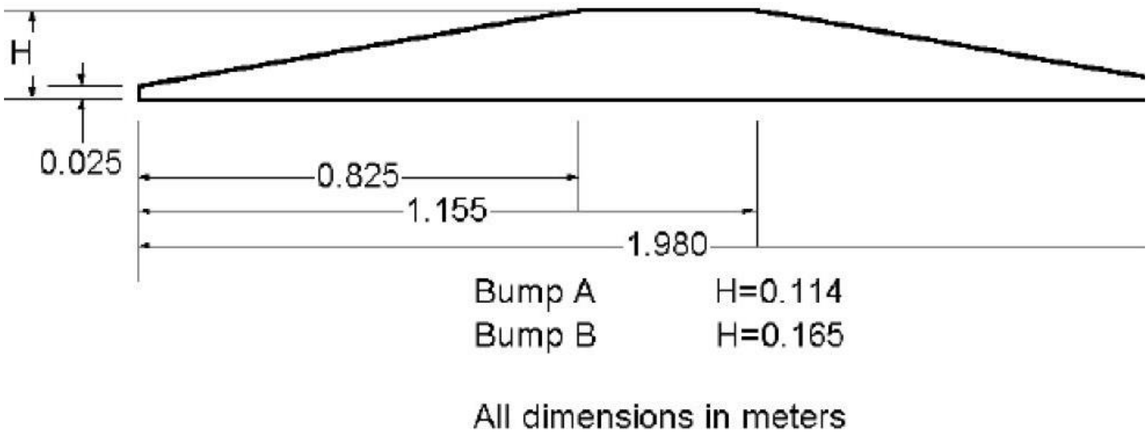

Figure 4-14 The APG course dimensions [3]

Simulink input of APG course for 15km/h was given in Figure 4-15.

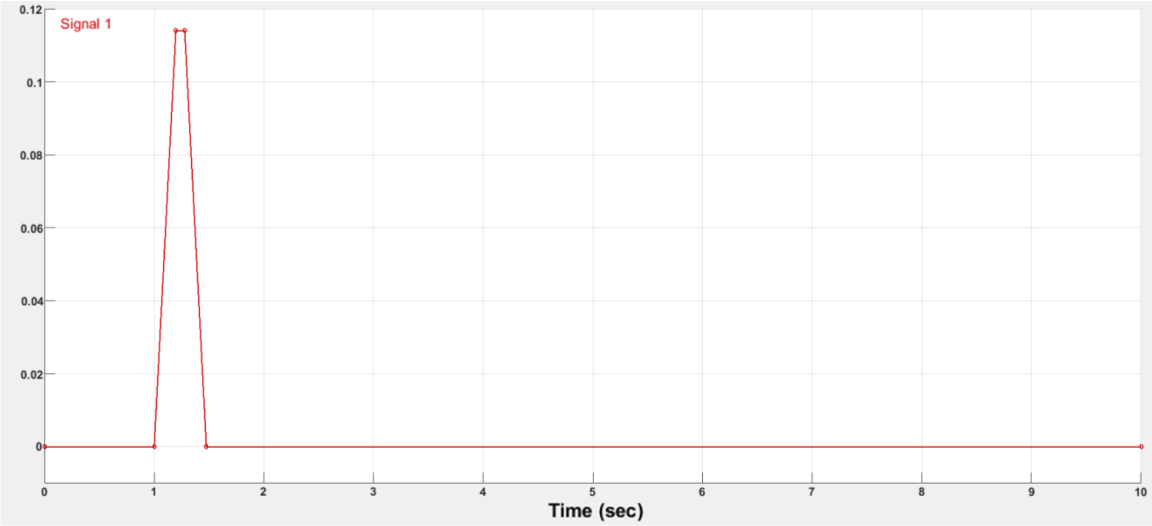

Figure 4-15 Track non-uniform input

APG courses are placed on track one of left side the other right side of the track as given in Figure 4-16. Distance of the obstacles is about 5 meters. Simulations were run according to these inputs.

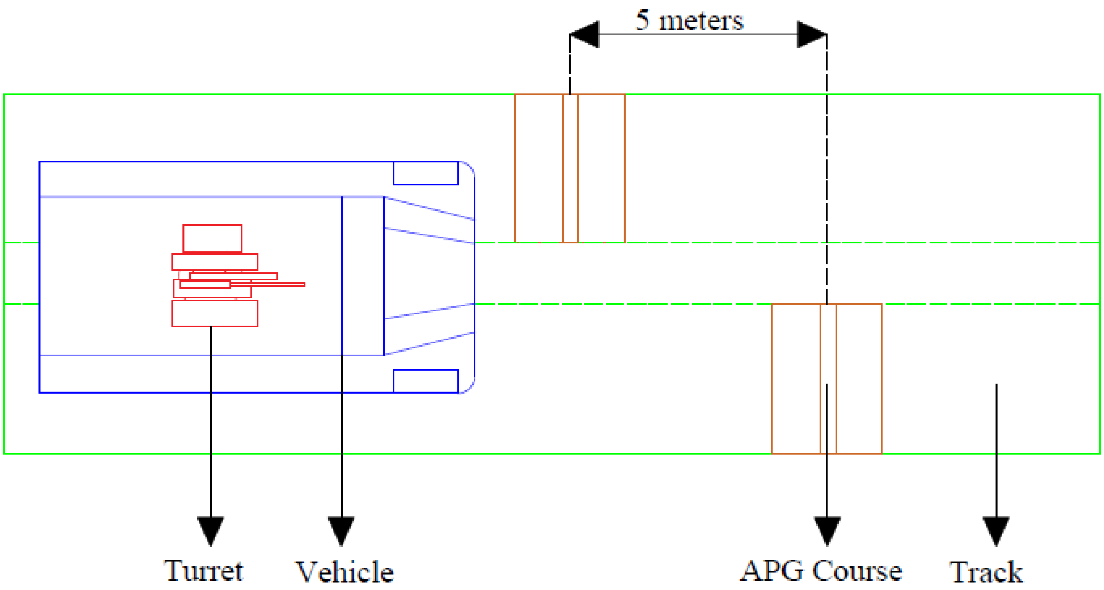

Figure 4-16 Simulation scenario of vehicle

4.2.2 Building Turret Mechanics in MATLAB SIMULINK

As mentioned in previous chapters, the degree of freedom of the turret is two. This means turret has to control two axis which is elevation and azimuth. The system rotate around these axes. Each axis includes gear mechanism.

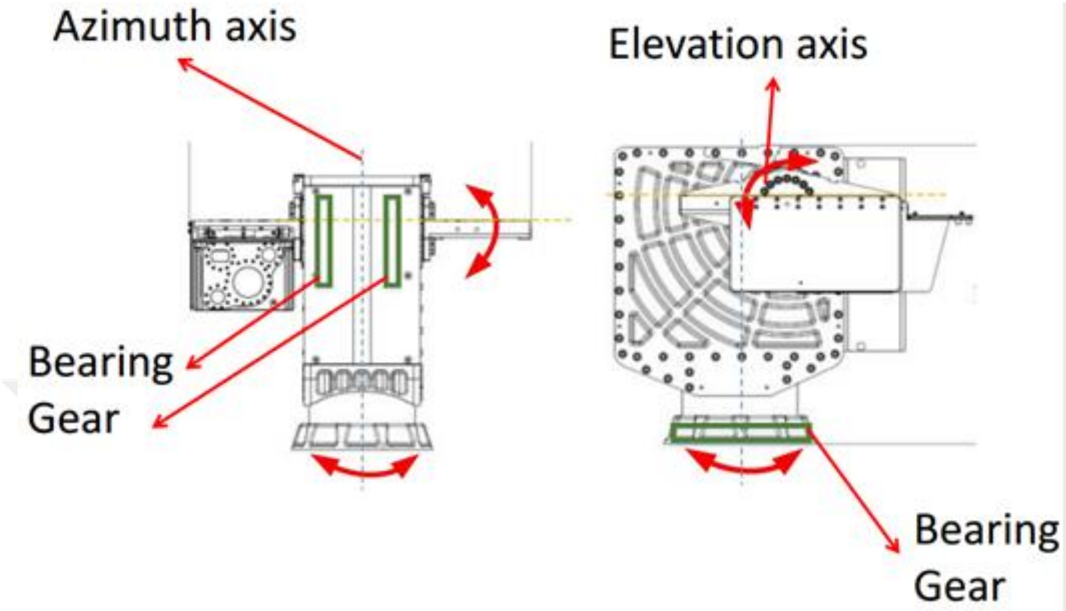

Figure 4-17 Structure of the turret

Simulink Sim-Mechanic tool is given a right approach for the dynamic analysis of the mobile mechanisms. 3D mechanical systems can be simulated with using this tool. Each part of the system can be represented with body blocks. Joints, constrains and sensors can be added and measured the dynamic parameters of the system.

Turret system was modeled in Simulink Sim-Mechanic. Then the turret was installed on the vehicle model in the Simulink. When vehicle move on z, pitch and roll axis, turret stabilize itself against to vehicle motions.

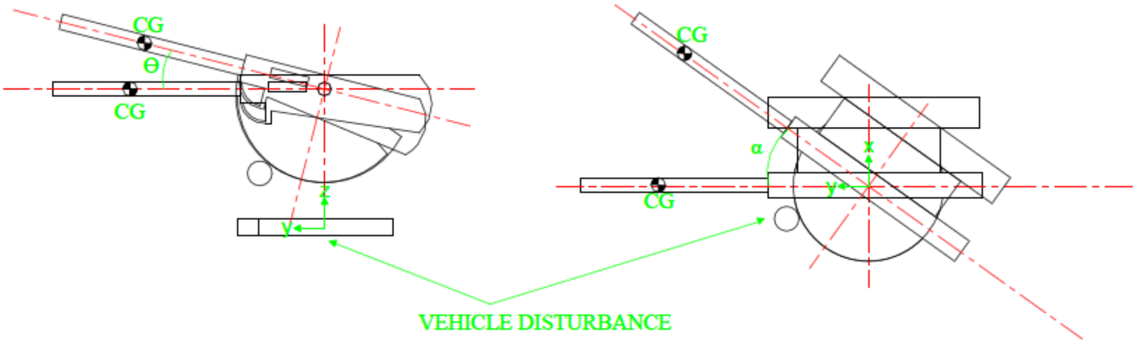

Figure 4-18 Turret motion axes

The turret is a mechanism, and muzzle endpoint is the point to be directed. Therefore the important thing for the SIMULINK model of the turret is that modeling to the position of muzzle endpoint with gear mechanism.

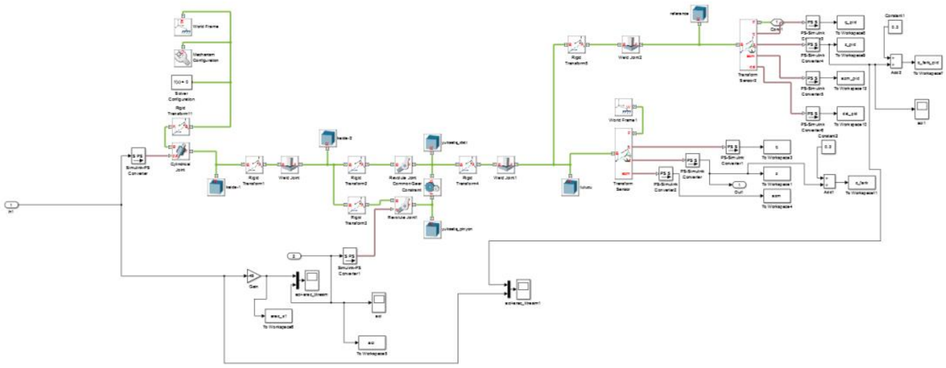

Figure 4-19 Simulink block diagram of the turret

Vehicle and turret are connected each other with relations. Block diagram of the connections as follows;

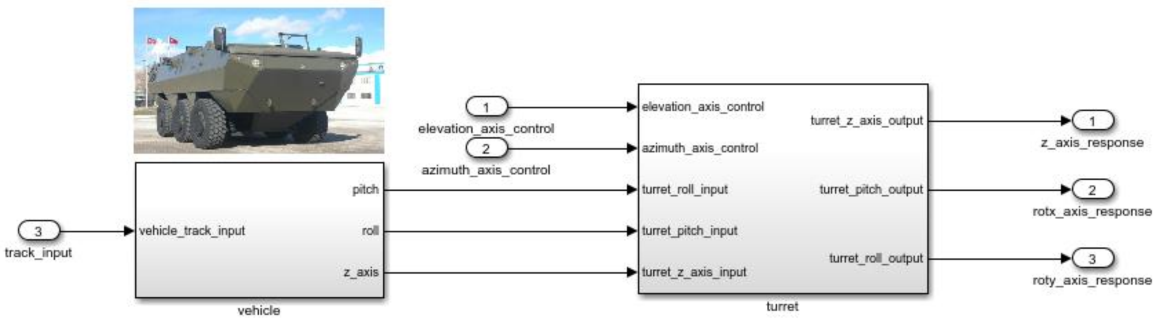

Figure 4-20 Turret-Vehicle connections

Turret controls, elevation and azimuth axis, with PID controller. PID is the primary controller, easy to tune, easy to apply and there are many works for it in the literature. PID controller can be mostly used this kind of steering processes.

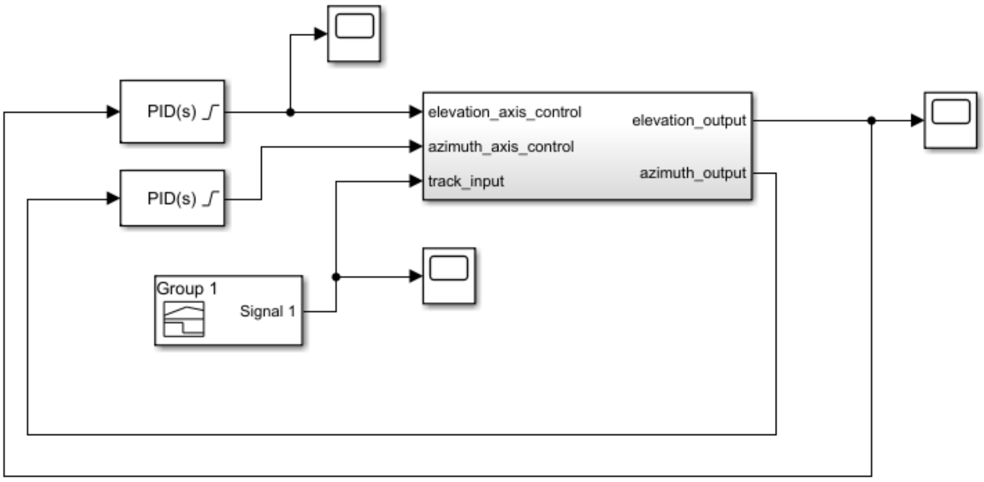

Figure 4-21 PID controlled plant

Disturbance of the system was detected a position sensor and proceed with PID controller. Control parameters were sent to elevation and azimuth motors and system correct itself against to disturbances. Figure 4-22 is shown control diagram of the system.

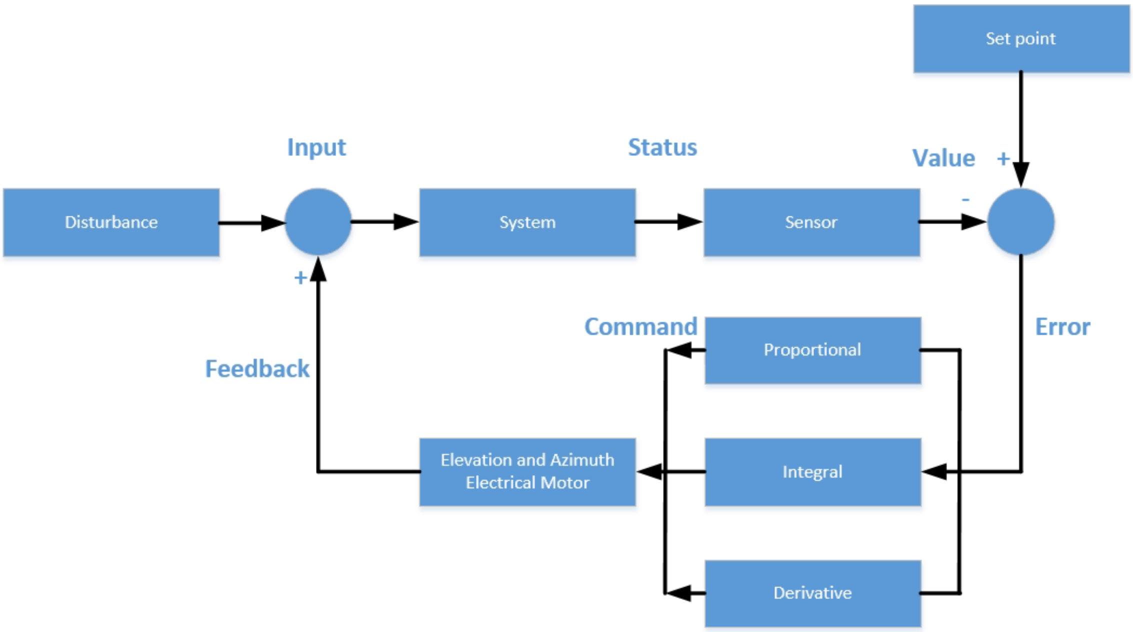

Figure 4-22 PID Control diagram of the turret

PID values, define for achieve performance and meet requirements. There are several methods for tuning to find value of proportional, integral and derivative gains. According to traditional method PID controller is tuned manually or rule-based methods. Traditional methods takes time because of iterative processes or include serious limitations. MATLAB Control System Toolbox provide to automatic tuning. In this scope this toolbox was used for PID tuning and values were given in Table 4-1.

Table 4-2 Proportional, Integral and Derivative values

	7 DOF Vehicle	9 DOF Vehicle
K_P	0.0165	0.0246
K_I	0.0135	0.0361
K_D	0.0148	0.0312

4.2.3 Modeling Turret System on ANSYS

Engineering systems usually have complex physical inputs and being many kinds of parts and their relations. Virtual simulation programs help to understand and optimize interactions between physic, control and environment effects. ANSYS is one of the dominant engineering analysis tools, and in this scope, ANSYS is used for physical simulations of the system. Turret has various kind of sub-systems like electrical motors, reductors, electro optic systems, gear systems, firing systems, etc. Flexibility of the sub-system mechanics are affected aiming precision of the weapon. It is hard to observing these effects for whole parts. However, gears are caused the most dominant flexibility effects on the turret system. For searching flexibility effects of the gears on the aiming, turret was modeled in ANSYS.

According to this model, elevation and azimuth gears are flexible and the other parts are rigid. For minimizing to simulation time and lighten the model, fasteners, electronic components, electrical motors, connectors and the other insignificant parts for this analysis were removed and point masses were assigned instead of these parts. Joints and contacts types were directly affected simulation time and accuracy. Some contact and joints types can be shown simple mathematical relations and givens right approach.

First step of the modeling turret in ANSYS is importing geometry, cleaning insignificant parts and assigning point mass instead of removed parts. Secondly, contacts and joints were assigned, this step is very important for accuracy of the analysis. Meshing operations are made automatically in Transient Structure tool of the ANSYS, but mesh size, relevance, shape can be tuned. Finally, inputs were introduced the simulation, for these simulations while turret fixed to the ground, azimuth and elevation motions values introduced.

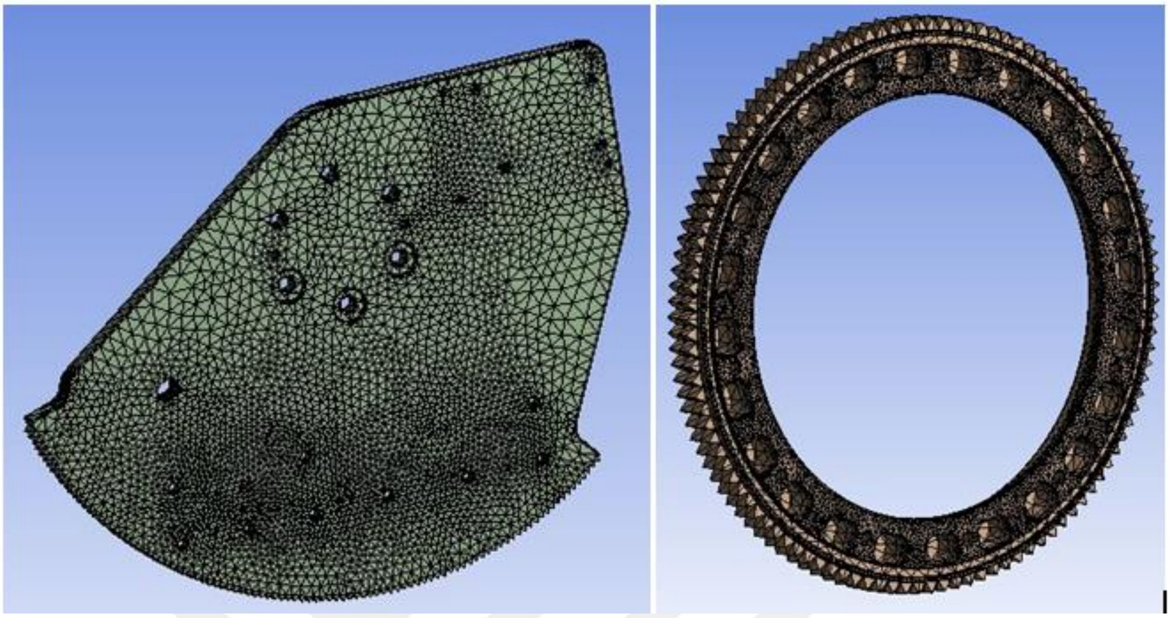

Figure 4-23 Elevation and Azimuth Gear meshing operation

Elevation and azimuth motions were investigated separately but system inputs are same. Basic inputs of the simulation were given following,

- Turret was fixed to the ground,
- Reaching 60º/s velocity with 90º/s^2 acceleration,
- Point masses instead of insignificant parts,
- Contacts and joints,
- Gravity (z direction 9,81m/s^2),
- Material properties

Outputs of the simulation,

- Muzzle displacements
- Fatigue life of the gears

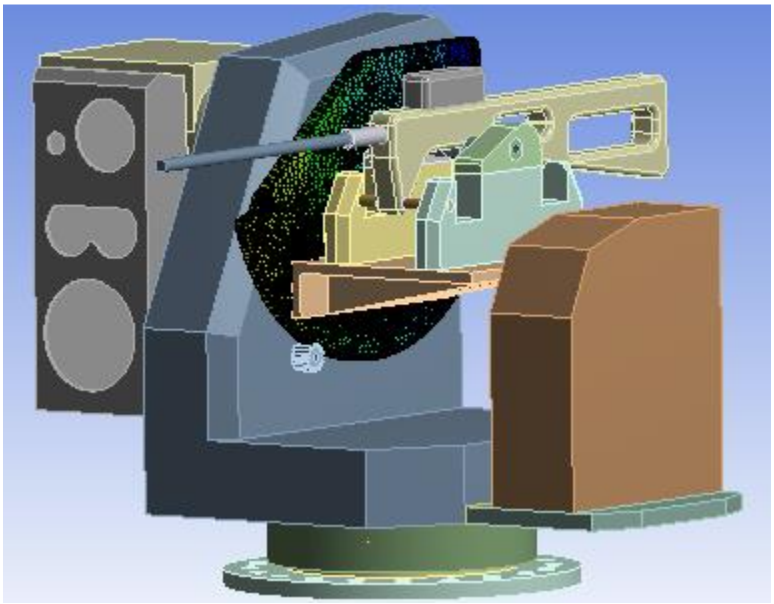

Figure 4-24 ANSYS Turret model

5 RESULTS AND DISCUSSIONS

5.1 MATLAB Vehicle Simulation Results

Two different vehicles were simulated under three cases for this section. Each vehicle is simulated 15km/h, 30km/h, and 50km/h velocities and observed the displacement of z, roll and pitch axes.

5.1.1 4 Wheels 7 DOF Vehicle Simulation Results

4 wheels 7 DOF vehicle is simulated at 15km/h velocity and displacements were given in Figure 5-1.

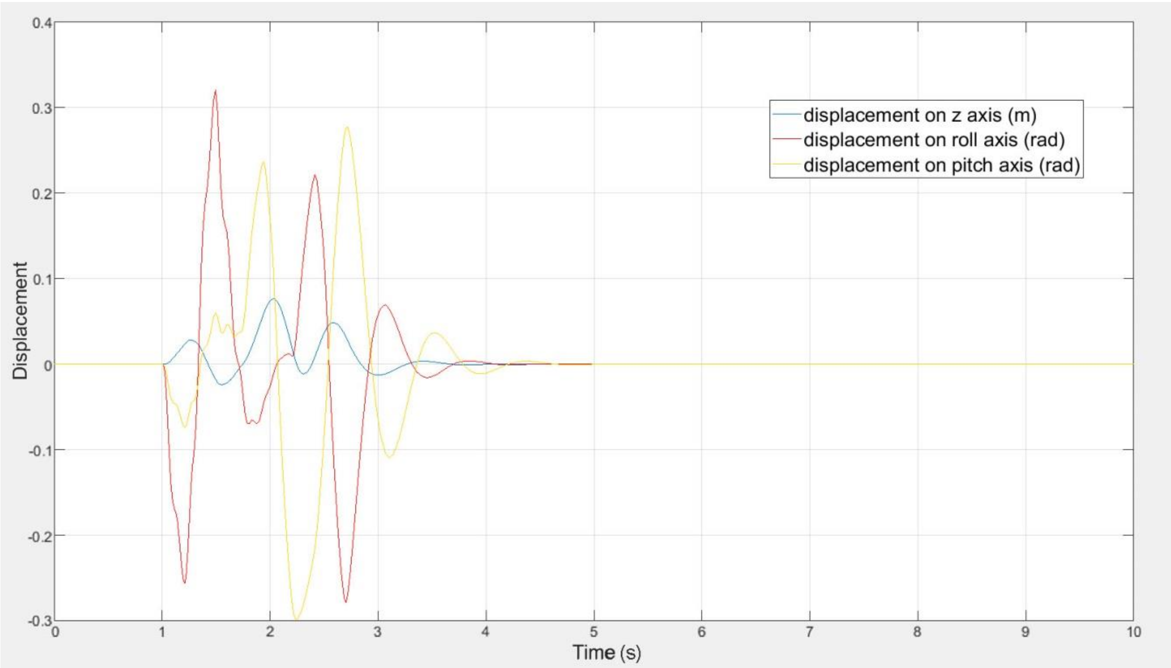

Figure 5-1 7 DOF vehicle 15km/h velocity displacements on z, roll and pitch axis

4 wheels 7 DOF vehicle is simulated at 30km/h velocity and displacements were given in Figure 5-2.

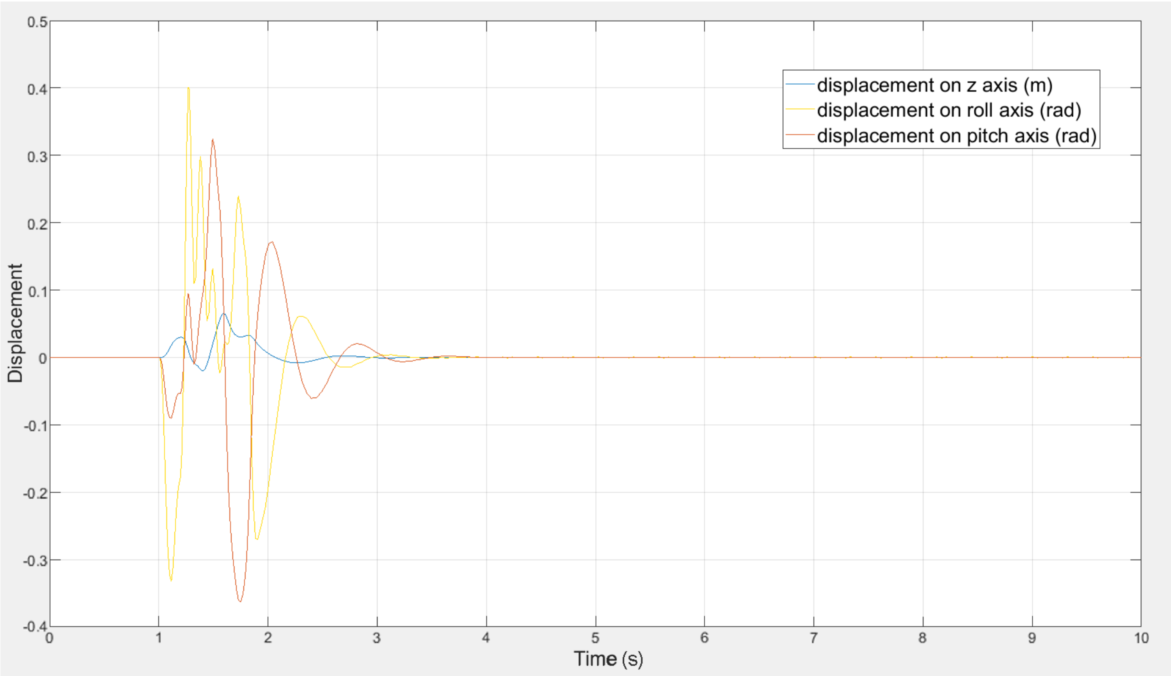

Figure 5-2 7 DOF vehicle 30km/h velocity displacements on z, roll and pitch axis

4 wheels 7 DOF vehicle is simulated at 50km/h velocity and displacements were given in Figure 5-3.

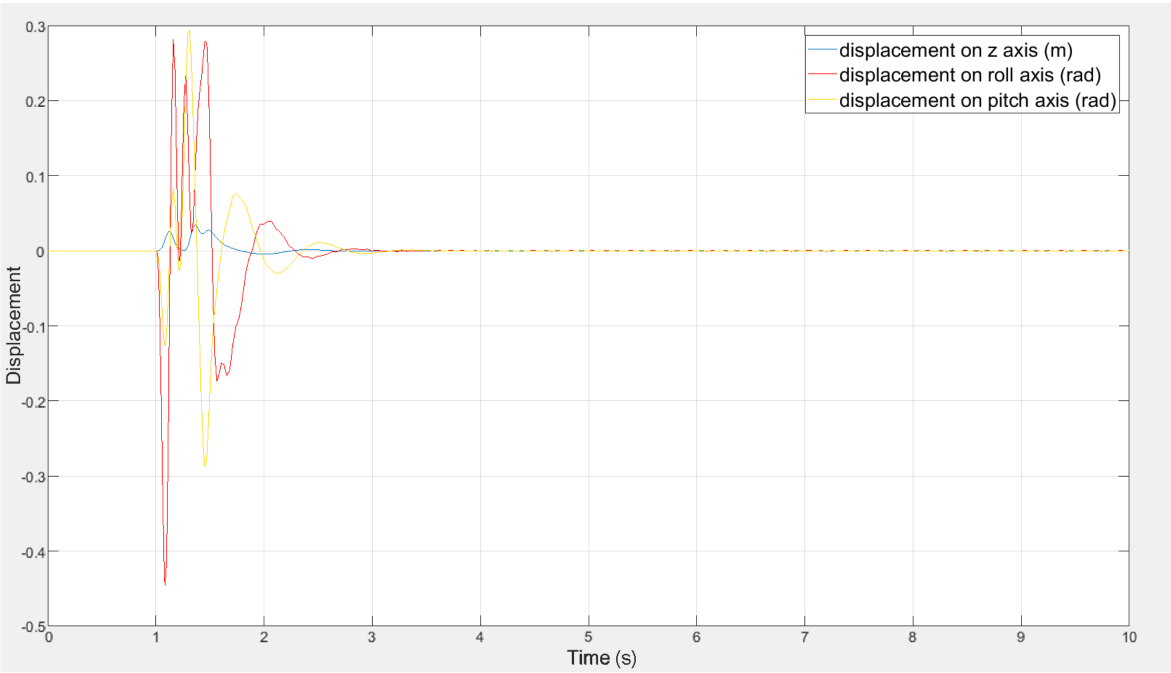

Figure 5-3 7 DOF vehicle 50km/h velocity displacements on z, roll and pitch axis

As seen the charts, the amplitude of the displacements changed with time. However, characteristics of the curves are similar for all velocities.

5.1.2 6 Wheels 9 DOF Vehicle Simulation Results

6 wheels 9 DOF vehicle is simulated at 15km/h velocity and displacements were given in Figure 5-4.

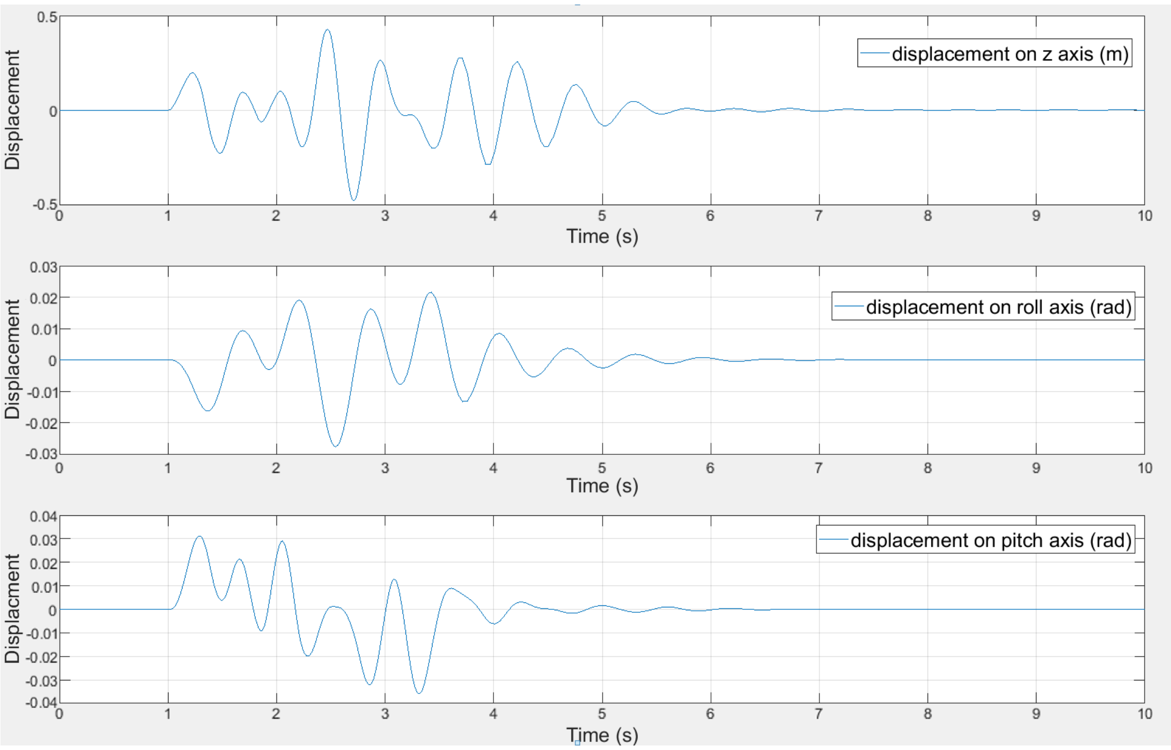

Figure 5-4 9 DOF vehicle 15km/h velocity displacements on z, roll and pitch axis

6 wheels 9 DOF vehicle is simulated at 30km/h velocity and displacements were given in Figure 5-5.

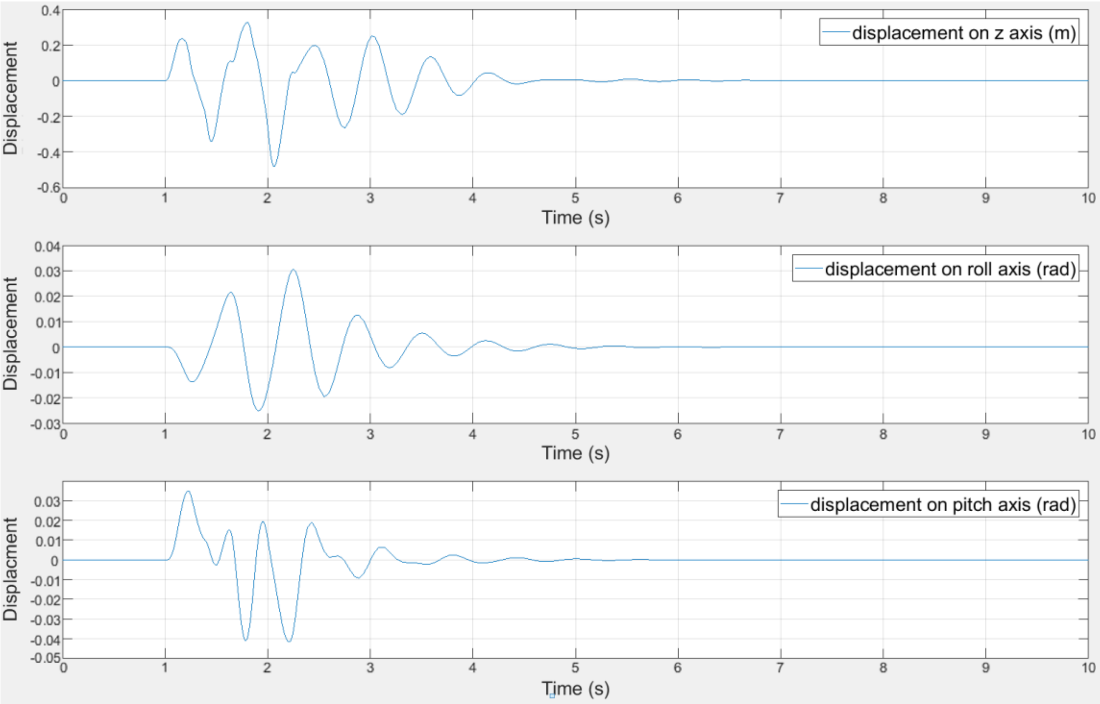

Figure 5-5 9 DOF vehicle 30km/h velocity displacements on z, roll and pitch axis

6 wheels 9 DOF vehicle is simulated at 50km/h velocity and displacements were given in Figure 5-6.

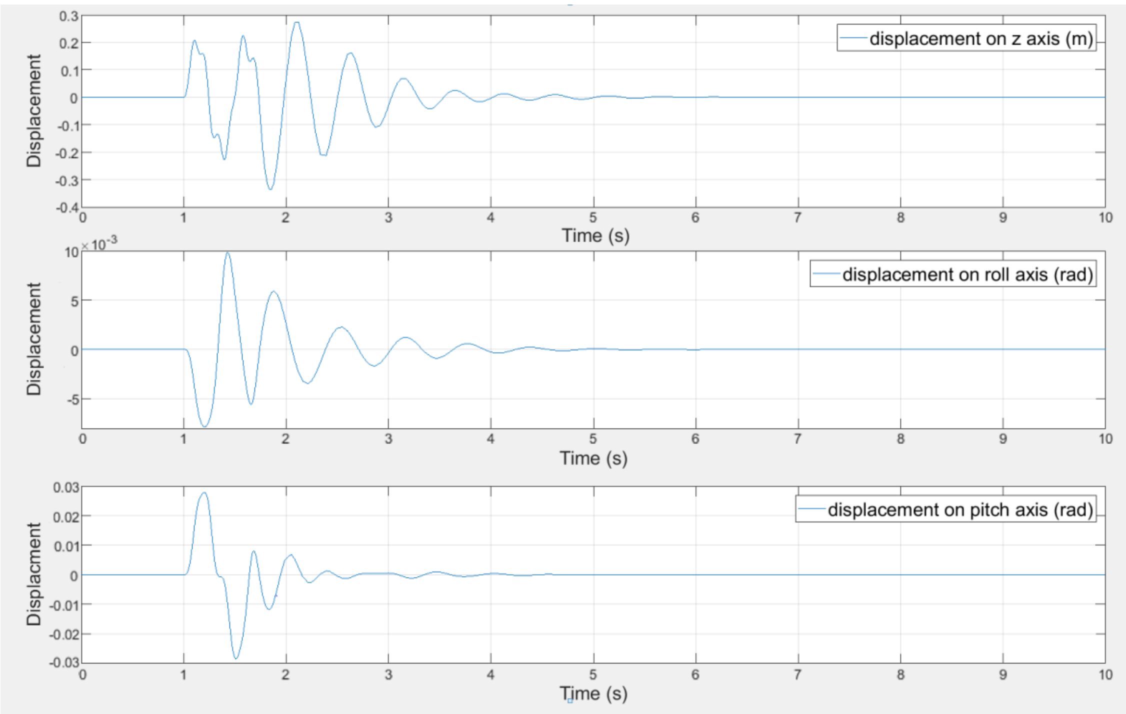

Figure 5-6 9 DOF vehicle 50km/h velocity displacements on z, roll and pitch axis

Results are similar to 4 wheels vehicle. As seen the charts, the amplitude of the displacements changed with time. However, characteristics of the curves are similar for all velocities.

5.2 MATLAB Turret Integrated and PID Controlled Vehicle Results

As seen the previous sections, when the vehicle passes on an obstacle, the physical structure of vehicle generate displacements. A muzzle endpoint has to affect as minimum as possible from these displacements for high accuracy target tracing. Turret compensates against the distributions because of to keeping weapon right position.

The turret steer against to distributions with PID controller at this section. The turret was integrated on the 4 wheels 7 DOF and 6 wheels 9 DOF vehicles. Moreover, vehicles passed obstacle track with 15km/h, 30km/h, and 50km/h velocities.

5.2.1 PID Controlled Turret Integrated 4 Wheels 7 DOF Vehicle

Displacement of the muzzle x, y and z-axis for 15km/h were given in Figure 5-7.

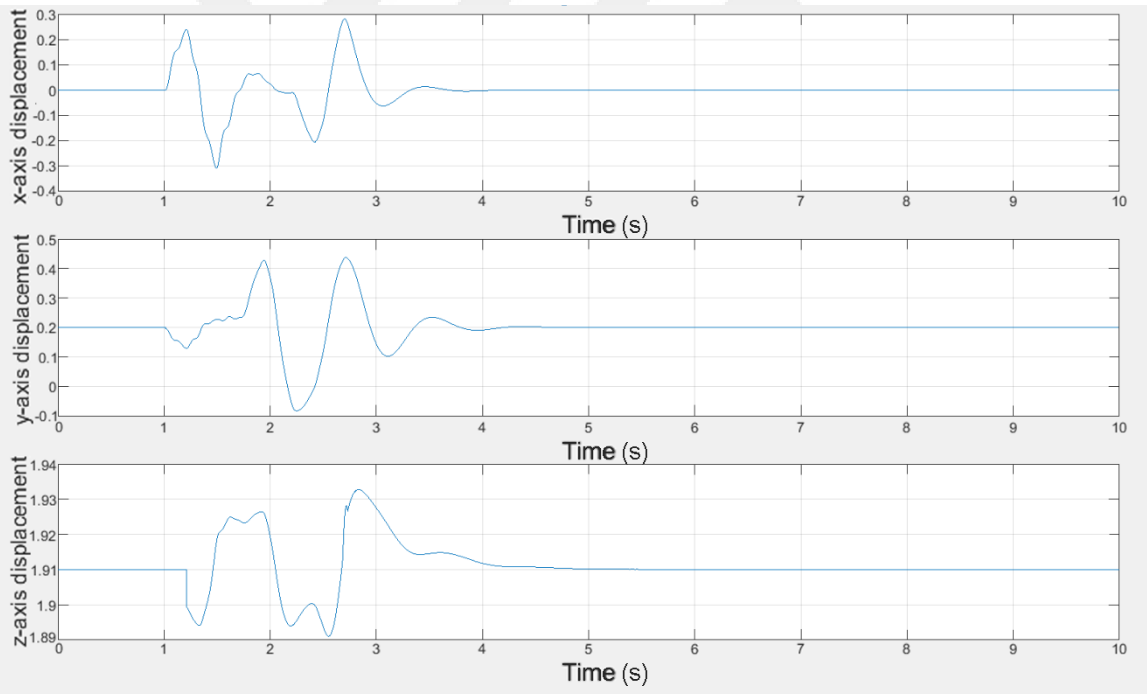

Figure 5-7 7 DOF vehicle 15km/h velocity PID controlled Turret displacements of muzzle (m)

,

Angular velocities of x, y and z-direction of the muzzle were given in Figure 5-8.

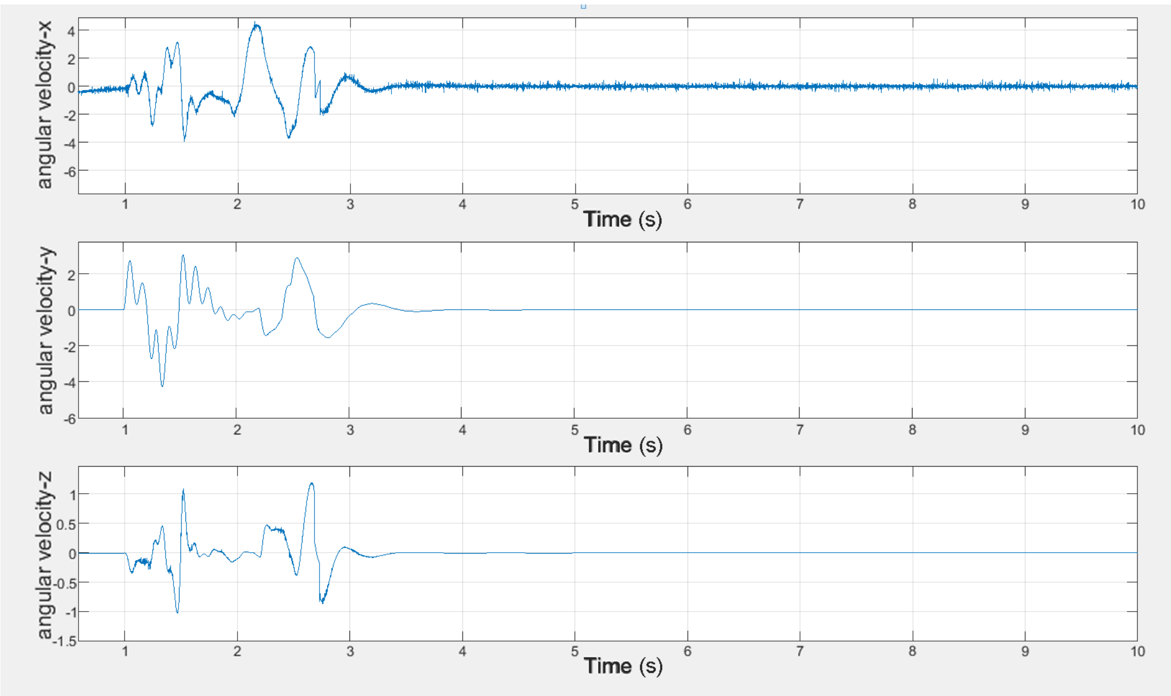

Figure 5-8 7 DOF vehicle 15km/h velocity PID controlled Turret angular velocities of muzzle (rad/s)

The weapon was affected mostly displacement of z and roll axis. Displacement difference on z-axis between muzzle and vehicle were given in Figure 5-9. As seen, the amplitude of the muzzle displacement lower than the vehicle.

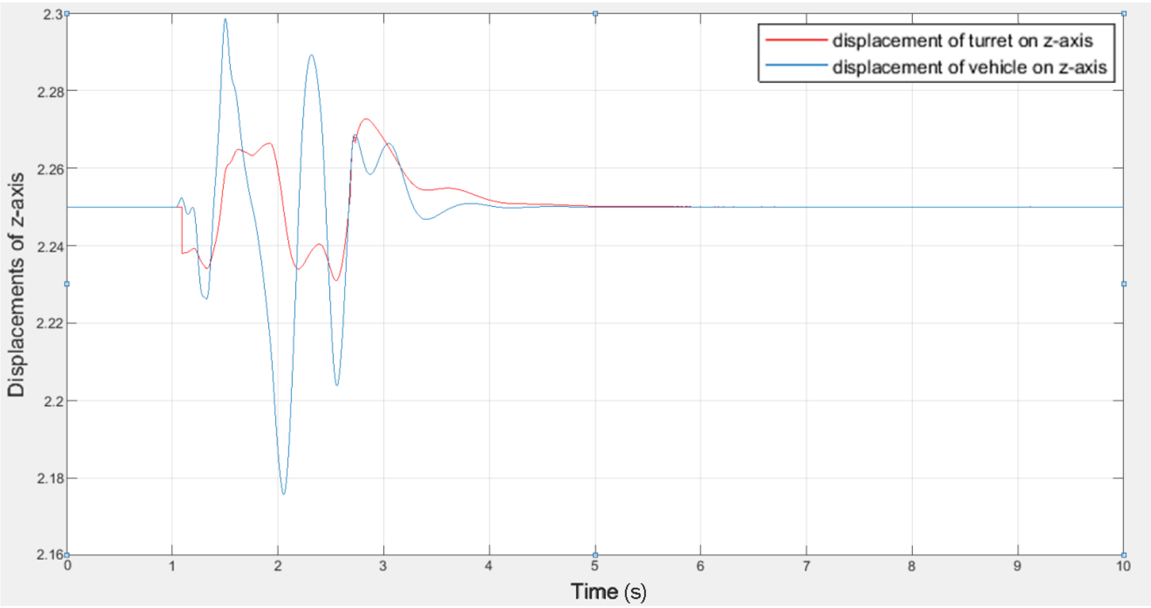

Figure 5-9 7 DOF vehicle 15km/h velocity PID controlled comparing z displacement between vehicle and muzzle (m)

Displacement of the muzzle x, y and z-axis for 30km/h were given in Figure 5-10.

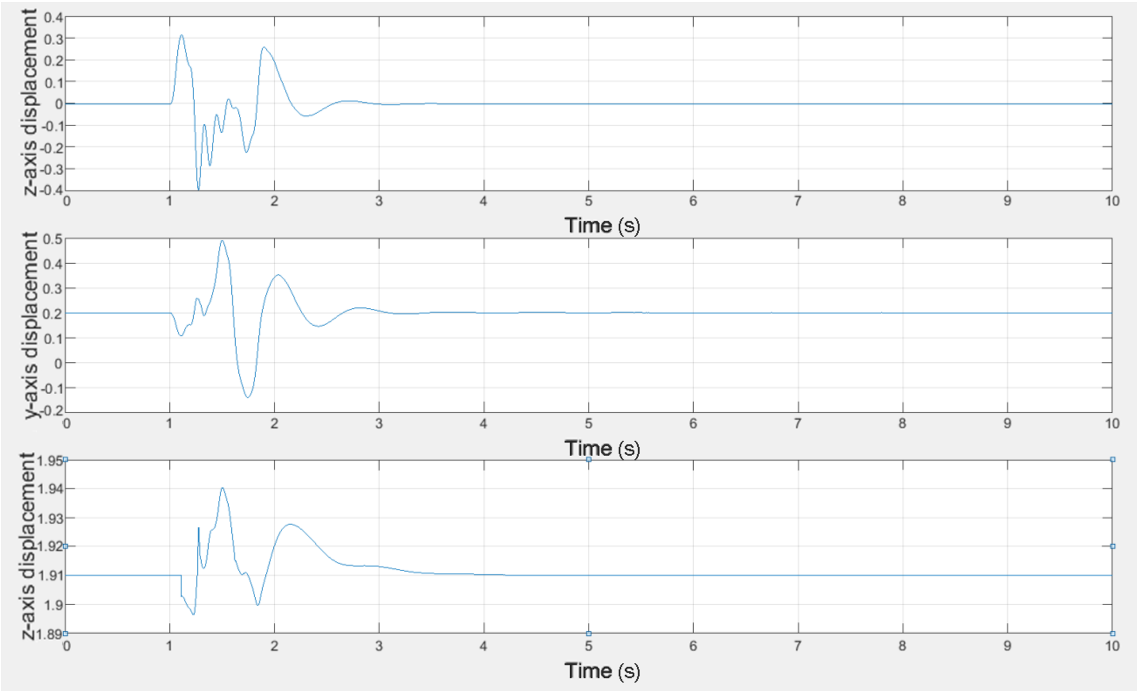

Figure 5-10 7 DOF vehicle 30km/h velocity PID controlled Turret displacements of muzzle (m)

Angular velocities of x, y and z-direction of the muzzle were given in Figure 5-11.

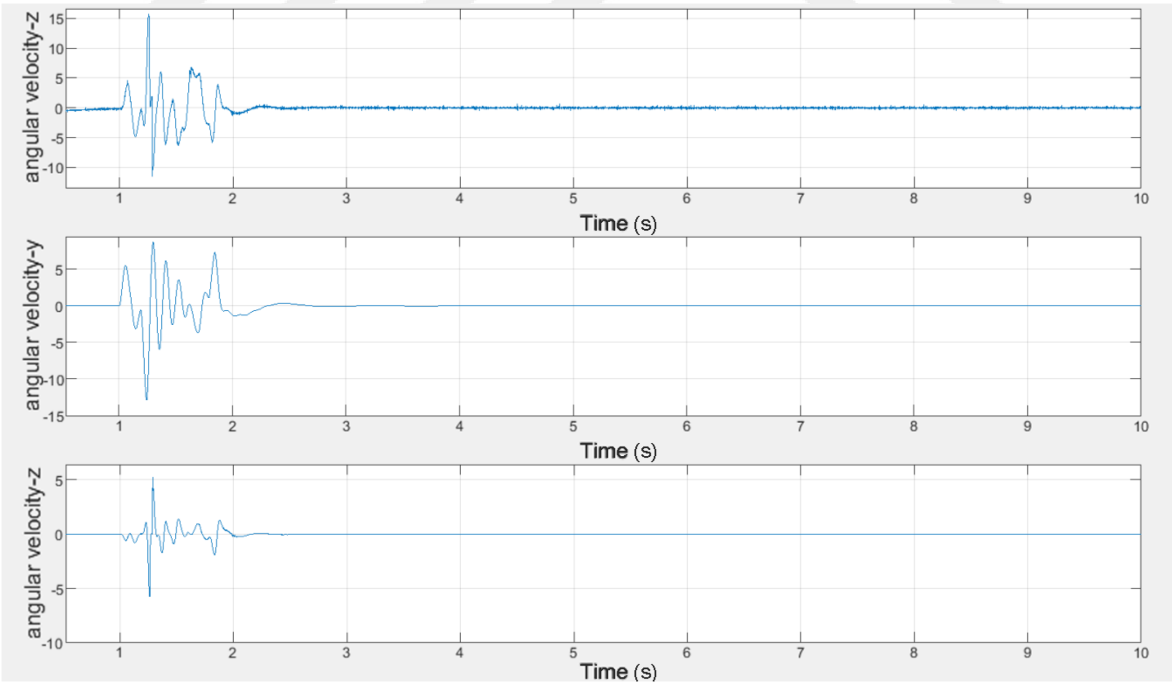

Figure 5-11 7 DOF vehicle 30km/h velocity PID controlled Turret angular velocities of muzzle (rad/s)

Displacement difference on z-axis for 30km/h between muzzle and vehicle were given in Figure 5-12.

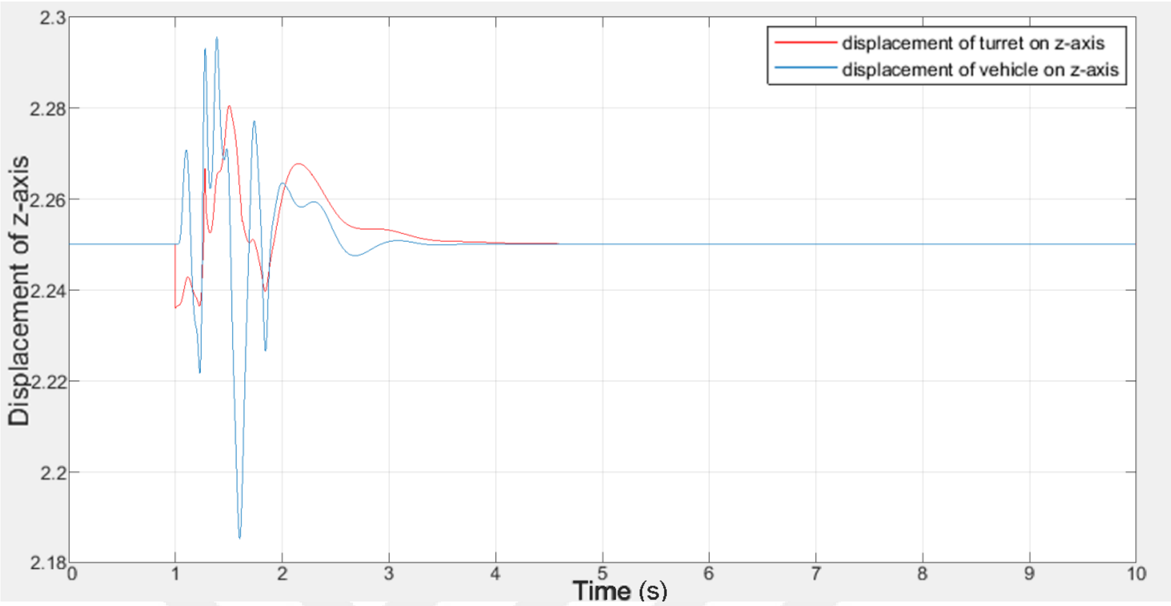

Figure 5-12 7 DOF vehicle 30km/h velocity PID controlled comparing z displacement between vehicle and muzzle (m)

Displacement of the muzzle x, y and z-axis for 50km/h were given in Figure 5-13.

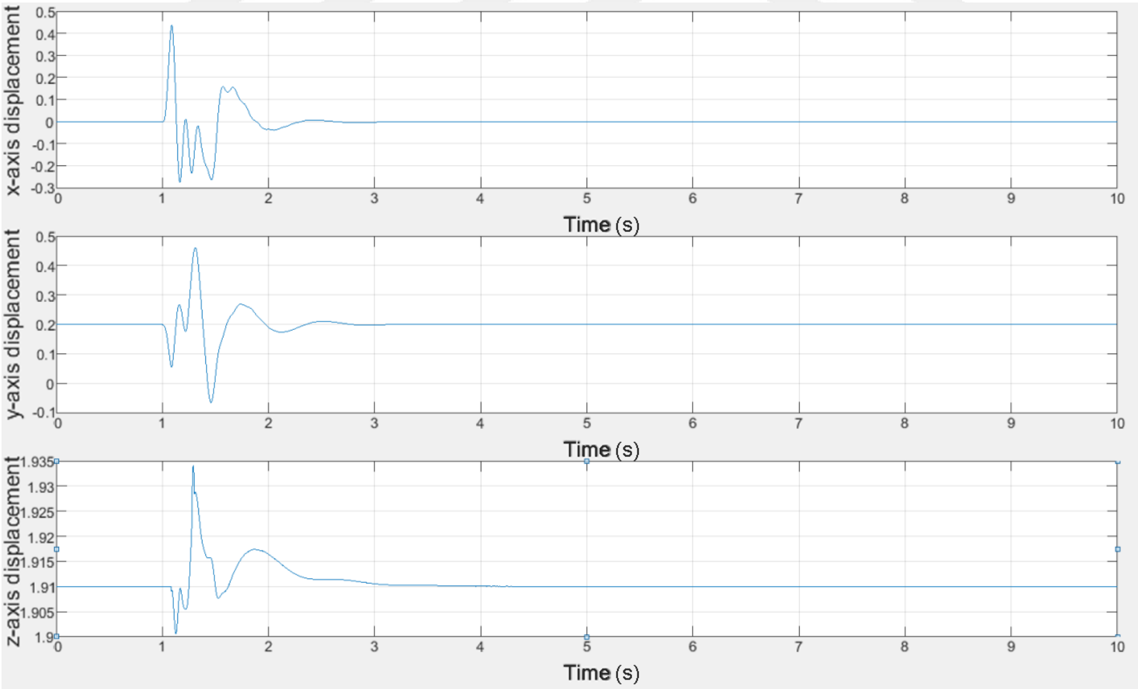

Figure 5-13 7 DOF vehicle 50km/h velocity PID controlled Turret displacements of muzzle (m)

Angular velocities of x, y and z-direction of the muzzle were given in Figure 5-14.

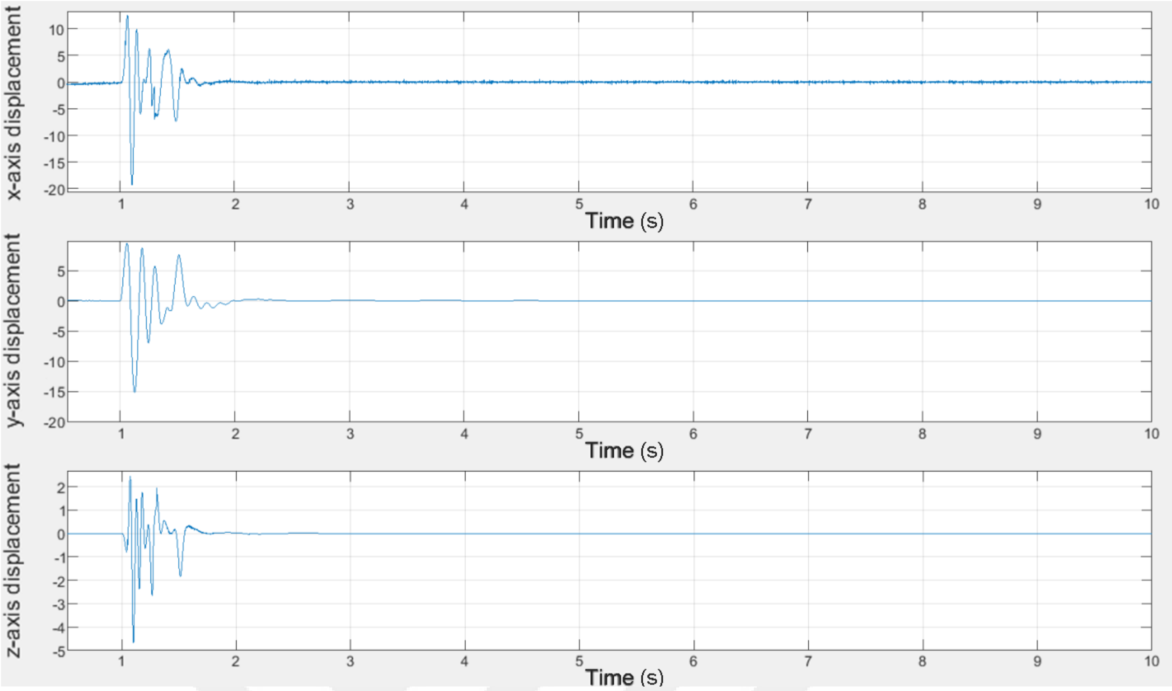

Figure 5-14 7 DOF vehicle 50km/h velocity PID controlled Turret angular velocities of muzzle (rad/s)

Displacement difference on z-axis for 50km/h between muzzle and vehicle were given in Figure 5-15.

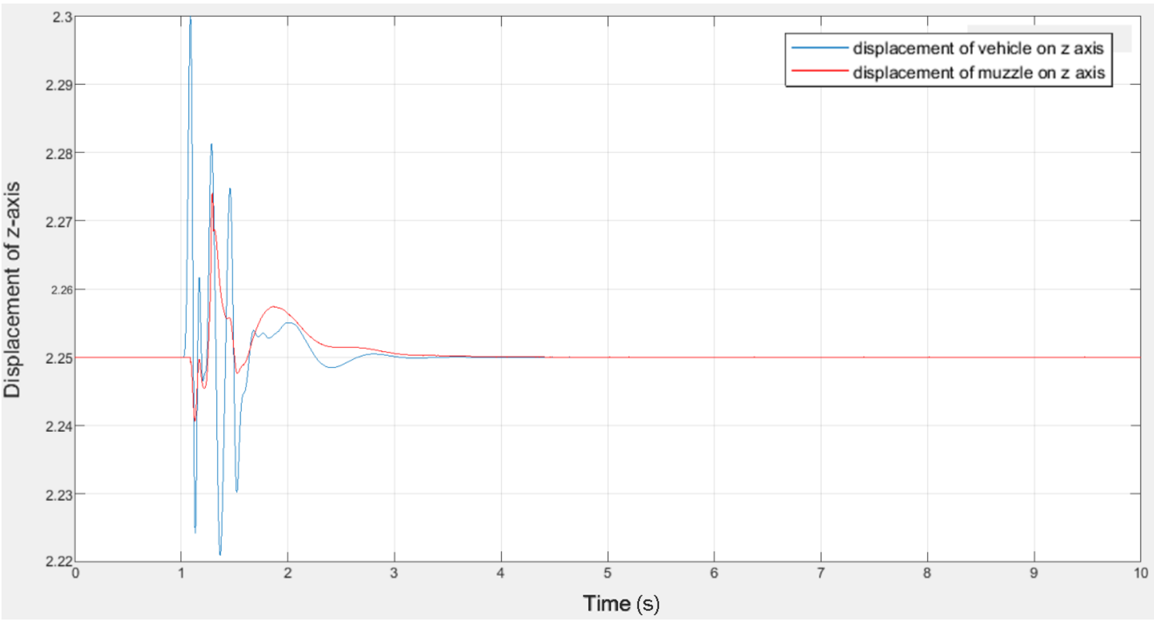

Figure 5-15 7 DOF vehicle 50km/h velocity PID controlled comparing z displacement between vehicle and muzzle (m)

5.2.2 PID Controlled Turret Integrated 6 Wheels 9 DOF Vehicle

Displacement of the muzzle x, y and z-axis for 15km/h were given in Figure 5-16.

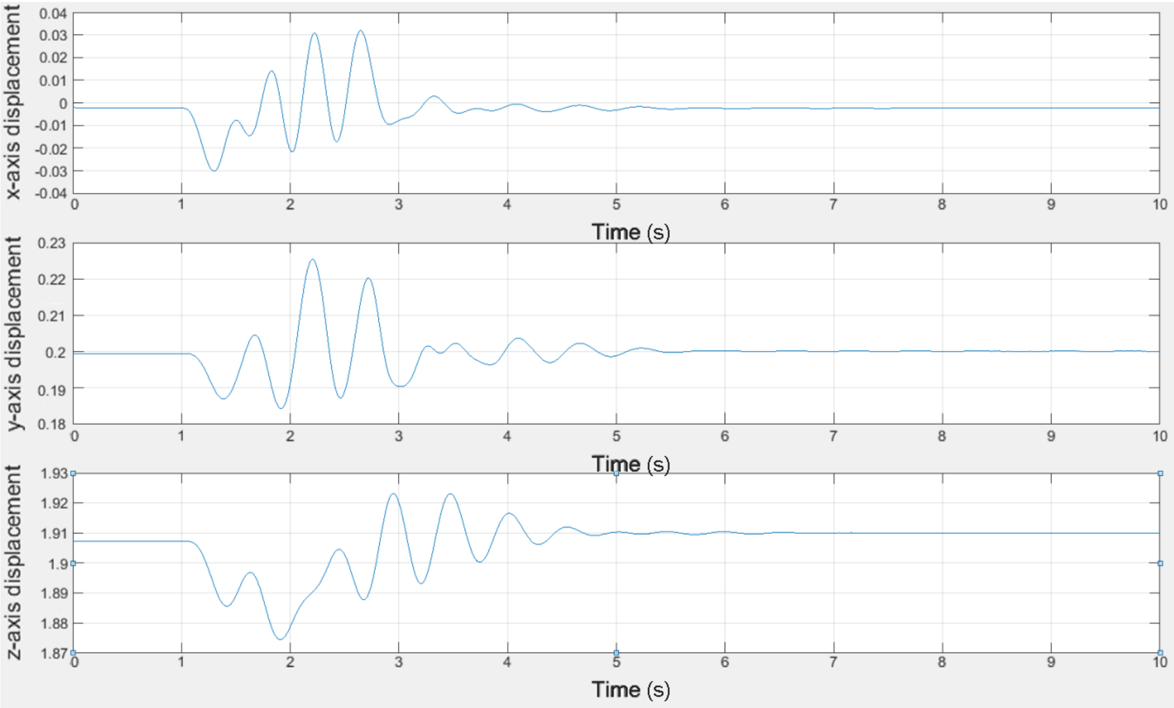

Figure 5-16 9 DOF vehicle 15km/h velocity PID controlled Turret displacements of muzzle (m)

Angular velocities of x, y and z-direction of the muzzle were given in Figure 5-17.

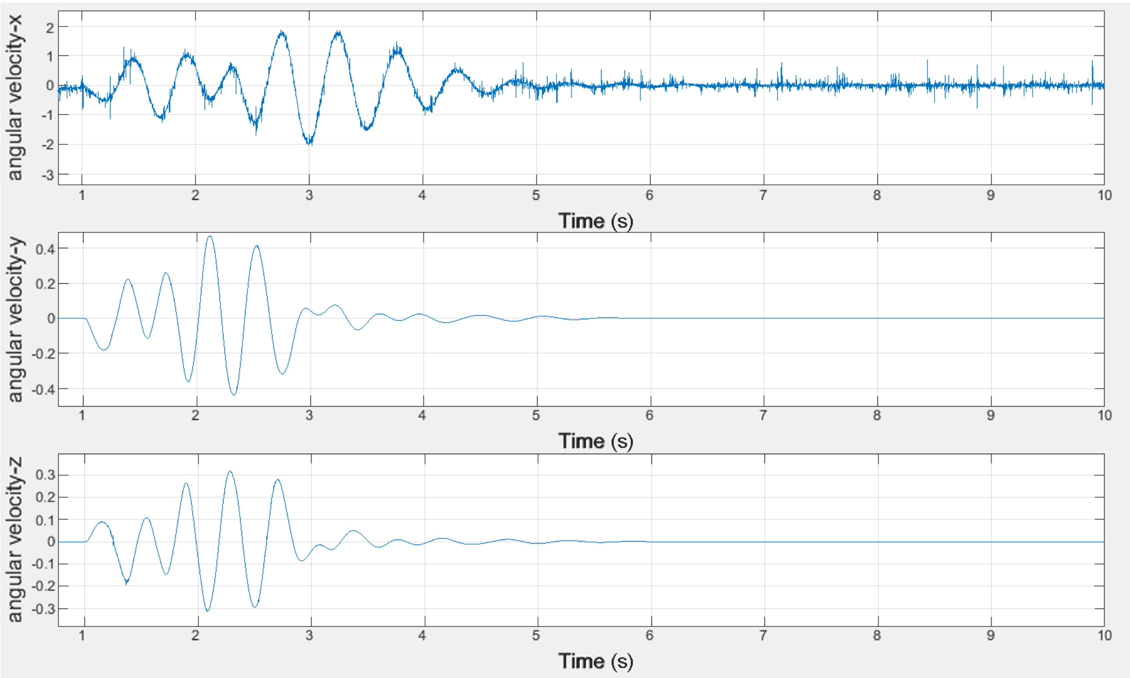

Figure 5-17 9 DOF vehicle 15km/h velocity PID controlled Turret angular velocities of muzzle (rad/s)

As seen Figure 5-18, amplitudes on the z-axis of the turret are half of the vehicles;

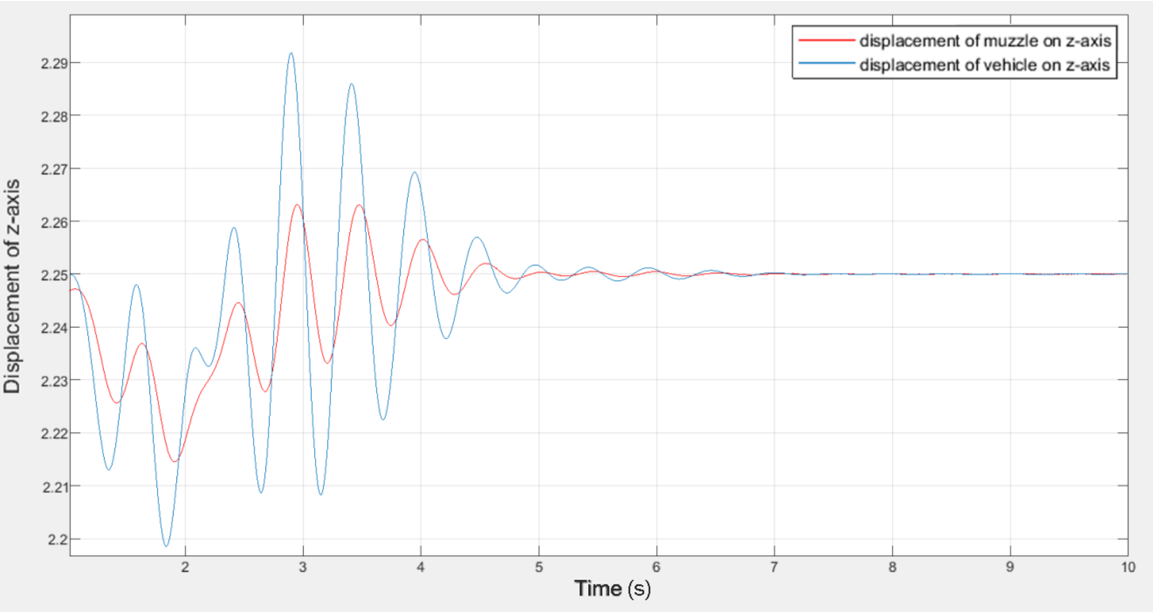

Figure 5-18 9 DOF vehicle 15km/h velocity PID controlled comparing z displacement between vehicle and muzzle (m)

Displacement of the muzzle x, y and z-axis for 30km/h were given in Figure 5-19.

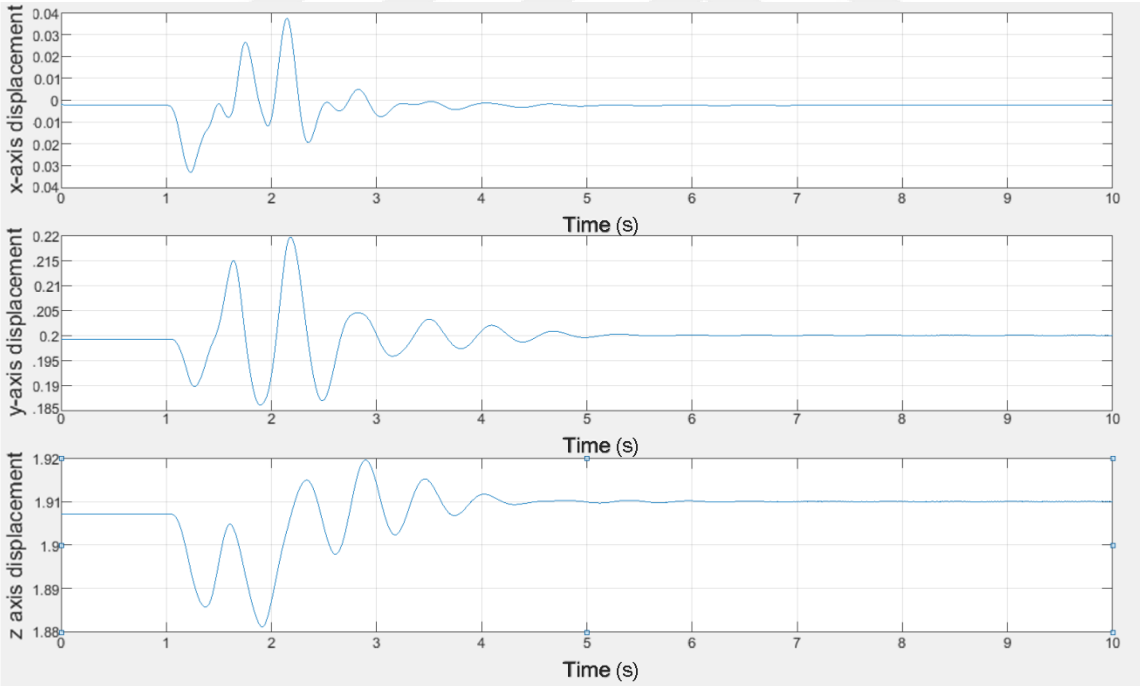

Figure 5-19 9 DOF vehicle 30km/h velocity PID controlled Turret displacements of muzzle (m)

Angular velocities of x, y and z-direction of the muzzle were given inFigure 5-20.

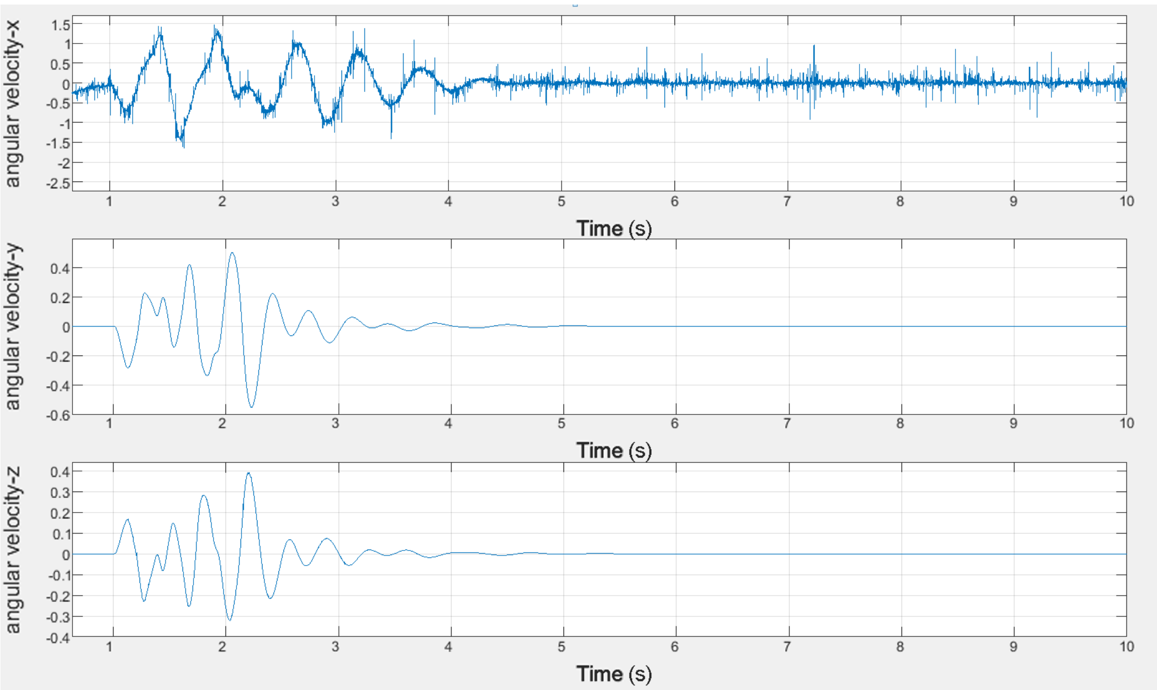

Figure 5-20 9 DOF vehicle 30km/h velocity PID controlled Turret angular velocities of muzzle (rad/s)

Amplitudes of the muzzle and vehicles on z-axis for 30km/h were given in Figure 5-21.

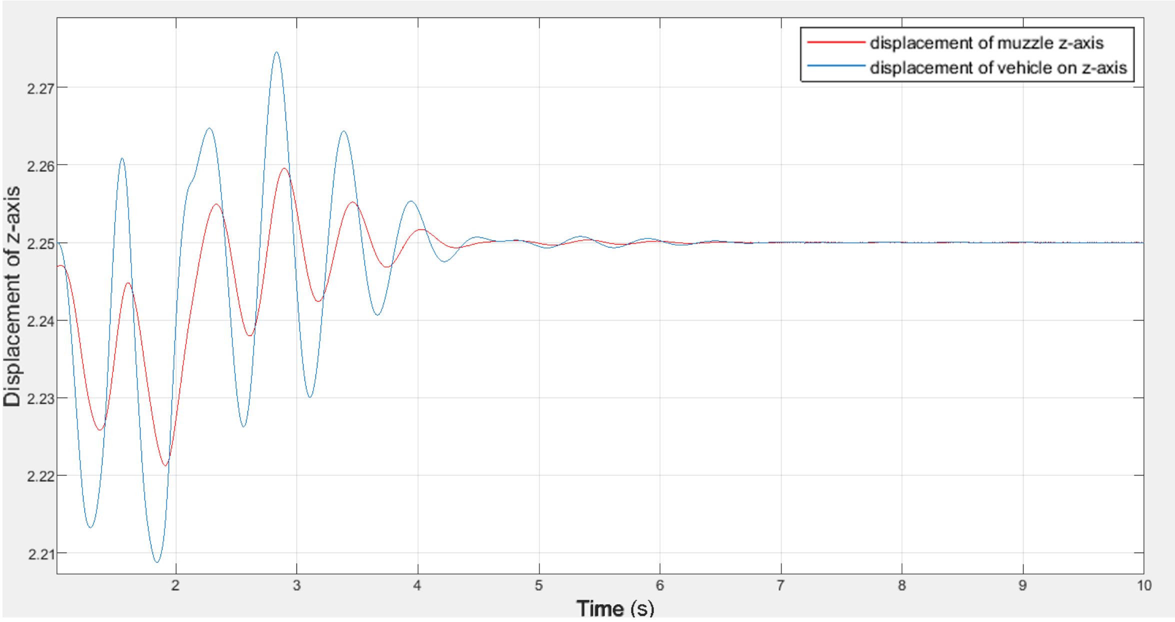

Figure 5-21 9 DOF vehicle 30km/h velocity PID controlled comparing z displacement between vehicle and muzzle (m)

Displacement of the muzzle x, y and z-axis for 50km/h were given in Figure 5-22.

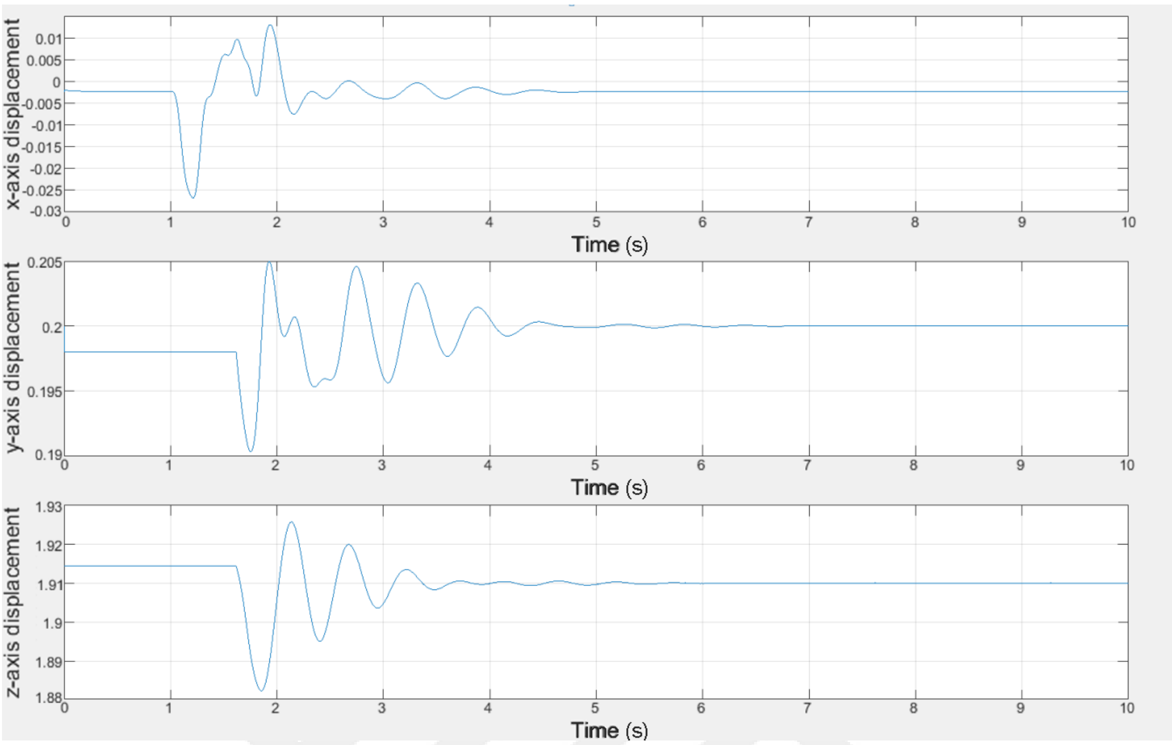

Figure 5-22 9 DOF vehicle 50km/h velocity PID controlled Turret displacements of muzzle (m)

Angular velocities of x, y and z-direction of the muzzle were given in Figure 5-23.

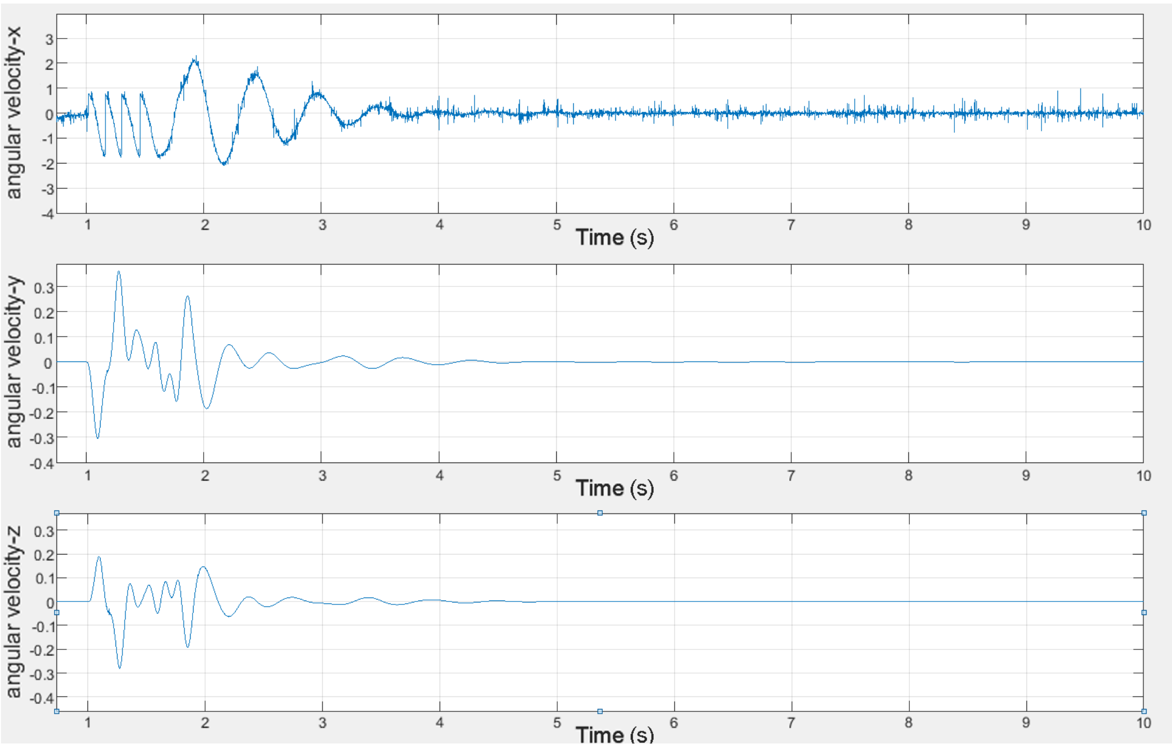

Figure 5-23 9 DOF vehicle 50km/h velocity PID controlled Turret angular velocities of muzzle (rad/s)

Amplitudes of the muzzle and vehicles for 50km/h were given in Figure 5-24.

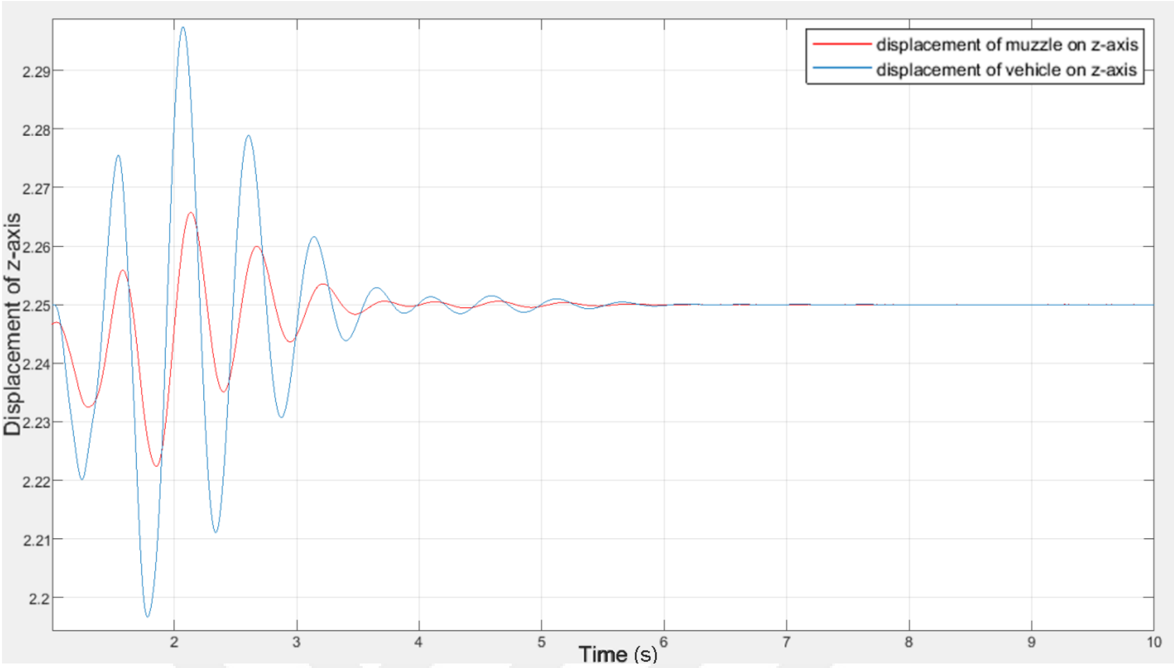

Figure 5-24 9 DOF vehicle 50km/h velocity PID controlled comparing z displacement between vehicle and muzzle (m)

5.3 ANSYS Results

5.3.1 Maximum Elevation Velocity While Elevation Gear is Flexible and Rigid

These simulations run for seeing the effect of elevation gear flexibilities. In this simulation, muzzle motion compares with rigid and flexible cases, when weapon reach maximum velocity position of weapon as Figure 5-25.

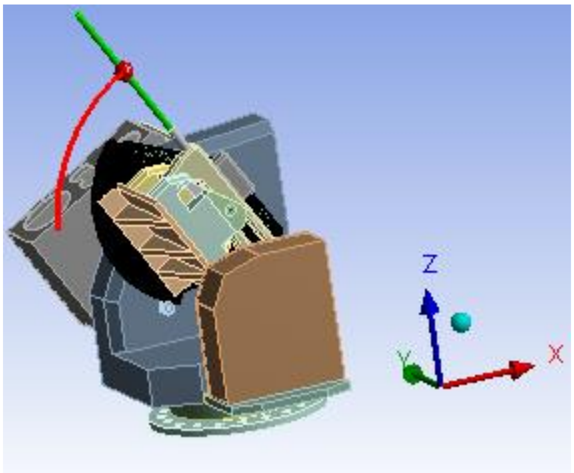

Figure 5-25 Flexible elevation gear maximum velocity analysis

Weapon position on z-axis can be seen in Figure 5-26.

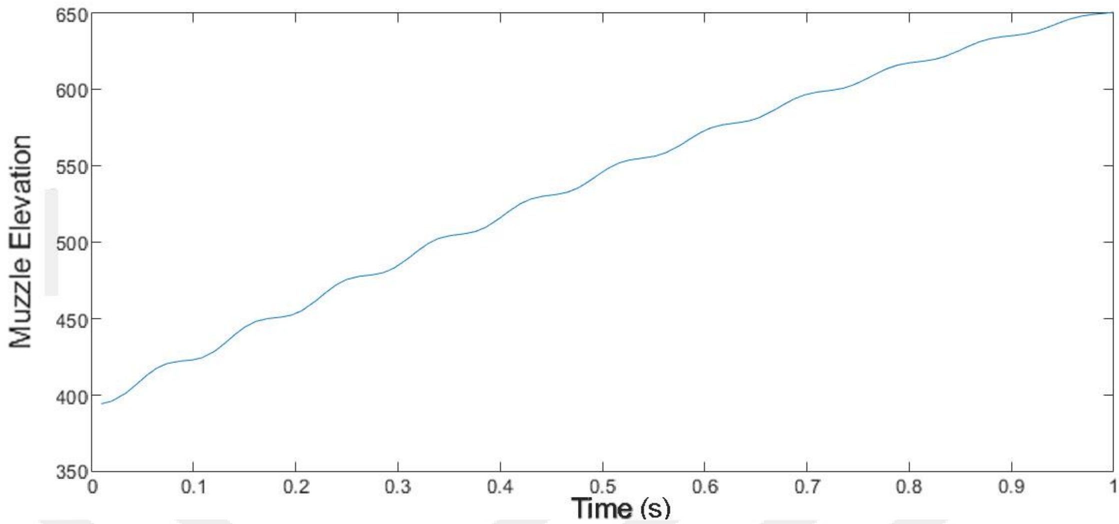

Figure 5-26 Maximum elevation velocity flexible gear analysis results (mm)

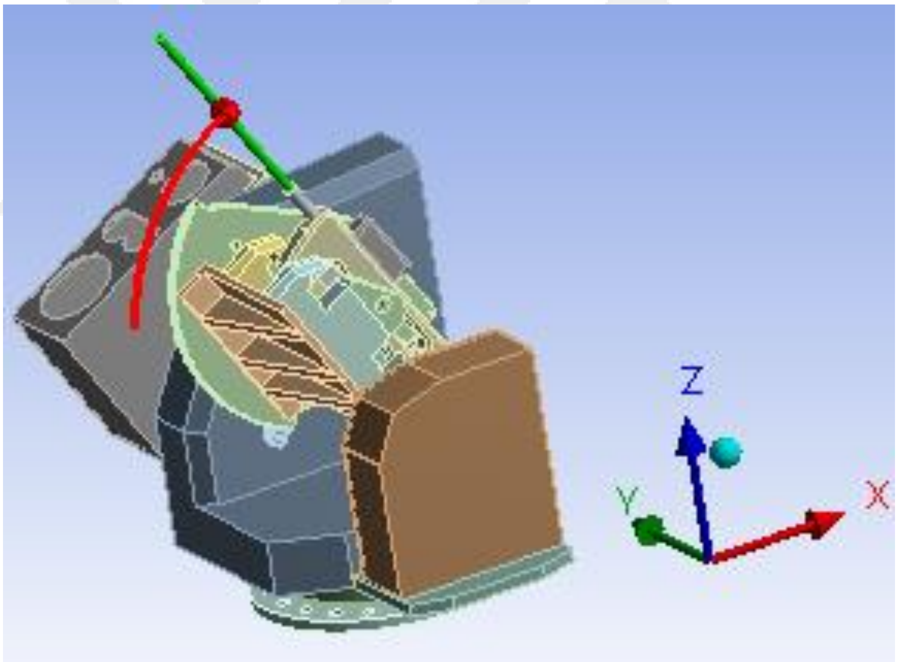

Figure 5-27 Rigid elevation gear maximum velocity analysis

Weapon motion on z-axis for rigid case was given in Figure 5-28.

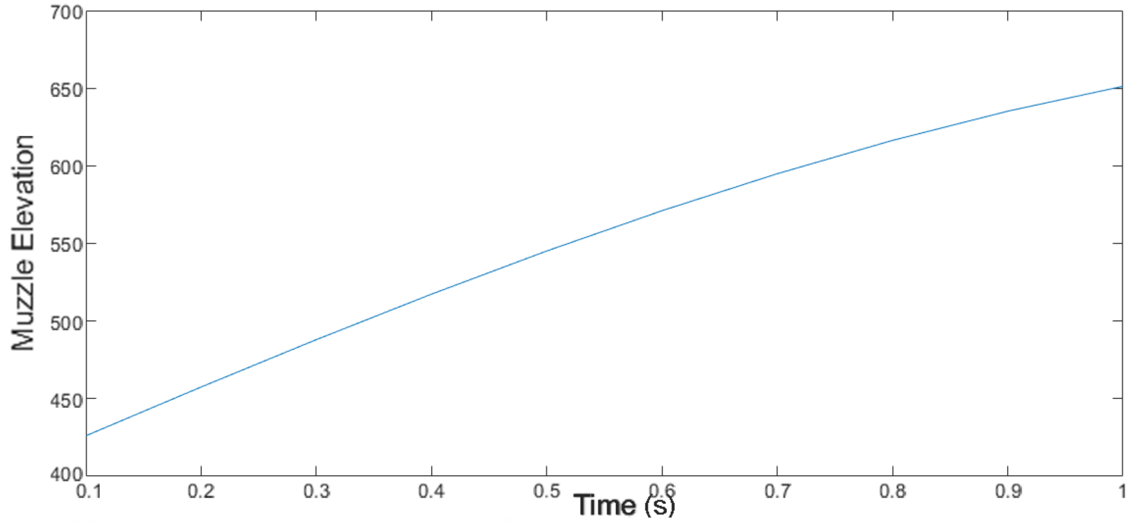

Figure 5-28 Maximum elevation velocity rigid gear analysis results (mm)

Flexible analysis solution line characteristic is more sinusoidal according to rigid solution. Muzzle motion for rigid an flexible gear is compared in Figure 5-29.

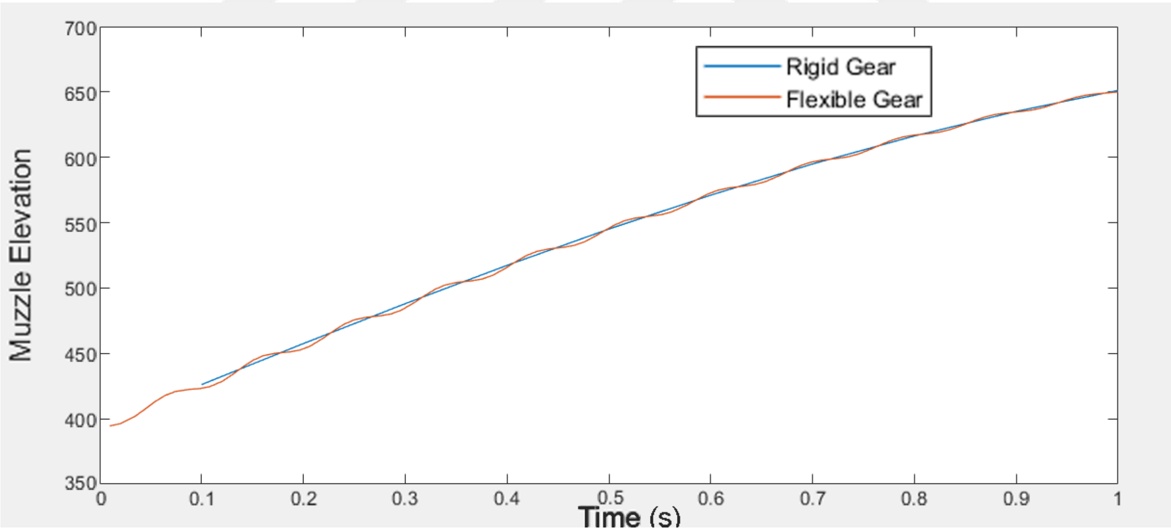

Figure 5-29 Comparing rigid and flexible cases at z-axis (mm)

Difference between rigid and flexible gear condition, muzzle positions with time can be seen easily. Simulation run for 1 second; differences are not significant until 1 second. The system takes desired position at 1 second. There is 1.2mm difference occurred end of the simulation between rigid and flexible gears conditons. Difference between rigid and flexible gears were given in Figure 5-30.

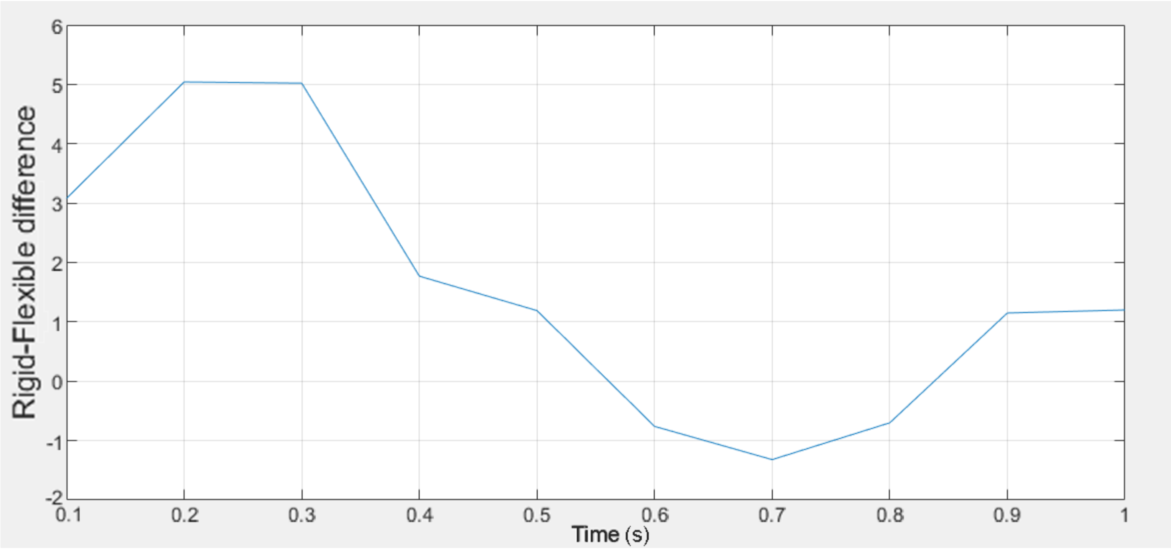

Figure 5-30 Rigid and flexible gear muzzle position difference at z-axis (mm)

Motion trajectories of rigid and flexible cases at x-axis wew given in Figure 5-31.

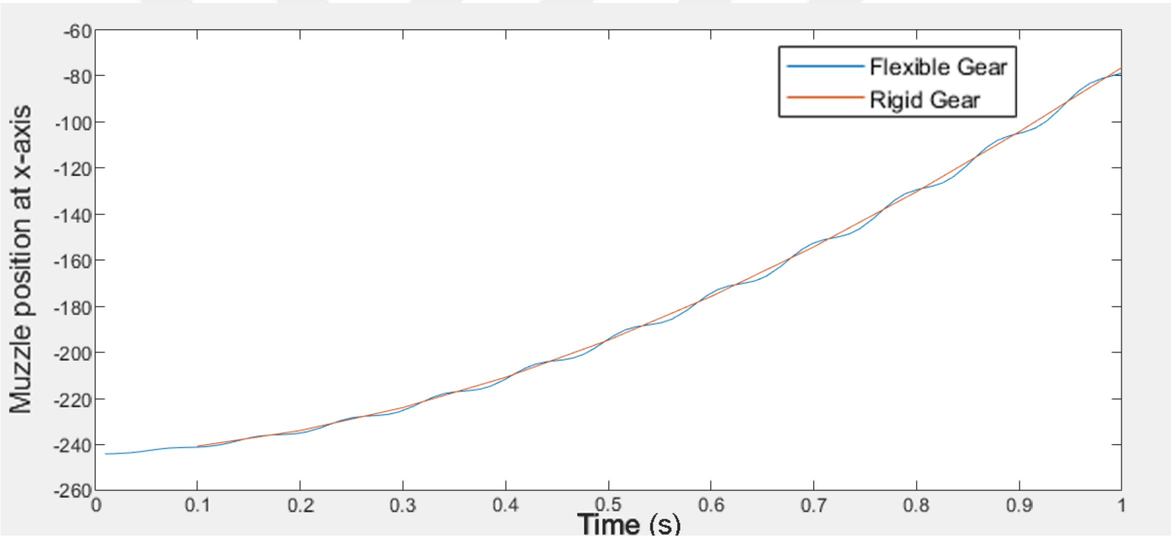

Figure 5-31 Comparing rigid and flexible cases at x-axis (mm)

Muzzle move at a different position along the time at the x-axis. At the final step, the muzzle is 2.345mm further under flexible conditions. Difference between rigid and flexible gears were given in Figure 5-32.

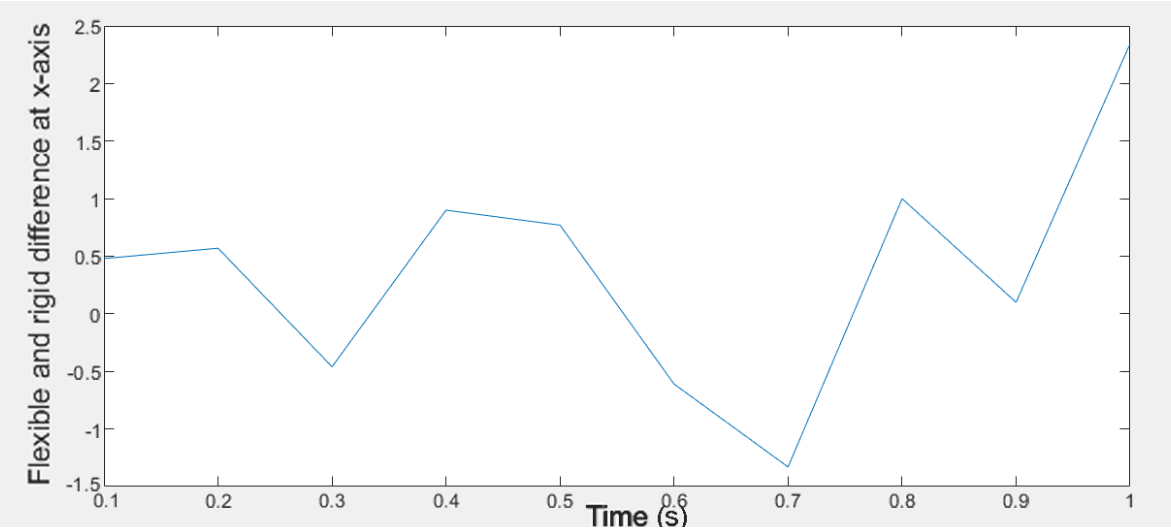

Figure 5-32 Rigid and flexible gear muzzle position difference at x-axis (mm)

No motion was observed at y-axis as Figure 5-33.

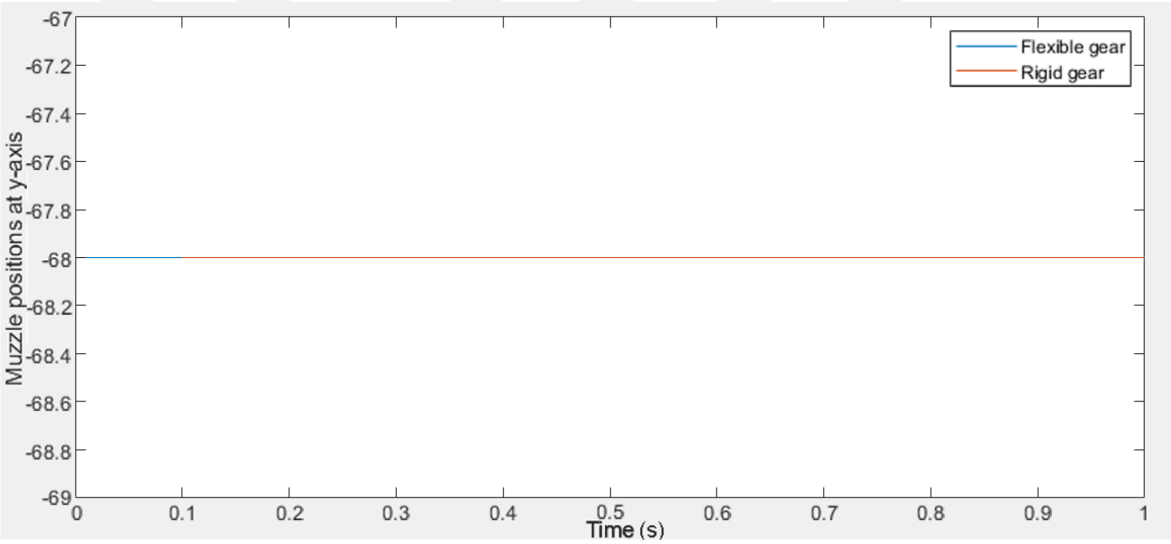

Figure 5-33 Comparing rigid and flexible cases at y-axis (mm)

5.3.2 Maximum Azimuth Velocity While Azimuth Gear is Flexible and Rigid

These simulations run for seeing the effect of azimuth gear flexibilities. In this simulation, Muzzle motion compares with rigid and flexible cases. Turret has a specific acceleration and velocity. Turret reach maximum velocity at 60º. Path of the motion was given in Figure 5-34.

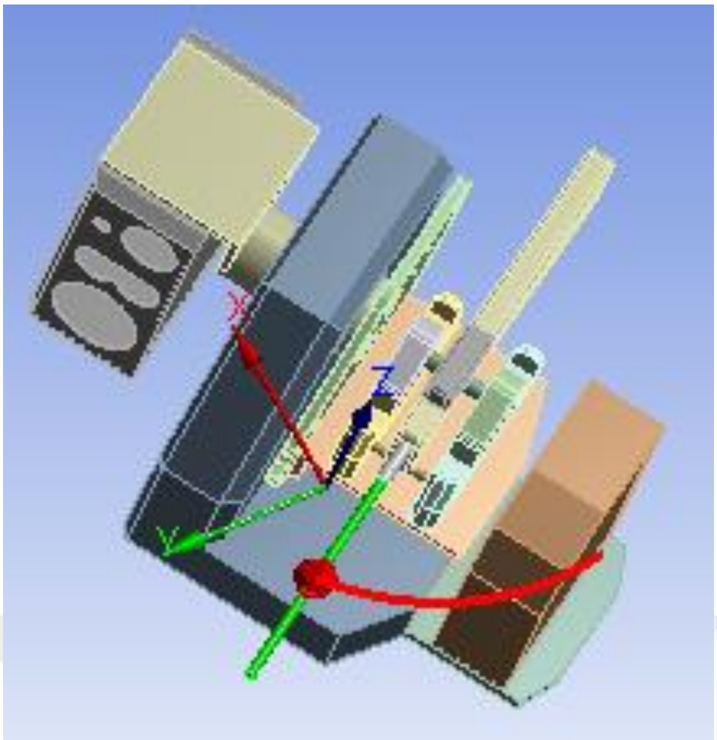

Figure 5-34 Azimuth gear maximum velocity analysis

Position at x-axis for rigid and azimuth gears were given in Figure 5-35.

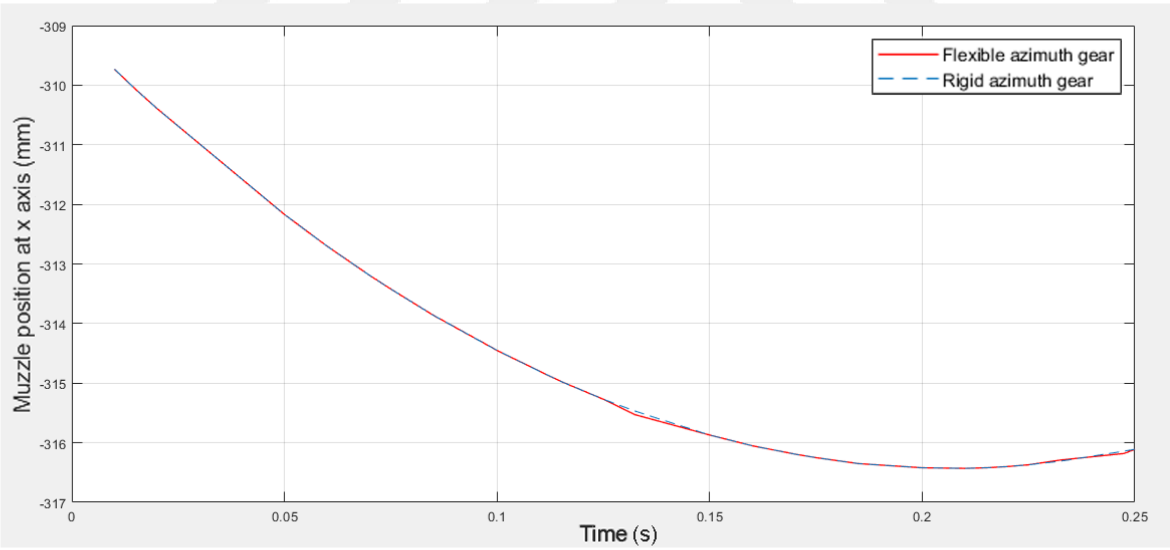

Figure 5-35 Muzzle position at x-axis for rigid and flexible azimuth gear

Difference between flexible and rigid at x-axis which is given below, it can be seen that there is no major difference between rigid and flexible cases. Maximum difference is about 0.06 mm.

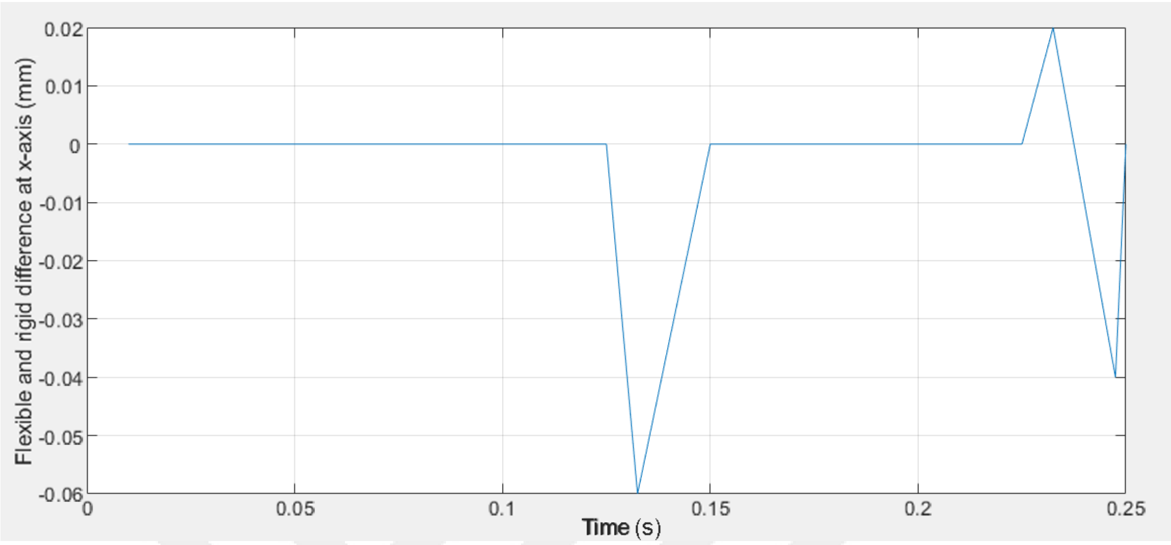

Figure 5-36 Displacement difference for rigid and flexible azimuth gear at x-axis

Position at y-axis for rigid and azimuth gears were given in Figure 5-37.

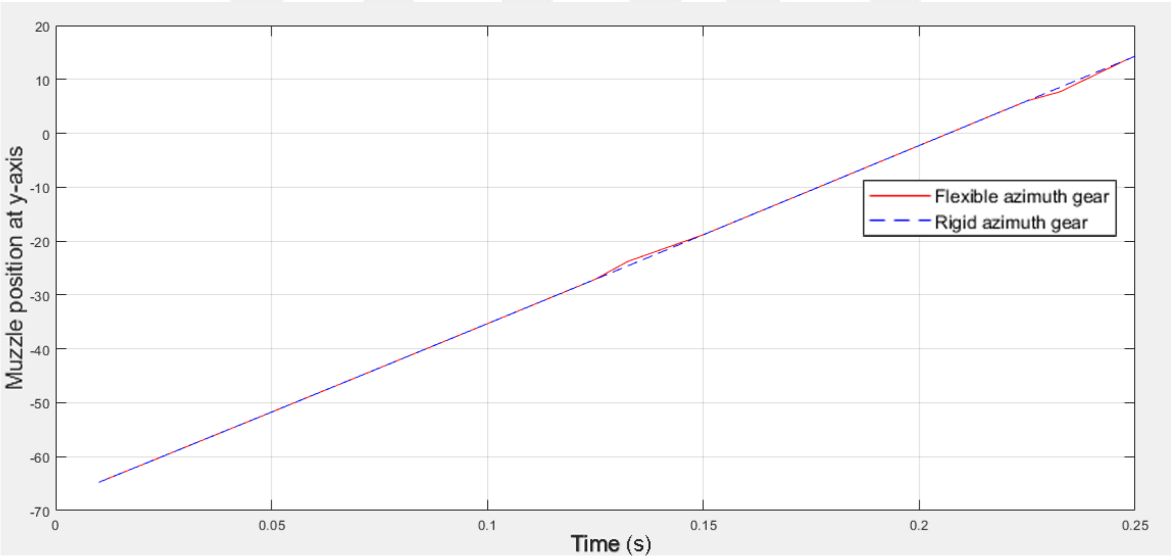

Figure 5-37 Muzzle position at y-axis for rigid and flexible azimuth gear (mm)

Difference between rigid and flexible azimuth gear at y-axis is the following the figure. The maximum difference is about 0.025mm.

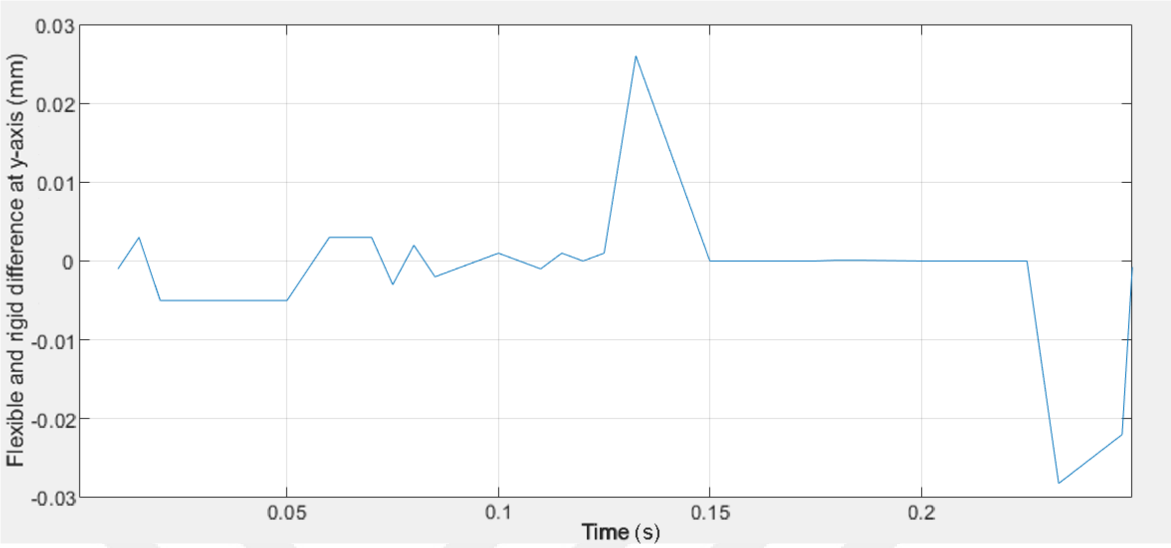

Figure 5-38 Displacement difference for rigid and flexible azimuth gear at y-axis

It was not observed any displacement on z-axis which was given in Figure 5-39.

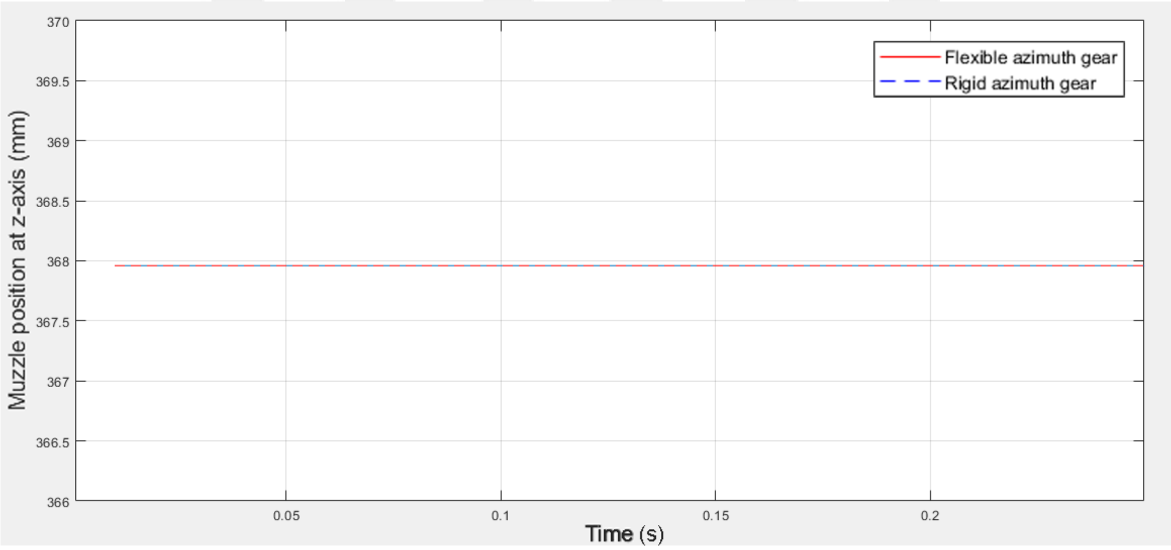

Figure 5-39 Muzzle position at z-axis for rigid and flexible azimuth gear

5.3.3 Gears Fatigue Failure Analysis

Machine elements usually fail under the repeated or fluctuating stresses. These loading types is called variable loading. Even if maximum stress is below the yield strength, elements can fail under the variable loading. Characteristic of these failures is that, stresses have been repeated a very large number of cycle and element fail suddenly, there is no alert.

Azimuth and elevation gear are loaded variable during to their lifelong. Steering and stabilization processes cause to load gears positive and negatively, therefore gears fatigue failure has to be analyzed.

Calculation of the fatigue life depends on following inputs [19],

- Fatigue analysis type
- Loading type
- Mean stress effects
- Multiaxial Stress Correction
- Fatigue Modification

Each inputs include sub-options. These options can be chosen according to analysis type.

In this scope, gears were analyzed strain life fatigue analysis type. Loading type of the gears are constant amplitude, proportional loading and for the mean stress calculation Goodman theory was chosen. Elevation and azimuth gear materials same and material properties is given in Table 5-1 Gear material Properties

Table 5-1 Gear material Properties

Properties	Value	Unit
Young’s Modulus	200	GPa
Tensile Yield Strength	250	MPa
Tensile Ultimate Strength	460	MPa

ANSYS include alternating stress – number of cycle curve for each material in its survey and curve of the using material in this analysis is given in Figure 5-40.

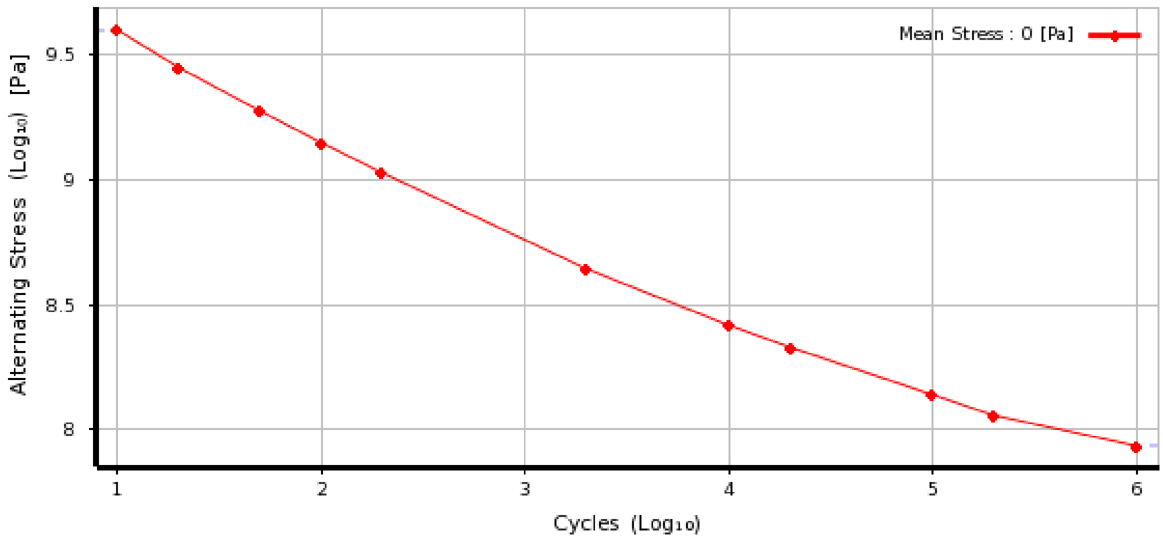

Figure 5-40 Stress-cycle chart of the steel

During the maximum elevation motions stresses were given in Figure 5-41 on the elevation gear.

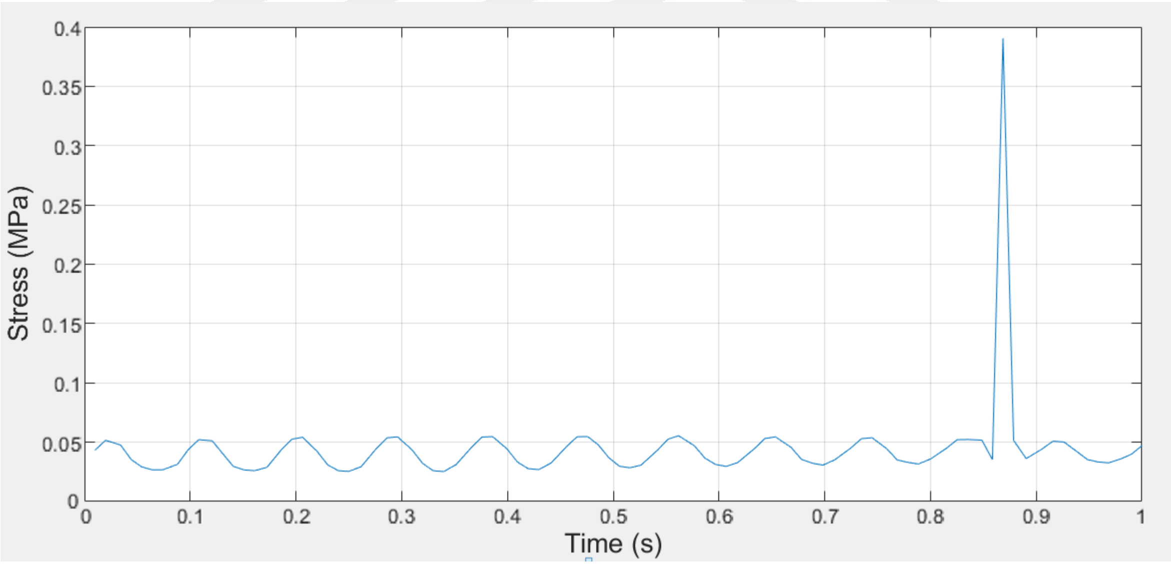

Figure 5-41 Elevation gear stress versus time

Elevation gear stress is very low according to material properties because gear was design for low flexibility and this cause to increasing strength. Solution of the fatigue life analysis was found 1e+006 cycles and this means that it is not foreseen to any damage. Gear could work under these conditions safely.

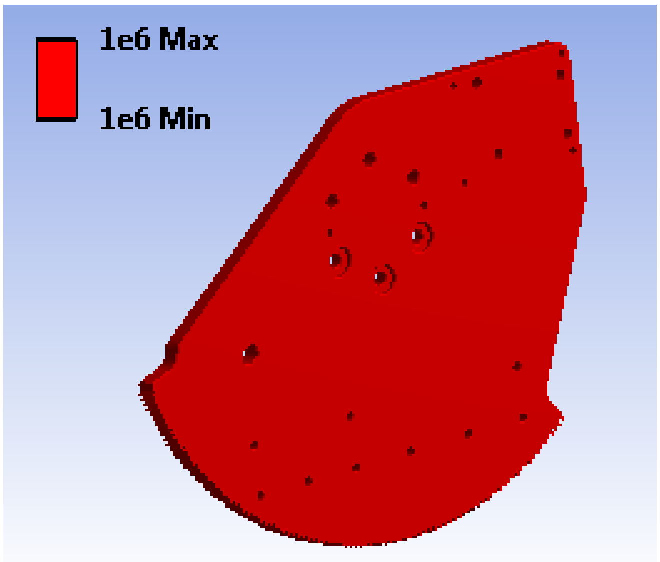

Figure 5-42 Fatigue life of elevation gear

During the maximum azimuth motions stresses were given in Figure 5-41 on the azimuth gear.

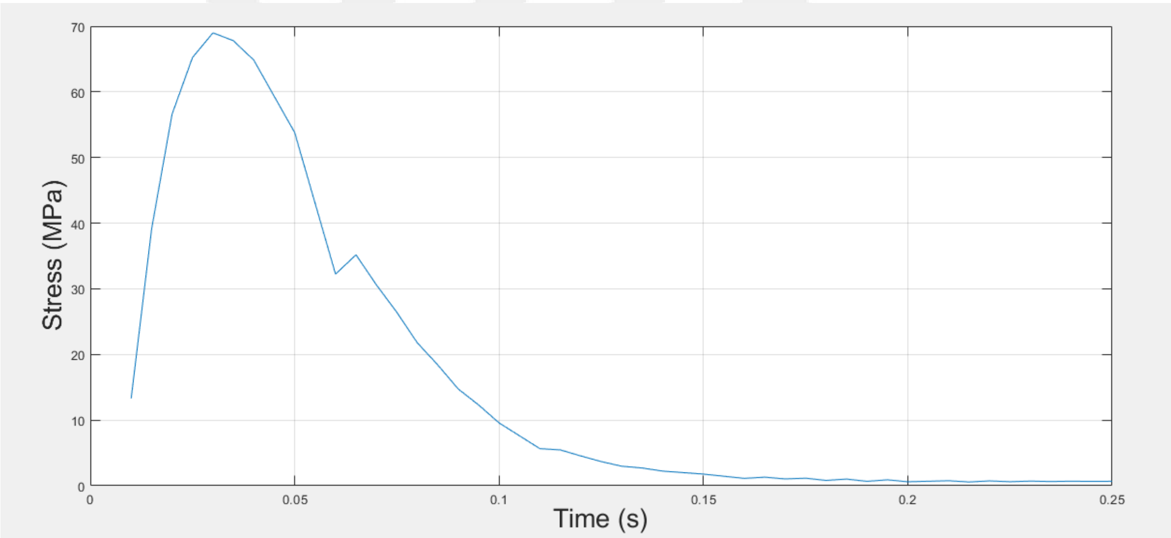

Figure 5-43 Azimuth gear stress versus time

Stresses on the azimuth gear were very low according to Young modulus of the material. Azimuth gear was design for low flexibility like elevation gear. Fatigue life cycle was found 1e+006 cycles and azimuth and elevation gears fatigue life were found endless.

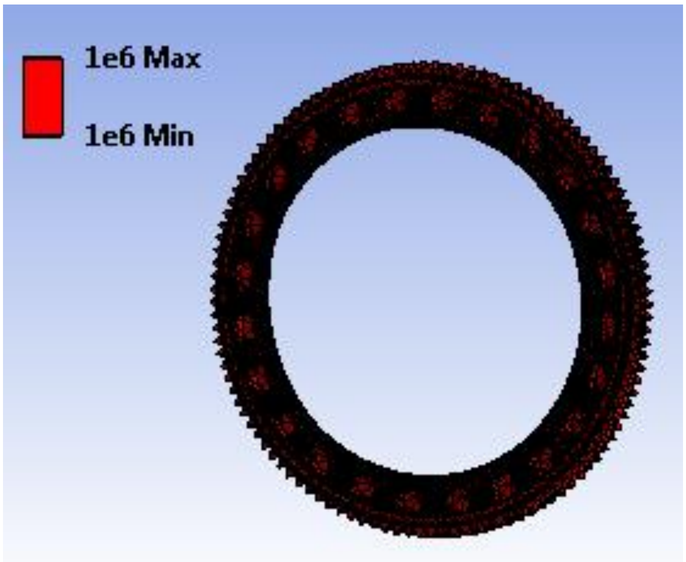

Figure 5-44 Fatigue life of azimuth gear

It is not foreseen to see fatigue failure to the gears with their lifelong according to these solutions.

5.4 MATLAB ANSYS Integrated Results

In this section, the scenario is that turret system was integrated on vehicle and vehicle pass on the obstacles at 30km/h velocity and turret stabilized itself according to 10 meters beyond the target. These simulations were run for 7 DOF and 9 DOF vehicles. Vibration profiles were generated by MATLAB SIMULINK. These profiles have ~10000 data point, therefore only peak points of the heave, roll and pitch motions were sent to ANSYS. However, peak times do not same for heave, roll and pitch profiles. Firstly, peaks points and peak times were found for each profile separately. Then times points have been merged for all profiles. Point quantities were reached 85 at this step. MATLAB has been sent to peaks of profiles with times and control parameters for each point to ANSYS. MATLAB has collapsed an output file for 85 iterations. In these simulations ANSYS was run in batch mode, there is not any interface like WORKBENCH. Whole commands were sent by MATLAB. Before the ANSYS APDL running,

Making a flexible analyze at ANSYS takes a time. One step calculations take approximately 5 hours depends on the performance of the computer. If these simulations were run under flexible conditions, it would need to ~425 hours for 85 iterations. A significant difference between flexible and rigid analysis for the small motion of elevation and azimuth axis is not foreseen. Proving this foresee one step analysis was run for maximum amplitude for heave, pitch and roll and maximum stabilization parameters at ANSYS WORKBENCH.

Table 5-2 Maximum motion condition

Motion	Maximum Value	Selected Value
Maximum heave for 7 DOF Vehicle	0.0761 m	0,5064 m
Maximum heave for 9 DOF Vehicle	0,5064 m	
Maximum roll for 7 DOF Vehicle	0.3200 rad	0.3200 rad
Maximum roll for 9 DOF Vehicle	0,0283 rad	
Maximum pitch for 7 DOF Vehicle	0.2766 rad	0.2766 rad
Maximum pitch for 9 DOF Vehicle	0,0311 rad	

According to Table 5-2 control parameters calculated by Artificial Neural Network functions as elevation axis -0.3151 rad and azimuth axis 0.0431 rad.

Elevation axis analysis was analyzed for rigid and flexible gear conditions. Positions were given in Figure 5-45.

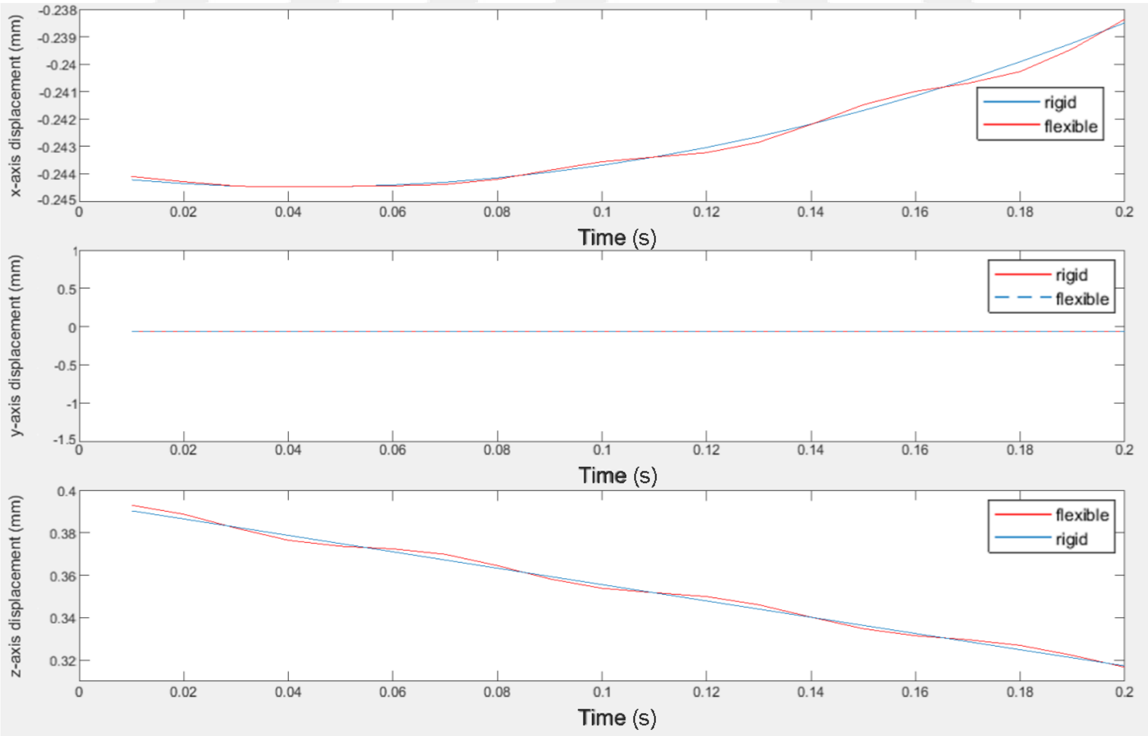

Figure 5-45 Displacement of the muzzle

Displacement difference between flexible and rigid conditions were given in Figure 5-46.

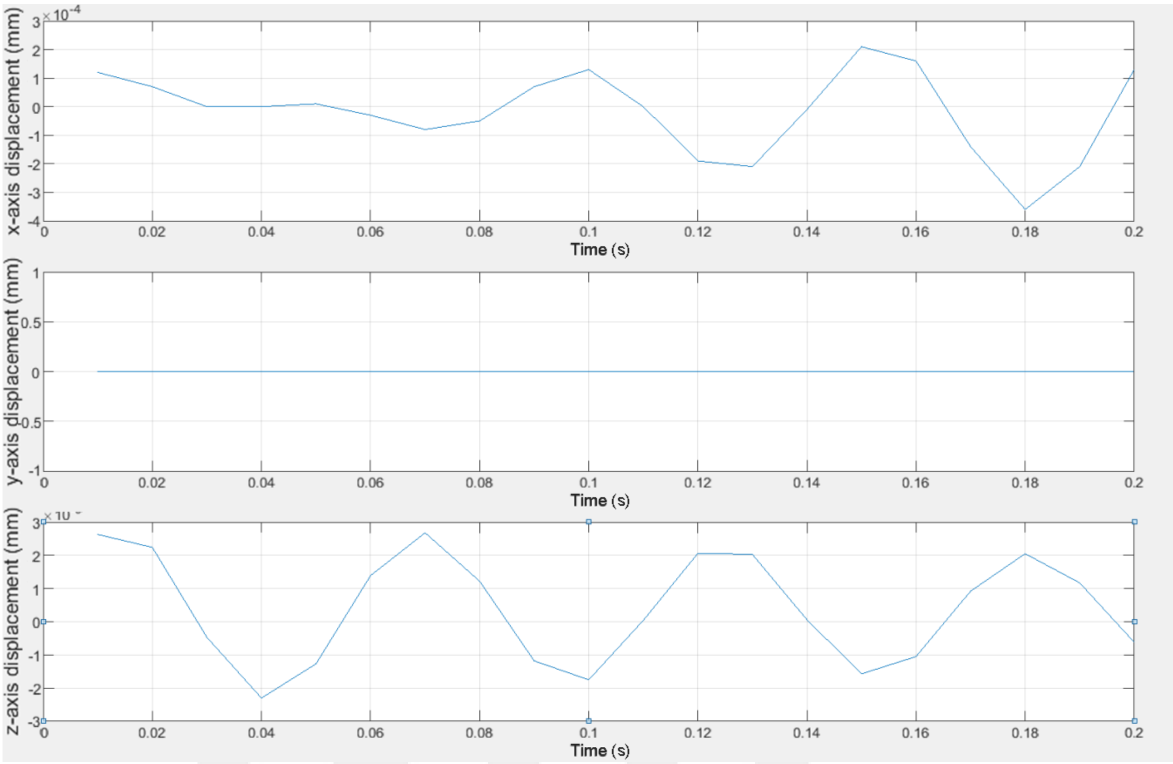

Figure 5-46 Displacement difference of the muzzle between rigid and flexible gears

Maximum value of the difference were given in Table 5-3.

Table 5-3 Maximum displacement difference (mm)

Axis	Maximum displacement difference
x	2.1000e-04
y	0
z	0.00270

As seen the Table 5-3, maximum displacement difference about 0.214 µm and 2.27µm for elevation axis. Maximum azimuth axis difference between rigid and flexible cases for maximum motion condition was given Heading 5.3.2 and this was found as 60µm.

Flexible and rigid case analysis were given almost same results. The differences are small enough to be ignored. Realistic results can be given by rigid analysis so simulations were run for rigid cases for simplifying to problem.

5.4.1 7 DOF Vehicle Analysis

Generated peak points profiles for 7 DOF vehicle were given as Figure 5-47. These are the inputs for elevation and azimuth motions of the turret systems.

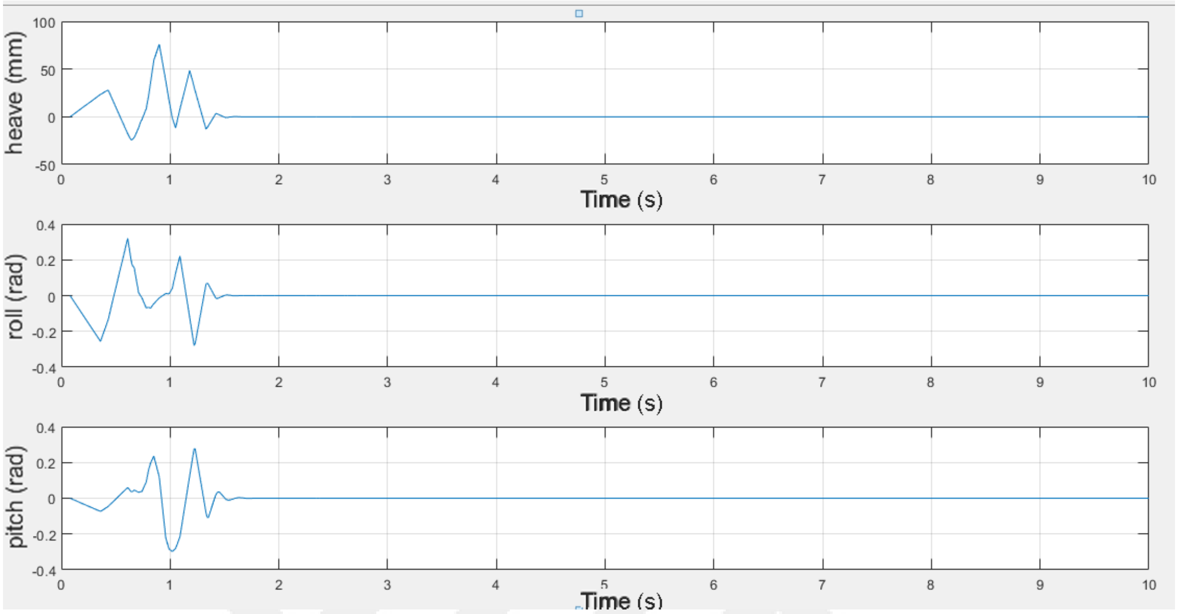

Figure 5-47 Picks of the heave, roll, and pitch motion for input

Turret stabilizes itself with Artificial Neural Network functions for elevation and azimuth axis. Simulation results of x, y and z-axis for muzzle endpoint were given in Figure 5-48.

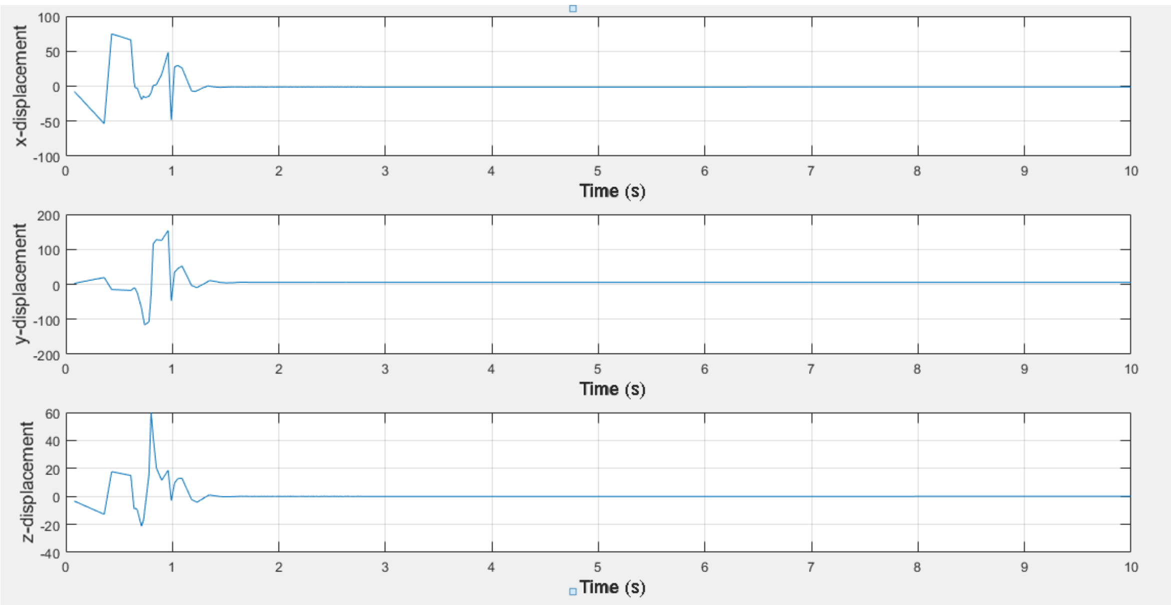

Figure 5-48 Muzzle position of x, y and z-axis (mm)

Simulation results of rotation on x, y and z-axis for muzzle endpoint were given in Figure 5-49.

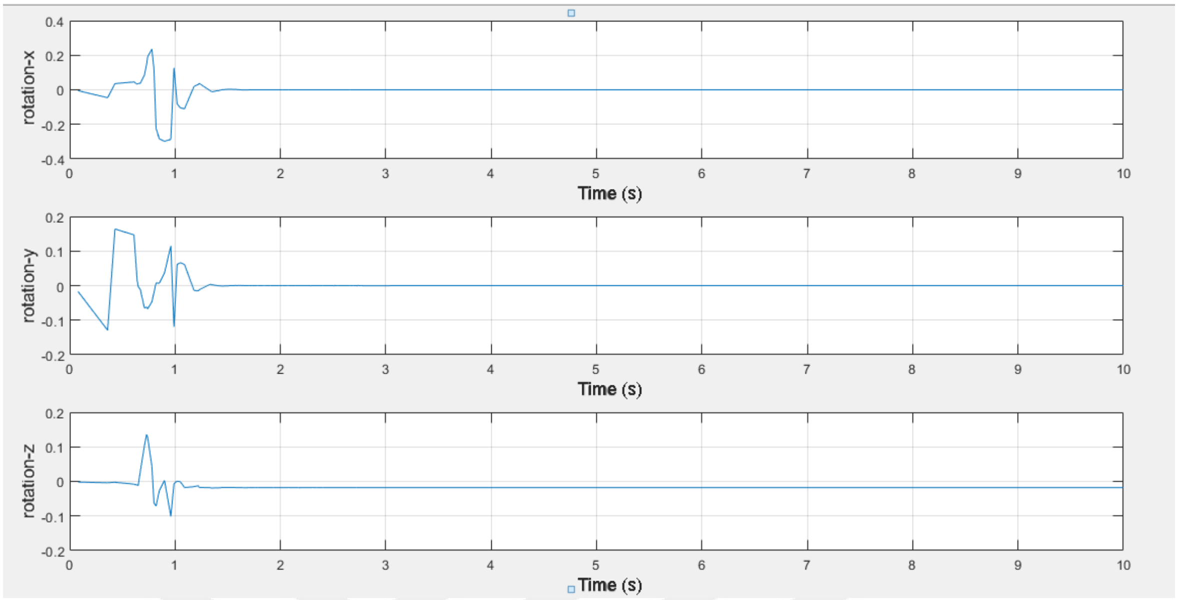

Figure 5-49 Muzzle rotation of x, y and z-axis (rad)

Heave displacement of vehicle and x, y, z displacement of muzzle were compared in Figure 5-50.

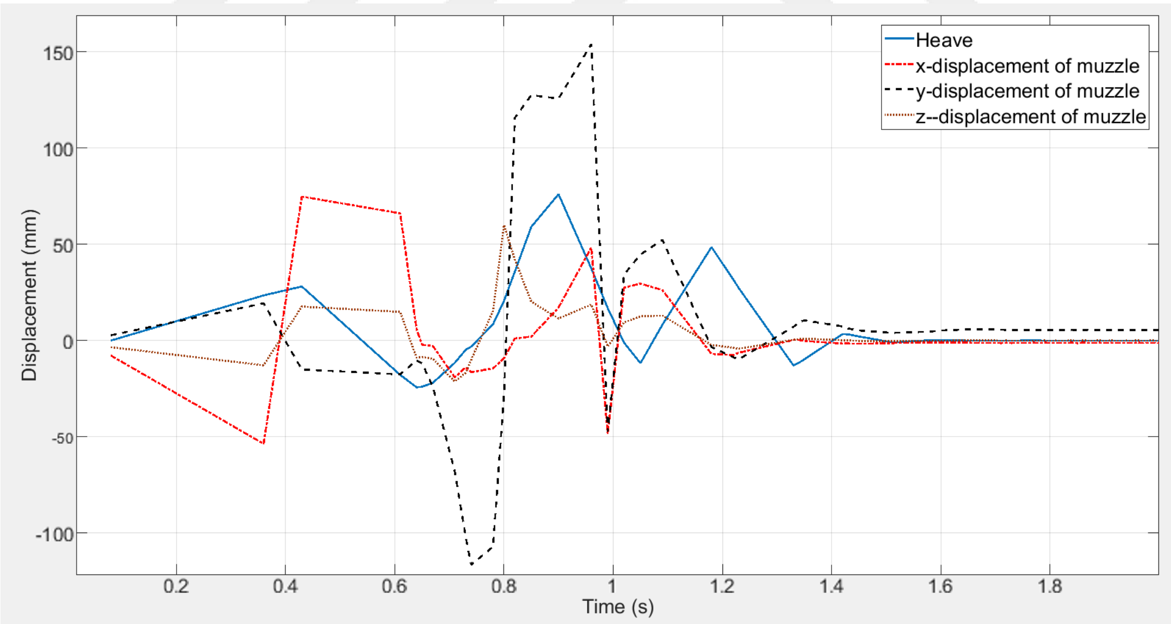

Figure 5-50 Muzzle and heave displacements

Roll, pitch rotational displacement of vehicle and x, y, z rotational displacement of muzzle were compared in Figure 5-51.

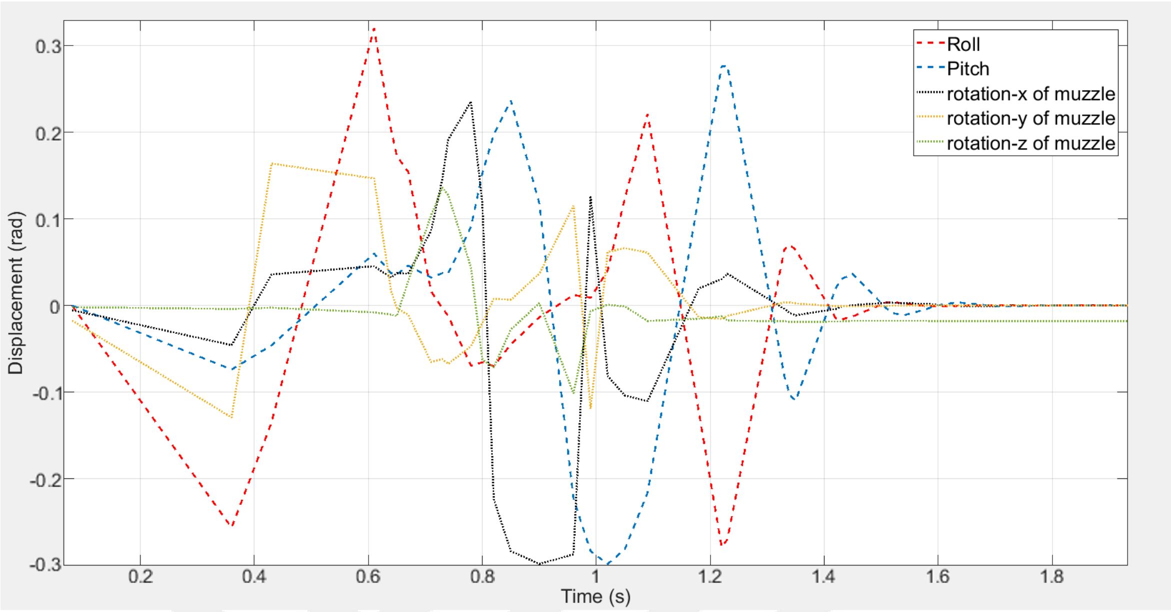

Figure 5-51 Muzzle rotational, roll and pitch displacements

5.4.2 9 DOF Vehicle Analysis

Generated peak points profiles for 9 DOF vehicle were given in Figure 5-52. These are the inputs for turret systems.

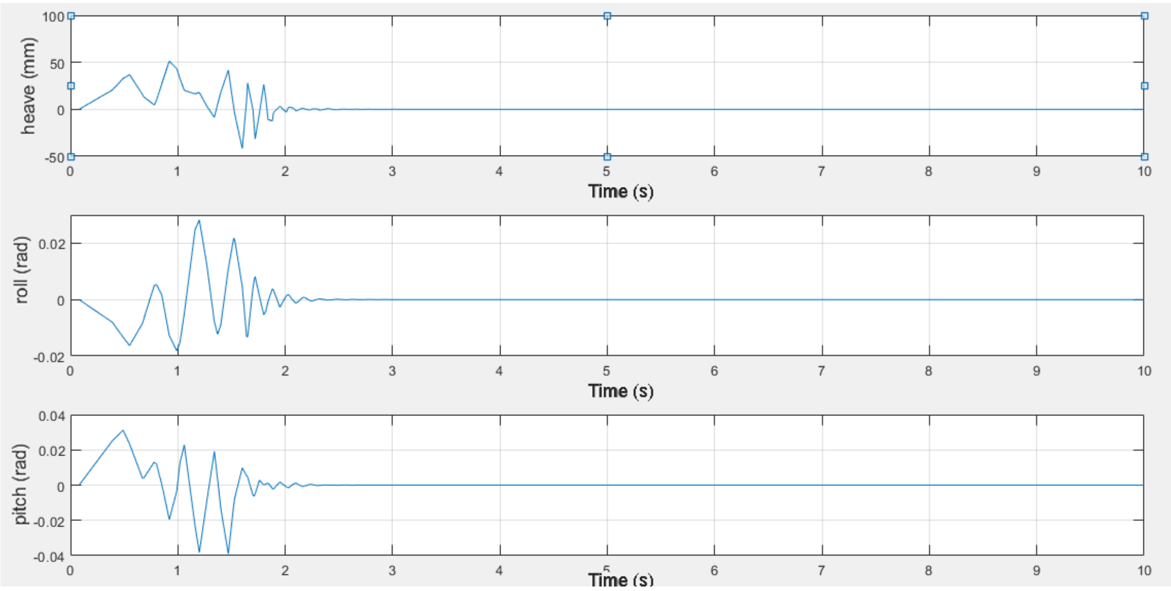

Figure 5-52 Picks of the heave, roll and pitch motion for input

Turret stabilizes itself with Artificial Neural Network functions for elevation and azimuth axis. Simulation results of x, y and z-axis for muzzle endpoint were given in Figure 5-53.

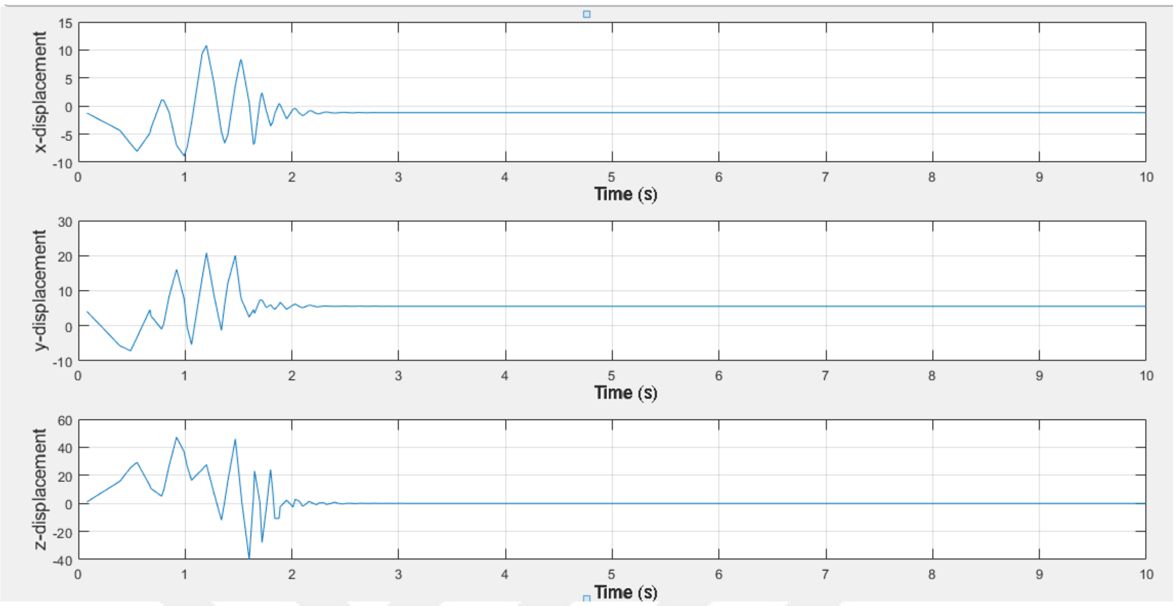

Figure 5-53 Muzzle position of x, y and z-axis (mm)

Simulation results of rotation on x, y and z-axis for muzzle endpoint were given in Figure 5-54.

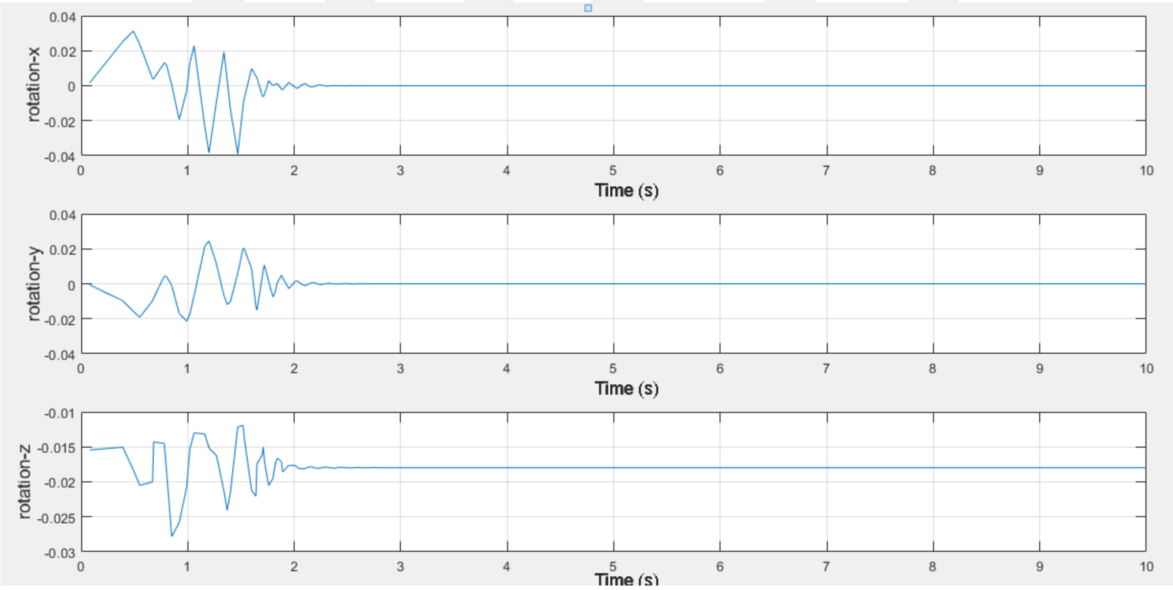

Figure 5-54 Muzzle rotation of x, y and z-axis (rad)

Heave displacement of vehicle and x, y, z displacement of muzzle were compared in Figure 5-55.

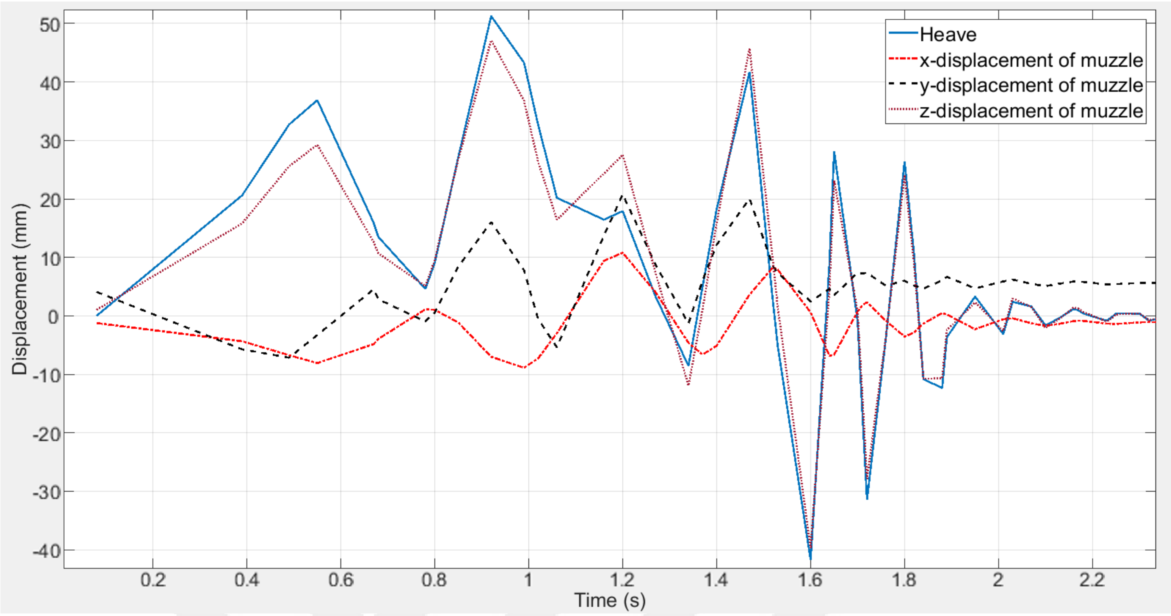

Figure 5-55 Muzzle and heave displacements

Roll, pitch rotational displacement of vehicle and x, y, z rotational displacement of muzzle were compared in Figure 5-56.

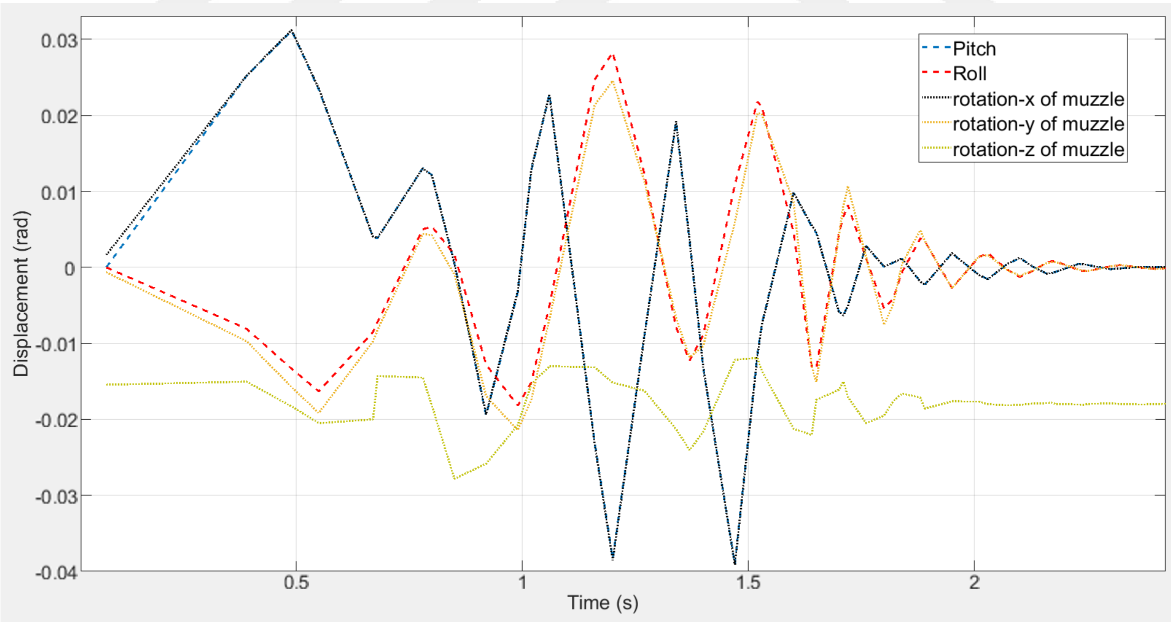

Figure 5-56 Muzzle rotational, roll and pitch displacements

6 CONCLUSIONS AND FUTURE WORK

Turret stabilization processes depend on various kinds of physical conditions. Flexibility of the turret mechanics, mounting types, usage area are effected these performances. Gear mechanisms are one of the most complicated systems in the turret. Backlash effects, unbalanced masses, friction forces and flexibility of the materials are the main problems for the gears.

This study was try to provide realistic simulation environment for the turret systems. These systems are mostly used for ground vehicles. Observing motion behaviors of the system, turret was installed two different vertical vehicle model and simulated with three different velocities. Then searching to flexibility effects of the gears, ANSYS model of the turret was created.

Firstly, vertical models were built for 4 wheel 7 DOf and 6 wheel 9 DOF vehicle. Vehicles were passed over obstacles which name is Aberdeen Proving Ground, widely used for military vehicle and system tests, and motions are observed at three different velocities. 7 DOF vehicle has more rough curve characteristics because of own stiffness, damping and mass dynamics. 9 DOF vehicle curve characteristics are smoother.

Turret mechanism can be built in MATLAB SIMULINK with using physical blocks. This model was installed two different vehicle models and vehicles were passed over obstacles, again. Turret steering mechanisms were controlled with PID controller. Controller parameters were tuned automatically with using MATLAB Control System Tuning. Each vehicle has own dynamics, therefore two different tuning operations were made for two different vehicles. PID Controller was successfully responded against to distributions. Because the muzzle moves more significant on the z-axis, vehicle heave motion and muzzle z-axis displacements were plot together and observed amplitude of the muzzle motions at z-axis are half of the vehicle heave motions.

For searching flexibility effects of the gears on aiming, physical model of the turret were built with using ANSYS software. If right approaches are applied, this model can give close to the real results. System was analyzed with flexible and rigid gear conditions and results were compared. Displacement difference between flexible and rigid gears on the muzzle at azimuth axis was found about 0.06mm. This value is equal 0.012º displacement difference on the azimuth gears for flexible and rigid conditions. At the elevation axis maximum displacement difference was found about 5mm on the muzzle and this value is equal to 0.96º on the elevation gear for flexible and rigid conditions.

Repeated or fluctuating stresses can be caused fail even if maximum stresses is below the yield strength. Variable loads are dangerous loading types for machine elements. Fatigue life of the mechanical parts can be analyzed with ANSYS software easily. With using loading types, means stresses effects, multiaxial stress correction and fatigue modifications information fatigue analysis can be performed. Gear systems in the turret is exposed to this kind of variable loadings during to its service life. Gears analyzed at the maximum loading conditions and no danger has been foreseen. Fatigue life of the gears were found endless.

In the last step, MATLAB vehicle model and ANSYS turret model were connected. MATLAB gives right approach for vehicle vibration model and it is possible to create physical model of the turret at ANSYS. Power of these two programs provides to see what is happening in the real conditions. Simulations were run 143 iteration for 7 DOF vehicle and 85 iteration for 9 DOF vehicle. Iteration quantities have determined by Peak points of the heave, roll and pitch motions. Moreover stabilization parameters of the turret were provided by MATLAB Artificial Neural Network Tool. According to this, responses of the systems tough to the program previously and until this point, turret was decided stabilization responses itself. Network can respond to disturbances coming from 6-axis.

This study shows that ANSYS and MATLAB software can be used effectively together. For example, suspension or chassis systems which is analyzing with ANSYS can be simulate under real track conditions. System can be loaded with realistic values with this connections. Either other parts on the vehicle can be simulated with this method. We can think about the reverse, it can observed to the impact of the firing shock of the weapon on the vehicle suspension and it can have an idea about changes on the driving characteristics. It is possible for the systems can produce own responses against the variable states with using artificial intelligences

7 REFERENCES

[1] "ASELSAN INC," [Online]. Available: http://www.aselsan.com.tr/tr-tr/cozumlerimiz/silah-sistemleri/uzaktan-komutali-atis-sistemleri/sarp-uzaktan-komutali-stabilize-silah-sistemi. [Accessed 15 01 2018].

[2] "WIKIPEDIA The Free Encylopedia," [Online]. Available: http://www.wikizero.info/index.php?q=aHR0cHM6Ly9lbi53aWtpcGVkaWEub3JnL3dpa2kvR3VuX3N0YWJpbGl6ZXI. [Accessed 10 01 2018].

[3] Ö. GÜMÜŞAY, Intelligent Stabilization Control of Turret Subsytems under Disturbances from Unstructured Terrain, ANKARA: Master Thesis, METU Electrical and Electronics Engineering, 2006.

[4] D. J. Purdy, «Comparison of balance and out of balance main battle tank armaments,» Royal Military College of Science, Swindon.

[5] «Rheinmetall Handbook on Weaponry, Rheinmetal GmbH,» second English edition,, 1992.

[6] H. Warwick, «A guide to the design of main armament gun,» DERA, Chobham Lane Chertsey UK.

[7] W. E. Kölbl, Fire Control Systems for Main Battle Tanks, Military Technology, 1981.

[8] L. L. YANG, «An Overview on Vehicle Dynamics,» *International Journal of Dynamics and Control,* no. 4, pp. pp 385-395, 2013.

[9] P. M. J. M. Tejas P. Turakhia, Mathematical Modeling and Simulation of a Simple Quarter Car, International Journal for Scientific Research & Development, 2016.

[10] D. CEBON, Handbook of Vehicle-Road Interaction, London: Taylor & Francis, 1999.

[11] F. KOST, Basic Principles of Vehicle Dynamics, Friedrichshafen: Part of the Bosch Professional Automotive Information book series (BPAI), 2014.

[12] G. RILL, Vehicle Dynamics, Brasil: Fachhochschule Regensburg University of Applied Sciences, 2007.

[13] T. D. Gillespie, Fundamentals of Vehicle Dynamics, Pennsylvania: Society of Automotive Engineers, Inc..

[14] N. N. MHASKE, «Stiffness Analysis of Passenger Car Tire Using Nitrogen,» *International Journal of Scientific and Research Publications,*, cilt 6, no. 1, pp. 140-148, 2016.

[15] MAYBACH, «Maybach,» 10 09 2012. [Çevrimiçi]. Available: http://maybach300c.blogspot.com.tr/2012/09/rigid-and-semi-rigid-crank-axle.html. [%1 tarihinde erişilmiştir10 01 2018].

[16] B. BAYSAL, Altı Taktik Tekerleği Tahrikli (6X6) Zırhlı Askeri Aracın Titreşim Analizi, İstanbul: Master Thesis, Yıldız Teknik Üniversitesi Graduate School of Nature and Applied Science, 2012.

[17] Jagreet, «Overview of Artificial Neural Networks and its Applications,» 05 05 2017. [Çevrimiçi]. Available: https://www.xenonstack.com/blog/data-science/overview-of-artificial-neural-networks-and-its-applications. [%1 tarihinde erişilmiştir10 01 2018].

[18] H. D. BEALE, Neural Network Toolbox, Massachuaetts: MathWorks, 2017.

[19] A. H. Raymond Browell, «Calculating and Displaying Fatigue Results,» ANSYS INC., 2006.

APPENDIX

```
%running vehicle_parameters
vehicle_value_4x4   %Values of 7DOF
%vehicle_value_6x6  %Values of 9DOF


%running simulink
model = 'Vehicle_4x4'; %7DOF vehicle model
%model = 'Vehicle_6x6'; %9DOF vehicle model
load_system(model)
sim(model)


%finding peaks of heave
A1=findpeaks(heave);
A2=findpeaks(-1*heave);
A3=-1*A2;
A4=[A1;A3];
[m, n]=size(A4);
for a=1:1:m
    A5(a,1)=(find(heave==A4(a,1)));
end
A6=[A5 A4];
A7=sortrows(A6);

%finding peaks of roll
B1=findpeaks(roll);
B2=findpeaks(-1*roll);
B3=-1*B2;
B4=[B1;B3];
[m1, n1]=size(B4);
for a=1:1:m1
    B5(a,1)=(find(roll==B4(a,1)));
end
B6=[B5 B4];
B7=sortrows(B6);

%finding peaks of pitch
C1=findpeaks(pitch);
C2=findpeaks(-1*pitch);
C3=-1*C2;
C4=[C1;C3];
[m2, n2]=size(C4);
for a=1:1:m2
    C5(a,1)=(find(pitch==C4(a,1)));
end
C6=[C5 C4];
C7=sortrows(C6);
```

```
 %Merginng peaks with time
D1= [A7(:,1); B7(:,1); C7(:,1)];
D2=sortrows(D1);
[D3]=unique(D2,'rows');
D4=pitch(D3(:,1),:);
PITCH=[D3/1000 D4];
D5=roll(D3(:,1),:);
ROLL=[D3/100 D5];
D6=heave(D3(:,1,:));
HEAVE=[D3/100 D6*1000];
[m3, n3]=size(D3);

%azimuth and elevation axis gear ratio;
d_yanal=10;
d_yukselis=16;

%step size
m4=m3-1;

for    i=1:1:m4

%elevation axis correction;
YUK1=(NN_alfa_heave(HEAVE(i,2))+NN_alfa_beta(ROLL(i,2)))*d_yukselis;
YUK2=(NN_alfa_heave(HEAVE(i+1,2))+NN_alfa_beta(ROLL(i+1,2)))*d_yukselis;


K0=400;      %elevation high
LW=450;      %muzzle-elevation axis distance
K1=K0+LW*sin(YUK1);
K2=K0+LW*sin(YUK2);

%azimuth axis correction;
YAN1=(NN_tetha_omega(PITCH(i,2)))*d_yanal*K1;
YAN2=(NN_tetha_omega(PITCH(i+1,2)))*d_yanal*K2;


%Putting inputs in the batch file
content = fileread( 'ANSYS_BATCH_V12.txt' );


content = regexprep( content, '(?<=_loadvari229\(1,1,1\) = )\S+', sprintf(
'%f', YUK1 )) ;
content = regexprep( content, '(?<=_loadvari229\(2,1,1\) = )\S+', sprintf(
'%f', YUK2 )) ;

content = regexprep( content, '(?<=_loadvari230\(1,1,1\) = )\S+', sprintf(
'%f', YAN1 )) ;
content = regexprep( content, '(?<=_loadvari230\(2,1,1\) = )\S+', sprintf(
'%f', YAN2 )) ;

%initial loads
content  =  regexprep(  content,  '(?<=_loadvari226uz\(1,1,1\)  =  )\S+',
sprintf( '%f', HEAVE(i,2) )) ;
content  =  regexprep(  content,  '(?<=_loadvari226uz\(2,1,1\)  =  )\S+',
sprintf( '%f', HEAVE(i+1,2 ));
```

```
content = regexprep( content, '(?<=_loadvari226roty\(1,1,1\) = )\S+',
sprintf( '%f', ROLL(i,2) ));
content = regexprep( content, '(?<=_loadvari226roty\(2,1,1\) = )\S+',
sprintf( '%f', ROLL(i+1,2) ));

content = regexprep( content, '(?<=_loadvari226rotx\(1,1,1\) = )\S+',
sprintf( '%f', PITCH(i,2 ) )) ;
content = regexprep( content, '(?<=_loadvari226rotx\(2,1,1\) = )\S+',
sprintf( '%f', PITCH(i+1,2) )) ;

%Putting time in the batch file
content = regexprep( content, '(?<=_loadvari229\(1,0,1\) = )\S+', sprintf(
'%f', HEAVE(i,1) )) ;
content = regexprep( content, '(?<=_loadvari229\(2,0,1\) = )\S+', sprintf(
'%f', HEAVE(i+1,1) ));

content = regexprep( content, '(?<=_loadvari230\(1,0,1\) = )\S+', sprintf(
'%f', HEAVE(i,1) )) ;
content = regexprep( content, '(?<=_loadvari230\(2,0,1\) = )\S+', sprintf(
'%f', HEAVE(i+1,1) ));

content = regexprep( content, '(?<=_loadvari226uz\(1,0,1\) = )\S+',
sprintf( '%f', HEAVE(i,1) )) ;
content = regexprep( content, '(?<=_loadvari226uz\(2,0,1\) = )\S+',
sprintf( '%f', HEAVE(i+1,1) ));

content = regexprep( content, '(?<=_loadvari226rotx\(1,0,1\) = )\S+',
sprintf( '%f', HEAVE(i,1) )) ;
content = regexprep( content, '(?<=_loadvari226rotx\(2,0,1\) = )\S+',
sprintf( '%f', HEAVE(i+1,1) ));

content = regexprep( content, '(?<=_loadvari226roty\(1,0,1\) = )\S+',
sprintf( '%f', HEAVE(i,1) )) ;
content = regexprep( content, '(?<=_loadvari226roty\(2,0,1\) = )\S+',
sprintf( '%f', HEAVE(i+1,1) ));

fId = fopen( 'ANSYS_BATCH_INPUT_V12.txt', 'w' ) ;
fwrite( fId, content ) ;
fclose( fId ) ;

%running ansys apdl at batch mode

!"C:\Program Files\ANSYS Inc\v162\ansys\bin\winx64\ANSYS162.exe" -b -i
ANSYS_BATCH_INPUT_V12.txt -o ANSYS_BATCH_OUTPUT_V12.txt

end

%Storing solutions

fileID=fopen('ANSYS_SOLUTIONS_V12.txt');
formatSpec='%f %f %f %f %f %f %f %f %f %f';
E = textscan(fileID,formatSpec);
TIME=1:1:10;
NODE=E{1,1};
XXCC=E{1,2};
YYCC=E{1,3};
```

```
ZZCC=E{1,4};
XXC=E{1,5};
YYC=E{1,6};
ZZC=E{1,7};
ROTXX=E{1,8};
ROTYY=E{1,9};
ROTZZ=E{1,10};
E1=[NODE XXCC YYCC ZZCC XXC YYC ZZC ROTXX ROTYY ROTZZ];
E2=(find(E1(:,1)==19));
EXXC=E1(E2(:,1),5);
EXXY=E1(E2(:,1),6);
EXXZ=E1(E2(:,1),7);
EROTXX=E1(E2(:,1),8);
EROTYY=E1(E2(:,1),9);
EROTZZ=E1(E2(:,1),10);
```

9 DOF Vehicle value

```
m1=17400;
m2=270;
m3=270;
m4=270;
m5=270;
m6=270;
m7=270;
k1=806170;
k2=806170;
k3=806170;
k7=806170;
k8=806170;
k9=806170;
k4=986849;
k5=986849;
k6=986849;
k10=986849;
k11=986849;
k12=986849;
c1=25333;
c2=25333;
c3=25333;
c7=25333;
c8=25333;
c9=25333;
c4=50;
c5=50;
c6=50;
c10=50;
c11=50;
c12=50;
Jteta=(1/12)*(m1*7.040*7.040);
Jalfa=(1/12)*(m1*2.770*2.770);
L1=5.160;
L2=3.520;
L3=3.340;
L4=3.260;
L5=1.760;
L6=1.200;
L7=1.056;
```

7 DOF vehicle value

```
m1=60;
m2=60;
m3=60;
m4=60;
m5=1200;
Jteta=4000;
Jalfa=950;
k1=30000;
k2=30000;
k3=30000;
k4=30000;
kt1=180000;
kt2=180000;
kt3=180000;
kt4=180000;
c1=3500;
c2=3500;
c3=3500;
c4=3500;
ct1=500;
ct2=500;
ct3=500;
ct4=500;
L1=1.5;
L2=1.5;
L3=0.75;
L4=0.75;
L5=0.75;
```

Neural Network files

```
function [Y,Xf,Af] = NN_alfa_heave(X,~,~)
%MYNEURALNETWORKFUNCTION neural network simulation function.
%
% Generated by Neural Network Toolbox function genFunction, 17-Jan-2018
17:14:13.
%
% [Y] = myNeuralNetworkFunction(X,~,~) takes these arguments:
%
%   X = 1xTS cell, 1 inputs over TS timesteps
%   Each X{1,ts} = Qx1 matrix, input #1 at timestep ts.
%
% and returns:
%   Y = 1xTS cell of 1 outputs over TS timesteps.
%   Each Y{1,ts} = Qx1 matrix, output #1 at timestep ts.
%
% where Q is number of samples (or series) and TS is the number of
timesteps.

%#ok<*RPMT0>

% ===== NEURAL NETWORK CONSTANTS =====

% Input 1
x1_step1.xoffset = -100;
x1_step1.gain = 0.01;
x1_step1.ymin = -1;

% Layer 1
b1                =                [13.875461113410157;-10.814515696869364;-
7.7223720164887206;4.6349391018868058;1.5611343696953928;1.5255269104088
851;-4.6465618340180166;-7.7631657131753311;-10.849401735432414;-
13.994450817343147];
IW1_1   =   [-14.101733556199362;14.000343937572172;13.960651654843305;-
13.946515564022523;-13.938606197604694;13.937080880628089;-
13.932577652471911;-13.939358074448947;-13.966471514712142;-
13.990050500998786];

% Layer 2
b2 = -0.027888946924097643;
LW2_1 = [-0.11102084435182702 0.10744439635774512 0.11021405216505954 -
0.11058887598367O8     -0.11042723815101603     0.11105104946528439     -
0.11234300808893408     -0.11108595803281078     -0.10810980047059961     -
0.13616017847348327];

% Output 1
y1_step1.ymin = -1;
y1_step1.gain = 100.003330110893;
y1_step1.xoffset = -0.009999667;

% ===== SIMULATION ========

% Format Input Arguments
isCellX = iscell(X);
if ~isCellX
    X = {X};
end
```

```
% Dimensions
TS = size(X,2); % timesteps
if ~isempty(X)
    Q = size(X{1},1); % samples/series
else
    Q = 0;
end

% Allocate Outputs
Y = cell(1,TS);

% Time loop
for ts=1:TS

    % Input 1
    X{1,ts} = X{1,ts}';
    Xp1 = mapminmax_apply(X{1,ts},x1_step1);

    % Layer 1
    a1 = tansig_apply(repmat(b1,1,Q) + IW1_1*Xp1);

    % Layer 2
    a2 = repmat(b2,1,Q) + LW2_1*a1;

    % Output 1
    Y{1,ts} = mapminmax_reverse(a2,y1_step1);
    Y{1,ts} = Y{1,ts}';
end

% Final Delay States
Xf = cell(1,0);
Af = cell(2,0);

% Format Output Arguments
if ~isCellX
    Y = cell2mat(Y);
end
end

% ===== MODULE FUNCTIONS ========

% Map Minimum and Maximum Input Processing Function
function y = mapminmax_apply(x,settings)
y = bsxfun(@minus,x,settings.xoffset);
y = bsxfun(@times,y,settings.gain);
y = bsxfun(@plus,y,settings.ymin);
end

% Sigmoid Symmetric Transfer Function
function a = tansig_apply(n,~)
a = 2 ./ (1 + exp(-2*n)) - 1;
end
% Map Minimum and Maximum Output Reverse-Processing Function
function x = mapminmax_reverse(y,settings)
x = bsxfun(@minus,y,settings.ymin);
x = bsxfun(@rdivide,x,settings.gain);
x = bsxfun(@plus,x,settings.xoffset);
end
```

```
function [Y,Xf,Af] = NN_alfa_beta(X,~,~)
%MYNEURALNETWORKFUNCTION neural network simulation function.
%
% Generated by Neural Network Toolbox function genFunction, 17-Jan-2018
17:28:14.
%
% [Y] = myNeuralNetworkFunction(X,~,~) takes these arguments:
%
%   X = 1xTS cell, 1 inputs over TS timesteps
%   Each X{1,ts} = Qx1 matrix, input #1 at timestep ts.
%
% and returns:
%   Y = 1xTS cell of 1 outputs over TS timesteps.
%   Each Y{1,ts} = Qx1 matrix, output #1 at timestep ts.
%
% where Q is number of samples (or series) and TS is the number of
timesteps.

%#ok<*RPMT0>

% ===== NEURAL NETWORK CONSTANTS =====

% Input 1
x1_step1.xoffset = -1;
x1_step1.gain = 1;
x1_step1.ymin = -1;

% Layer 1
b1                =               [6.9048436540193245;3.1986130043361998;-
2.1963080058602431;1.1260085879614732;-
0.31248262130632803;0.45059078902978161;-1.3727545768525198;-
2.6972951654306527;2.9997877660792991;3.5528608172033458];
IW1_1   =   [-6.0317015596130474;-3.1972719546469941;2.9639852633594157;-
2.2238897623026785;2.0086989712263121;2.0256885873310901;-
2.5096444233901525;-
3.9590030927713995;3.4608881579980157;2.99427961405897];

% Layer 2
b2 = 0.071131493129348439;
LW2_1  = [0.048634807242525703 0.15655224485922731 -0.077326710250261665
0.1892654825983382       -0.20570976170952265       -0.22332451753929769
0.15333034948536409    0.017304970528547934    -0.079099812394712 74    -
0.24212552228034559];

% Output 1
y1_step1.ymin = -1;
y1_step1.gain = 1;
y1_step1.xoffset = -1;

% ===== SIMULATION ========

% Format Input Arguments
isCellX = iscell(X);
if ~isCellX
    X = {X};
end
```

```
% Dimensions
TS = size(X,2); % timesteps
if ~isempty(X)
    Q = size(X{1},1); % samples/series
else
    Q = 0;
end

% Allocate Outputs
Y = cell(1,TS);

% Time loop
for ts=1:TS

    % Input 1
    X{1,ts} = X{1,ts}';
    Xp1 = mapminmax_apply(X{1,ts},x1_step1);

    % Layer 1
    a1 = tansig_apply(repmat(b1,1,Q) + IW1_1*Xp1);

    % Layer 2
    a2 = repmat(b2,1,Q) + LW2_1*a1;

    % Output 1
    Y{1,ts} = mapminmax_reverse(a2,y1_step1);
    Y{1,ts} = Y{1,ts}';
end

% Final Delay States
Xf = cell(1,0);
Af = cell(2,0);

% Format Output Arguments
if ~isCellX
    Y = cell2mat(Y);
end
end

% ===== MODULE FUNCTIONS ========

% Map Minimum and Maximum Input Processing Function
function y = mapminmax_apply(x,settings)
y = bsxfun(@minus,x,settings.xoffset);
y = bsxfun(@times,y,settings.gain);
y = bsxfun(@plus,y,settings.ymin);
end

% Sigmoid Symmetric Transfer Function
function a = tansig_apply(n,~)
a = 2 ./ (1 + exp(-2*n)) - 1;
end
% Map Minimum and Maximum Output Reverse-Processing Function
function x = mapminmax_reverse(y,settings)
x = bsxfun(@minus,y,settings.ymin);
x = bsxfun(@rdivide,x,settings.gain);
x = bsxfun(@plus,x,settings.xoffset);
end
```

```
function [Y,Xf,Af] = NN_tetha_omega(X,~,~)
%MYNEURALNETWORKFUNCTION neural network simulation function.
%
% Generated by Neural Network Toolbox function genFunction, 17-Jan-2018
18:07:04.
%
% [Y] = myNeuralNetworkFunction(X,~,~) takes these arguments:
%
%   X = 1xTS cell, 1 inputs over TS timesteps
%   Each X{1,ts} = Qx1 matrix, input #1 at timestep ts.
%
% and returns:
%   Y = 1xTS cell of 1 outputs over TS timesteps.
%   Each Y{1,ts} = Qx1 matrix, output #1 at timestep ts.
%
% where Q is number of samples (or series) and TS is the number of
timesteps.

%#ok<*RPMT0>

% ===== NEURAL NETWORK CONSTANTS =====

% Input 1
x1_step1.xoffset = -1;
x1_step1.gain = 1;
x1_step1.ymin = -1;

% Layer 1
b1               =              [14;-10.888888888888889;7.7777777777777786;-
4.666666666666667;1.5555555555555562;1.5555555555555562;-
4.6666666666666661;-7.7777777777777786;10.888888888888888;14];
IW1_1 = [-14;14;-14;14;-14;14;-14;-14;14;14];

% Layer 2
b2 = 0.415049600702315;
LW2_1 = [-0.87715899273550724 0.63309706017023171 0.17228641383283438 -
0.38021296133042348    -0.76197744139229551    0.42370030634048939    -
0.39872310315991744      -0.30154144986970888      -0.53339422731047503
0.39698294257594058];

% Output 1
y1_step1.ymin = -1;
y1_step1.gain = 6420.91677849763;
y1_step1.xoffset = -0.000155741;

% ===== SIMULATION ========

% Format Input Arguments
isCellX = iscell(X);
if ~isCellX
    X = {X};
end
```

```
% Dimensions
TS = size(X,2); % timesteps
if ~isempty(X)
    Q = size(X{1},1); % samples/series
else
    Q = 0;
end

% Allocate Outputs
Y = cell(1,TS);

% Time loop
for ts=1:TS

    % Input 1
    X{1,ts} = X{1,ts}';
    Xp1 = mapminmax_apply(X{1,ts},x1_step1);

    % Layer 1
    a1 = tansig_apply(repmat(b1,1,Q) + IW1_1*Xp1);

    % Layer 2
    a2 = repmat(b2,1,Q) + LW2_1*a1;

    % Output 1
    Y{1,ts} = mapminmax_reverse(a2,y1_step1);
    Y{1,ts} = Y{1,ts}';
end

% Final Delay States
Xf = cell(1,0);
Af = cell(2,0);

% Format Output Arguments
if ~isCellX
    Y = cell2mat(Y);
end
end

% ===== MODULE FUNCTIONS ========

% Map Minimum and Maximum Input Processing Function
function y = mapminmax_apply(x,settings)
y = bsxfun(@minus,x,settings.xoffset);
y = bsxfun(@times,y,settings.gain);
y = bsxfun(@plus,y,settings.ymin);
end

% Sigmoid Symmetric Transfer Function
function a = tansig_apply(n,~)
a = 2 ./ (1 + exp(-2*n)) - 1;
end
% Map Minimum and Maximum Output Reverse-Processing Function
function x = mapminmax_reverse(y,settings)
x = bsxfun(@minus,y,settings.ymin);
x = bsxfun(@rdivide,x,settings.gain);
x = bsxfun(@plus,x,settings.xoffset);
end
```

```
% Dimensions
TS = size(X,2); % timesteps
if ~isempty(X)
    Q = size(X{1},1); % samples/series
else
    Q = 0;
end

% Allocate Outputs
Y = cell(1,TS);

% Time loop
for ts=1:TS

    % Input 1
    X{1,ts} = X{1,ts}';
    Xp1 = mapminmax_apply(X{1,ts},x1_step1);

    % Layer 1
    a1 = tansig_apply(repmat(b1,1,Q) + IW1_1*Xp1);

    % Layer 2
    a2 = repmat(b2,1,Q) + LW2_1*a1;

    % Output 1
    Y{1,ts} = mapminmax_reverse(a2,y1_step1);
    Y{1,ts} = Y{1,ts}';
end

% Final Delay States
Xf = cell(1,0);
Af = cell(2,0);

% Format Output Arguments
if ~isCellX
    Y = cell2mat(Y);
end
end

% ===== MODULE FUNCTIONS ========

% Map Minimum and Maximum Input Processing Function
function y = mapminmax_apply(x,settings)
y = bsxfun(@minus,x,settings.xoffset);
y = bsxfun(@times,y,settings.gain);
y = bsxfun(@plus,y,settings.ymin);
end

% Sigmoid Symmetric Transfer Function
function a = tansig_apply(n,~)
a = 2 ./ (1 + exp(-2*n)) - 1;
end
% Map Minimum and Maximum Output Reverse-Processing Function
function x = mapminmax_reverse(y,settings)
x = bsxfun(@minus,y,settings.ymin);
x = bsxfun(@rdivide,x,settings.gain);
x = bsxfun(@plus,x,settings.xoffset);
end
```

CURRICULUM VITAE

Credentials

Name, Surname : Ahmet TATAR

Place of Birth : Denizli, TURKEY

Material Status : Single

E-mail : tatar0ahmet@gmail.com

Adress : Ankara, TURKEY

Education

BSc. : Yıldız Technical University

MSc. : -

PhD. : -

Foreign Language

English

Work Experience

Design Engineer, ASELSAN INC (2014 -)

Areas of Experiences

-

Projects and Budgets

-

Publications

-

Oral and Poster Presentation

-

HACETTEPE UNIVERSITY
GRADUATE SCHOOL OF SCIENCE AND ENGINEERING
THESIS/DISSERTATION ORIGINALITY REPORT

HACETTEPE UNIVERSITY
GRADUATE SCHOOL OF SCIENCE AND ENGINEERING
TO THE DEPARTMENT OF MECHANICAL ENGINEERING

Date: 15/05/2018

Thesis Title / Topic: "MODELING OF NON-LINEAR EFFECT IN REMOTE CONTROLLED STABILIZED GUN SYSTEMS"

According to the originality report obtained by my thesis advisor by using the *Turnitin* plagiarism detection software and by applying the filtering options stated below on 14/05/2018 for the total of 113 pages including the a) Title Page, b) Introduction, c) Main Chapters, d) Conclusion sections of my thesis entitled as above, the similarity index of my thesis is 5 %.

Filtering options applied:

1. Bibliography/Works Cited excluded
2. Quotes excluded
3. Match size up to 5 words excluded

I declare that I have carefully read Hacettepe University Graduate School of Sciene and Engineering Guidelines for Obtaining and Using Thesis Originality Reports; that according to the maximum similarity index values specified in the Guidelines, my thesis does not include any form of plagiarism; that in any future detection of possible infringement of the regulations I accept all legal responsibility; and that all the information I have provided is correct to the best of my knowledge.

15.05.2018

I respectfully submit this for approval.

Date and Signature

Name Surname:	AHMET TATAR
Student No:	N14121261
Department:	MECHANICAL ENGINEERING
Program:	Master
Status:	☒ Masters ☐ Ph.D. ☐ Integrated Ph.D.

ADVISOR APPROVAL

APPROVED.

PROF. DR. BORA YILDIRIM